ABSTRACT

ANTIGEN-SPECIFIC TOLEROGENIC VACCINES INHIBIT AUTOIMMUNE

DISEASE IN A RODENT MODEL OF MULTIPLE SCLEROSIS

by

Jennifer Lori Blanchfield

(Under the direction of Mark D. Mannie, Ph.D.)

May 21, 2010

Chair: Jeffrey C. Smith, Ph.D.

Department: Microbiology and Immunology at East Carolina University Brody School of

Medicine

Multiple sclerosis (MS) is considered to be a T cell-mediated autoimmune disease directed against myelinated nerves within the central nervous system. Current therapies available to MS patients have low efficacy and are immunosuppressive. Novel therapies that negatively regulate or delete autoreactive T cells, i.e., induce antigen-specific T cell tolerance, are key for the development of more efficacious and perhaps curative therapies. Our laboratory has developed a vaccine platform comprised of cytokine-antigen fusion proteins to promote T cell tolerance. In this study, GM-CSF and M-CSF cytokines were tested as domains in cytokine-neuroantigen (NAg) fusion proteins to assess targeting of NAg to different antigen presenting cell (APC) subsets. Fusion proteins were designed with a cytokine N-terminal domain and the encephalitogenic peptide 69-88 of guinea pig myelin basic protein (GP69-88) as the C-terminal

domain. Studies measuring T cell activation *in vitro*, prevention of experimental autoimmune encephalomyelitis (EAE), and treatment of EAE showed that GMCSF-NAg was the most potent fusion protein, with the following rank order of activity (GMCSF-NAg > MCSF-NAg > GP69-88). GMCSF-NAg was 1000-fold more potent than GP69-88 in stimulating myelin basic protein (MBP)-specific T cell proliferation. The mechanism by which GMCSF-NAg promoted T cell activation involved cytokine receptor-mediated uptake of NAg by APC, since free GM-CSF inhibited the GMCSF-NAg potentiated response. GMCSF-NAg potently targeted NAg to dendritic cells and macrophages *in vitro*, but not to B or T cell APC. Covalent linkage between GM-CSF and NAg was required for enhanced potency of GMCSF-NAg *in vitro* and for the prevention and treatment of EAE *in vivo*. In conclusion, GMCSF-NAg potently targeted self-antigen to myeloid APC subsets and caused profound antigen-specific tolerance in EAE. In the future, cytokine-NAg fusion proteins may provide a novel tool to develop antigen-specific, tolerogenic vaccines for the treatment of MS.

ANTIGEN-SPECIFIC TOLEROGENIC VACCINES INHIBIT AUTOIMMUNE

DISEASE IN A RODENT MODEL OF MULTIPLE SCLEROSIS

A Dissertation Presented to

The Faculty of the Department of Microbiology and Immunology

Brody School of Medicine at East Carolina University

In Partial Fulfillment of the Requirements of the Degree of

Doctor of Philosophy in Microbiology and Immunology

by

Jennifer Lori Blanchfield

May 21, 2010

ANTIGEN-SPECIFIC TOLEROGENIC VACCINES INHIBIT AUTOIMMUNE

DISEASE IN A RODENT MODEL OF MULTIPLE SCLEROSIS

by

Jennifer Lori Blanchfield

APPROVED BY:

DIRECTOR OF DISSERTATION: _____
Mark D. Mannie, Ph.D.

COMMITTEE MEMBER: _____
Donald R. Hoffman, Ph.D.

COMMITTEE MEMBER: _____
Everett C. Pesci, Ph.D.

COMMITTEE MEMBER: _____
Rachel L. Roper, Ph.D.

COMMITTEE MEMBER: _____
Mary Jane Thomassen, Ph.D.

CHAIR OF THE DEPARTMENT OF
MICROBIOLOGY AND
IMMUNOLOGY: _____
Jeffrey C. Smith, Ph.D.

DEAN OF THE GRADUATE SCHOOL: _____
Paul J. Gemperline, Ph.D.

ACKNOWLEDGEMENTS

with you. I could not make it through this life without your love, support and friendship. Coldplay said it best when they sang, "Honey you are a rock, upon which I stand." I hope my life choices have shaped our future, and the future of our baby, for the better.

TABLE OF CONTENTS

PAGE

CHAPTER 3: RESULTS

CHAPTER 4: DISCUSSION

LIST OF FIGURES AND TABLES

LIST OF ABBREVIATIONS

ADEM	**acute disseminated encephalomyelitis**
ALUM	**aluminum salt adjuvant**
ANOVA	**analysis of variance**
APC	**antigen presenting cells**
APL	**altered peptide ligand**
B7 molecules	**CD80 or CD86**
CBD	**chitin binding domain**
CD	**cluster of differentiation**
CFA	**complete Freund's adjuvant**
CFSE	**carboxyfluorescein succinimidyl ester**
CH3	**constant heavy chain, domain 3**
CIITA	**MHC II transcriptional activator**
CNS	**central nervous system**
CPM	**counts per minute**
CSF-1R	**colony stimulating factor-1 receptor**
CTLA-4	**cytotoxic T lymphocyte antigen-4**
DC	**dendritic cell**
DHFR	**dihydrofolate reductase**
DNA	**deoxyribonucleic acid**
DQ α / β	**MHC class II molecule DQ alpha and beta chains**
DRβ	**MHC class II molecule DR beta chain**

EAE	**experimental allergic or autoimmune encephalomyelitis**
ELISA	**enzyme-linked immunosorbent assay**
FDA	**US Food and Drug Administration**
fM	**femtomolar**
GFP	**green fluorescent protein**
GM-CSF	**granulocyte macrophage-colony stimulating factor**
GP69-88	**guinea pig myelin basic protein, amino acids 69-88**
GPMBP	**entire guinea pig myelin basic protein**
HLA	**human leukocyte antigen**
hmAb	**humanized monoclonal antibody**
Hsp	**heat shock protein**
HSV-1	**herpes simplex virus-1**
ICAM-1	**intercellular adhesion molecule-1**
IFN	**interferon**
IgG	**immunoglobulin G**
IL	**interleukin**
iNOS	**inducible nitric oxide synthase**
IP-10	**interferon inducible protein-10**
JAK-STAT	**janus kinase-signal transducer and activator of transcription**
LacZ	**beta-galactosidase**
LAG-3	**lymphocyte activation gene-3**
LFA-1	**lymphocyte function-associated antigen-1**
LPS	**lipopolysaccharide**

MAG	**myelin associated glycoprotein**
MAPK	**mitogen activated protein kinase**
MBP	**myelin basic protein**
M-CSF	**macrophage-colony stimulating factor**
MHC	**major histocompatibility complex**
MOG	**myelin oligodendrocyte glycoprotein**
MRI	**magnetic resonance imaging**
MS	**multiple sclerosis**
MTS / PMS	**tetrazolium salt / phenazine methosulfate**
NAg	**encephalitogenic peptide of MBP**
NK	**natural killer cell**
nM	**nanomolar**
PAP	**pulmonary alveolar proteinosis**
PCR	**polymerase chain reaction**
PI3-K	**phosphoinositol-3 kinase**
PLP	**proteolipid protein**
RA	**receptor antagonist**
RANTES	**regulated upon activation, normal T cell expressed and secreted**
scFv	**single chain variable region**
sIg	**surface immunoglobulin**
TCR	**T cell receptor**
TGF	**transforming growth factor**
Th	**T cell helper**

TNFa   tumor necrosis factor alpha

VCAM-1   vascular cell adhesion molecule-1

VLA-4   very late antigen-4

CHAPTER 1

INTRODUCTION

1.1 MULTIPLE SCLEROSIS: A BRIEF OVERVIEW

In the late 14th century, patients presenting with multiple sclerosis-like symptoms were documented as exhibiting paraplegias, a vague descriptor referring to paralysis of the lower extremities (1). Jean-Martin Charcot first comprehensively characterized multiple sclerosis in 1868 as 'sclerose en plaques'. He compiled clinical observations with detailed microscopic illustrations of disease lesions from the central nervous system of patients upon autopsy. Charcot found multiple sclerosis to be distinct from other neurological disorders based on these clinical and pathological observations (1).

The classification of multiple sclerosis (MS) has evolved over time and it is now characterized as a chronic, inflammatory demyelinating disease of the central nervous system (CNS) (2). Patients with MS commonly exhibit multiple plaques or lesions, defined as areas of inflammation and demyelination, within the white matter of the CNS. White matter predominantly consists of nerve axons encased in a lipid sheath, i.e. myelin, which aids in the conduction of nerve impulses from the brain to the periphery. Based on the pattern of demyelination, a patient may present with numbness, muscle weakness and spasticity, bladder and bowel dysfunction, cognitive and speech impairment, pain, and vision impairment among other symptoms. Approximately 85% of patients are initially diagnosed with a relapsing-remitting course of disease marked by an acute attack of neurological dysfunction that is followed by a remission of symptoms for at least 30 days before a subsequent relapse (2). Other forms of the disease include: primary progressive MS, marked by neurological dysfunction that

increases in severity without distinct relapses; secondary progressive MS, marked by relapsing-remitting disease that eventually progresses in the absence of distinct relapses; and progressive relapsing MS, described as a steady increase in neurological dysfunction with acute relapses (3). The clinical course of MS can vary among patients and usually culminates in a progressive loss of neurologic dysfunction over time (3).

Currently, MS is proposed to be a $CD4^+$ Th1 T cell mediated autoimmune disease (2). This hypothesis is based on studies in animal models and is supported by the histopathology of lesions from the CNS of MS patients. Histologically, human lesions are comprised of T lymphocytes, characterized with $CD4^+$ or $CD8^+$ (cluster of differentiation) co-receptors, plus macrophage (foam cells) infiltrates and are marked by the loss of myelin with or without axonal damage. In some MS patients however, there is evidence of B cell mediated pathology due to the presence of antibody and complement at sites of demyelination. Antibodies found in patient lesions and sera exhibit antigenic reactivity to proteolipid protein (PLP), myelin oligodendrocyte glycoprotein (MOG), myelin associated glycoprotein (MAG), glycolipids and heat shock proteins, however these antibodies are not specific to MS patients. Future research is needed to elucidate the complex immunopathology of the disease in order to determine if MS is one disease that evolves over time or if it is a disease that incorporates multiple, distinct diseases (2, 4). Understanding the pathology of MS will be important for providing patients with efficacious treatments (4).

MS is estimated to affect approximately 1.1 – 2.5 million people worldwide and 350, 000 people in the United States (5). A gender bias is seen among MS patients where women are approximately twice as likely to develop the disease than men (2). The age of onset is typically between 20 to 40 years, but children are also susceptible. All ethnicities are prone to developing

MS but there is a higher incidence of disease found in people of northern European descent, i.e. Scandinavia, Iceland, North America and the British Isles. High incidences of MS among select populations indicates a role for genetic and environmental factors in the etiology of the disease (2).

The etiology of MS is not currently known. A number of susceptibility factors have been suggested, but no one factor has been identified as a causative agent of MS (2). This has caused speculation that multiple sclerosis could be a polygenic disease, where multiple genes act in concert to influence disease susceptibility. Susceptibility genes most reproducibly associated with MS are HLA (human leukocyte antigen or major histocompatibility complex) class II alleles DQβ1*0602, DQα1*0102, DRβ1*1501, and DRβ1*0101. Non-HLA candidates include genes that encode for receptors of T cell growth factors (i.e., IL-2 receptor alpha and IL-7 receptor alpha) as well as immune response genes (i.e., inducible nitric oxide synthase, chemokines and their receptors, and the MHC II transcriptional activator CIITA). The increased risk of MS among families and populations may be the culmination of genetic and environmental factors. Potential environmental factors include exposure to toxins, organic solvents and infectious agents, yet there has been no direct evidence linking these factors to MS (2).

1.2 EXPERIMENTAL AUTOIMMUNE ENCEPHALOMYELITIS: THE ANIMAL MODEL OF MULTIPLE SCLEROSIS

MS is a difficult disease to study in human patients due to the inability of obtaining CNS samples. Therefore animal models are a crucial alternative for providing insights into MS pathogenesis. The animal model for MS, known as experimental autoimmune encephalomyelitis (EAE), has features in common with the human disease. These features include damage to the

myelin sheath and nerve fibers, lymphocyte infiltration in the CNS, and multiple perivascular CNS lesions (6). Discrepancies between EAE and MS pertain to the clinical course and immunopathology of the disease, the lack of genetic variation in the animal models, and that EAE has to be induced while MS is considered to be spontaneous; although EAE can be spontaneous in TCR transgenic models (7, 8). It is important to keep in mind that the clinical and pathological presentations are variable among MS patients such that it is unlikely to have one animal model replicate all aspects of MS (7). Despite the discrepancies, EAE prevails as a relevant model to study the mechanism of disease onset and recovery, immunopathology and genetics of the disease, as well as novel therapeutic strategies. EAE can continue to provide insights into MS but the relevance will ultimately have to be supported by clinical studies (7).

The animal model for MS was initially developed in monkeys during the 1930s in order to understand the etiology of acute disseminated encephalomyelitis that was seen in patients recovering from infection with small pox and measles or following rabies vaccination (9, 10). Acute disseminated encephalomyelitis (ADEM) is defined by an acute attack of the central nervous system leading to demyelination and inflammation of the brain. ADEM was induced in monkeys through repeated (greater than 50) intramuscular injections of brain extracts from normal rabbits (9-11). In 1944, Ferraro postulated that the induced encephalomyelitis was an allergic response to antigens within the brain tissue and thus coined the term experimental allergic encephalomyelitis (EAE) (12). With the advent of Complete Freund's Adjuvant (CFA; *Mycobacterium* in an oil-in-water emulsion) in 1942, the efficiency of EAE induction in monkeys was enhanced significantly (13). The field of EAE was advanced when researchers showed that the disease could be induced in smaller animal models including rabbits, guinea pigs, mice, rats, dogs, sheep and chickens (14).

Researchers suspected that EAE was an immunological based disease (ie, an allergic response, or a CFA induced humoral response to brain tissue) but there was no supporting evidence (15). Lymphocyte involvement in encephalomyelitis came to the forefront in 1960. Paterson showed that EAE could be transferred to naïve recipients through the adoptive transfer of lymph node cells from donor rats presenting with EAE (15). Subsequent research established that T cells were required for the induction of EAE. For instance, neonatal rats were refractory to EAE when thymectomized and sublethally irradiated (16, 17). Susceptibility to EAE was restored when rats were reconstituted with syngeneic thymocytes and not when reconstituted with normal B cells (16-18). Furthermore, B cells and antigen presenting cells (APC) from EAE donors were unable to adoptively transfer disease to thymectomized and irradiated recipients (18). Additional studies supported the role for T cells in EAE pathogenesis. Treatment of rats and mice with anti-CD4 antibodies, post encephalitogenic challenge, diminished EAE severity and duration when compared to treatment with non-specific antibodies (19, 20). Furthermore, $CD4^+$ T cells have been detected in CNS lesions of EAE induced mice (14).

Research examining T cell mediated induction of EAE was advanced with the identification of specific protein antigens, as opposed to whole brain homogenates, that were capable of inducing encephalomyelitis in the presence of adjuvant. In 1947, Kabat postulated that myelin was the source of encephalitogenic antigen because monkeys injected with emulsions of fetal rabbit brain, known to be devoid of myelin, did not induce encephalomyelitis (21). By 1977 myelin basic protein (MBP; 17 kDa) was shown to induce EAE in numerous animal models (14, 22). The major encephalitogenic determinant of myelin basic protein in Lewis rats, the model utilized in this project, was localized to amino acids 68-88 (14, 22). In the 1980s MBP specific T cell clones were found to be encephalitogenic and served as a platform for future

studies regarding T cell mediated pathogenesis in EAE (14). Based on these data, EAE was proposed to be an autoimmune response orchestrated by CD4^{+} T cells specific for myelin self peptides (23).

Theoretically, autoreactive T cells of low and high affinity for antigen are present in the periphery, despite thymic selection, and could potentially become activated in the absence of peripheral tolerance mechanisms (23). Typically T cells with low affinity for self-antigen:MHC complexes are positively selected for survival by thymic stromal cells, while potentially autoreactive T cells with high affinity for self-antigen:MHC complexes are negatively selected / deleted. However, autoreactive, high affinity T cells may escape thymic selection as a result of inefficient negative selection. For instance, if antigen inefficiently binds MHC then the T cell may exhibit weak affinity for the antigen:MHC complex and be positively selected (23). On the other hand, low affinity, autoreactive T cells that are positively selected in the thymus can become activated in the presence of high dose antigen: MHC complexes present within the CNS, in the case of MS (24). Low affinity T cells recruited to the CNS are postulated to sustain an autoimmune response thought to be previously initiated by high affinity autoreactive T cells (24).

In the EAE model, naïve, autoreactive T cells are activated in the presence of neuroantigen in CFA. Naïve CD4^{+} T cell activation occurs when TCR and CD4 recognize / bind antigen:MHC II complexes concurrently with co-stimulatory signaling between CD28, on T cells, and B7 molecules, on APC, for example (25). CFA promotes enhanced phagocytosis and maturation of APC, resulting in increased antigen uptake, expression of MHC class II and co-stimulatory molecules required to differentiate naive CD4^{+} T cells into Th1 effector T cells (25). Effector T cells then migrate through blood vessels via interactions between upregulated adhesion molecules on T cells (i.e., LFA-1 and VLA-4) and endothelium (i.e., ICAM-1 and

VCAM-1) (2). Activated T cells produce matrix metalloproteinases (MMP-2 and MMP-9) that promote diapedesis through the blood brain barrier. Effector T cells become reactivated in the CNS upon recognition of antigen:MHC II complexes on microglial cells (aka, resident CNS macrophages). Effector CD4^{+} T cells are thought to indirectly promote demyelination via the production of inflammatory cytokines (i.e., IFNγ and TNFα) that activate effector cells, i.e. macrophages, within the CNS and through the production of chemokines (i.e., RANTES and IP-10) that recruit additional macrophages. Activated macrophages can mediated cellular damage through enhanced phagocytosis and release of oxygen radicals (2). Research suggests that T cells may directly mediate cellular damage in the CNS through the production of cytotoxic / cytostatic cytokines such as IFNγ and TNFβ (14).

1.3 THERAPIES CURRENTLY AVAILABLE FOR MULTIPLE SCLEROSIS PATIENTS

Currently there are no curative therapies for MS patients. The most effective therapies available, IFNβ-1α (Avonex and Rebif), IFNβ-1β (Betaseron and Extavia), and an anti-VLA-4 monoclonal antibody (Tysabri) are generally immunosuppressive (2). IFNβ is generally well tolerated although patients have presented with flu-like symptoms, reactions at the injection site, liver toxicity and antibodies that neutralize IFNβ (2). IFNβ is established as an effective treatment to reduce MS activity (lesions measured by MRI) and disease severity during onset of MS. IFNβ is a cytokine typically considered to have antiviral properties, yet IFNβ also exerts antiproliferative and immunomodulatory effects that may account for the beneficial effects in MS patients (26, 27). For instance, IL-10 expression was upregulated in MS patients that received IFNβ therapy, which potentially promoted a switch from the pathogenic Th1 response

to a non-pathogenic, Th2 humoral response (26, 27). This idea of immune deviation is controversial because the humoral response is seen in MS lesions and has a role in exacerbating EAE. The antiproliferative effects of IFNβ, potentially via cell cycle regulation as documented in hematopoietic progenitors, and cytotoxic effects on T cells may be a more plausible mechanism of IFNβ in MS patients (26, 28).

Tysabri is a humanized monoclonal antibody against the α4 subunit of VLA-4 (α4 β1) and is postulated to block adhesion between immune cells (B cells, T cells, NK cells, macrophages) and vasculature endothelium, thereby inhibiting leukocyte migration into the CNS (2). Tysabri has proven to be effective in reducing MS activity and disease severity. However approximately 1 in 1,000 patients treated with Tyasbri for 18 months developed progressive multifocal leukoencephalopathy, a fatal inflammation of the CNS caused by reactivation of a latent JC (John Cunningham isolate) polyomavirus (2).

Other therapies available to MS patients include Copaxone (glatiramer acetate) and mitoxantrone. Mitoxantrone is a chemotherapeutic drug that promotes DNA damage by introducing double stranded breaks and DNA crosslinking. It has the potential to reduce disease activity and severity in some patients but carries an increased risk of cardiotoxicity and cancer (2). Copaxone is a random polypeptide of tyrosine, glutamic acid, lysine and alanine designed to mimic MBP and compete for binding on MHC class II molecules; based on the hypothesis that Copaxone would antagonize MBP specific T cell clones an inhibit their activation (2, 29). Copaxone is well tolerated by patients yet the efficacy of the drug in reducing disease severity is controversial (2). The mechanism of Copaxone activity is also unclear, however the drug appears to non-specifically suppress T cell activation by a mechanism associated with anergy and Th2 cytokine bias (29).

The treatments available confer some therapeutic relief to patients, however the benefits are dependent on frequent administration. The need for repeated administration indicates that the drugs have low efficacy. For instance, Avonex (IFNβ-1α) is administered intramuscularly once a week, while Rebif (IFNβ-1α), Betaseron and Extavia (IFNβ-1β) are administered subcutaneously every other day (30). Copaxone is administered subcutaneously once a day and Tysabri is administered intravenously once a month. Mitoxantrone is administered intravenously once every three months, however patients can only receive a limited number of doses due to toxicity (30). Overall, the therapies available to MS patients are not highly effective, are typically immunosuppressive, and have potential serious side effects. This highlights the need to develop alternative therapies that specifically target the autoimmune response, leaving adaptive immunity intact.

1.4 NOVEL, ANTIGEN-SPECIFIC THERAPEUTIC APPROACHES DEVELOPED IN EAE MODELS

Neuroantigen specific therapies are considered an important alternative to immunosuppressive drugs (31). The idea is to specifically delete or inhibit the autoreactive T cell repertoire and restore tolerance to autoantigens in order to develop a more efficacious and perhaps curative therapy. Antigen-specific therapies studied in the EAE model have included myelin proteins, synthetic peptides, altered peptide ligands, MHC variant peptides, plasmid DNA encoding myelin proteins, and antibody-antigen fusion proteins (discussed below). A number of peripheral tolerance mechanisms have been associated with these antigen-specific therapies including deletion through apoptosis, anergy, immune deviation and induction of a regulatory T cell response. In perspective, EAE has been a significant animal model for the development of

MS therapies because three of the six FDA approved drugs were developed after successful trials in EAE models (9).

Administration of self antigen (myelin basic protein or altered myelin peptide), subcutaneously or intravenously, at high doses during or after an encephalitogenic challenge suppressed the autoimmune response in EAE through a mechanism associated with apoptosis of both T cells and oligodendrocytes (myelin producing cells) (32, 33). This form of tolerance, known as high dose tolerance, involved the upregulation of IFNγ, TNFα and iNOS transcripts in the CNS (33, 34). Nitric oxide production, associated with increased apoptosis and EAE recovery, can be induced through iNOS via Th1 proinflammatory cytokines IFNγ and TNFα (33). A drawback of high dose tolerance is that the mechanism of tolerance is transiently cytotoxic and does not establish active tolerance (2). This means that antigen-specific memory would not be established and that high dose antigen would have to be administered regularly to be efficacious.

The amount of self-antigen administered also influences the tolerogenic mechanism. For instance, mucosal tolerance induced by the administration of low dose antigen occurs via a mechanism that promoted an antigen-specific regulatory T cell phenotype (35). Antigen-specific regulatory T cells can be induced in the periphery in the presence of antigen plus IL-10 and TGFβ during an immune response or after encountering a tolerogenic, IL-10 secreting DC (36). Induced regulatory T cells suppress T cell responses by a cytokine dependent manner through the secretion of IL-10 and TGFβ (36). Oral or intranasal administration of low dose MOG antigen, prior to encephalitogenic challenge, suppressed EAE by a regulatory T cell phenotype marked by increased IL-10 and decreased Th1 cytokines IFNγ and IL-2 (37). Furthermore, the development of severe EAE was prevented in naïve mice that received CD4^{+} T cells from MOG fed donors

prior to encephalitogenic challenge (37). A drawback of oral tolerance is that some models have indicated a limited window in which orally administered antigens effectively induce tolerance (35, 38). In fact, a previous clinical trial with a combination of bovine derived myelin, MBP and PLP was ineffective in MS patients in a placebo controlled trial (35). Nasal tolerance may provide a promising alternative because nasal administration of self antigen was also tolerogenic (35).

Antibody-antigen fusion proteins have been found to expand regulatory T cells and diminish autoimmunity in animal models of EAE (39). For example, initial studies with IgG-PLP indicated enhanced PLP uptake via the Fcγ receptor and augmented antigen presentation to PLP specific T cells *in vitro* (40). Aggregated IgG-PLP was more effective at inducing PLP specific tolerance than soluble Ig-PLP, and tolerance induction was associated with the production of the IL-10 tolerogenic cytokine by macrophages and dendritic cells (40). Upon further study with transgenic EAE models, aggregated IgG-PLP was found to promote expansion of antigen-specific regulatory T cells (CD4$^+$ CD25$^+$ CTLA-4$^+$ T cells) *in vivo* (39). These regulatory T cells suppressed proliferation of antigen-specific CD4$^+$ CD25$^-$ *in vitro* and promoted bystander suppression of T cells against CNS homogenate, MOG and MBP *in vivo*. Bystander suppression against MOG and MBP was mediated only when regulatory T cells were reactivated *in vitro* with PLP (39). The discovery of bystander suppression, where one regulatory T cell clone can potentially mediate suppression of heterogeneous, autoreactive T cell clones, is an advancement for the field because it is unclear which neuroantigens should be targeted to alleviate disease in MS patients.

Antigen-specific T cell tolerance has also been manipulated by altering the strength of binding between the TCR and peptide:MHC complex via altered peptide ligands (24). The idea

being that altering amino acid (s) in contact with the TCR will be nonstimulatory and prevent activation of antigen-specific T cells (41). EAE severity was significantly diminished by altered peptide ligands of PLP (41), MOG (42), and MBP(43). Drawbacks of APL therapies included switching from a pathogenic Th1 to a nonpathogenic Th2 cytokine response, which could promote hypersensitivity reactions and anaphylaxis (41). Additionally, some altered peptide ligands activated myelin reactive T cell clones *in vivo*, which is a concern when trying to prevent disease through the regulation of myelin reactive clones (41). In fact, clinical trials were halted when patients presented with exacerbated disease symptoms and hypersensitivity reactions after treatment with altered peptide ligands (44). An alternative to altered peptide ligands is MHC variant peptides, which have amino acid modifications at sites in contact with the MHC binding pocket, as opposed to sites in contact with the TCR. MHC variant peptides have shown promise in ameliorating EAE by promoting anergy in polyclonal T cell populations, but it is unclear if this therapy will stimulate the same side effects seen in clinical trials with altered peptide ligands (45, 46).

DNA vaccines encoding myelin antigens were devised as an alternative means to suppress EAE (47-49). These vaccines utilized bacterial plasmid DNA where unmethylated CpG served as an adjuvant to enhance Th1 and Th2 responses. Antigen-specific DNA vaccines were postulated to circumvent disease by either increasing IFNγ production, which has been shown to suppress EAE as IFNγ knockout mice exhibit worse disease, or by promoting the switch to a nonpathogenic Th2 response (50). DNA vaccines encoding myelin antigens (MBP, MOG, PLP, MAG) were mildly tolerogenic. To improve efficacy, plasmids encoding IL-4 were co-injected with plasmids encoding MOG or PLP in order to drive a Th2 immune response. This strategy significantly enhanced tolerance in comparison to individual vaccines of MOG, PLP, or

IL-4 (47-49). However, one report indicated that pre-treatment with DNA vaccines encoding MOG enhanced EAE upon encephalitogenic challenge 4-6 weeks later possibly due to enhanced MOG antibodies or IFNγ production (51). Despite the concern that DNA vaccines may worsen disease, plasmid DNA vaccines encoding MBP were well tolerated in Phase II clinical trials (52). Patients exhibited diminished activity (lesions) in the CNS and reduced numbers of MBP reactive antibodies in the cerebral spinal fluid (52).

The successful development of antigen-specific therapies for the treatment of autoimmune diseases, such as multiple sclerosis, will represent an advancement for the field of immunology. Antigen-specific therapies hold promise to selectively inhibit autoimmune responses against self antigens, leaving adaptive immunity intact. Drawbacks to antigen-specific therapies include potential worsening of disease, hypersensitivity reactions, sensitization to additional myelin epitopes and the uncertainty of which antigens to therapeutically target in patients. The hope is that continued research will alleviate the concerns associated with antigen-specific therapies and ultimately provide a effective or curative therapy for MS patients by promoting tolerance to self antigens.

1.5 DEVELOPMENT OF CYTOKINE-NEUROANTIGEN FUSION PROTEINS IN THE LEWIS RAT MODEL OF EAE

Our laboratory has generated cytokine-NAg fusion proteins as a means to inhibit the autoreactive T cell response against myelin epitopes in the Lewis rat model of EAE. Studies in other laboratories had previously shown the importance of cytokines to modulate the T cell response in various EAE models. For instance Th2 cytokines such as IL-4, IL-10 and IL-13 have been shown to diminish EAE severity. Plasmids encoding IL-4 synergistically enhanced

tolerogenic activity of myelin based DNA vaccines in the EAE model (47, 48). Additionally, intranasal administration of the IL-4 cytokine plus MBP peptide during disease onset was shown to reduce EAE (53). The tolerogenic mechanism was associated with increased expression of tolerogenic cytokines IL-10 and TGFβ concurrent with decreased IFNγ protein production by lymph node mononuclear cells 14 days post challenge (53). Encephalitogenic T cell clones transduced with IL-10, under control of the IL-2 promoter, suppressed EAE when administered as a pre-treatment or treatment regimen (54). Furthermore, transgenic mice expressing IL-10 under the MHC promoter were resistant to EAE induction on the BALB / c and SJL / J backgrounds (55). IL-13 transfected Chinese hamster ovary cells reduced EAE severity when administered concurrently during encephalitogenic challenge of Lewis rats, as compared to non-transfected controls (56).

IFNα and IFNβ have also been shown to diminish EAE severity when administered as a treatment after disease onset (57, 58). These effects were dose dependent such that EAE suppression was seen at higher doses of IFN. The mechanism of action was associated with decreased cellular infiltrates in the CNS, which was associated with reduced expression of VCAM-1 and ICAM-1 adhesion molecules on brain endothelial cells (59). These studies indicated the potential of cytokines to modulate the T cell mediated autoimmune response. Cytokine therapies could be improved by targeting the cytokine effects to antigen-specific T cells through covalent linkage between the cytokine and antigen.

Cytokine – antigen fusion proteins have been explored for the development of novel adjuvants in viral and cancer vaccines. For instance, an anti-viral vaccine comprised of the HSV-1 surface glycoprotein D covalently linked to IL-2 enhanced viral specific antibody production at titers comparable to or better than glycoprotein D in alum, an adjuvant approved

for human use (60). The fusion of glycoprotein D to IL-2 also enhanced the cytolytic response against virally infected macrophages and protected mice from a lethal challenge with HSV when compared to glycoprotein D or glycoprotein D plus IL-2 as separate molecules (60). In cancer vaccines, fusion proteins comprised of cytokines and a malignant B cell antigen, such as a tumor specific idiotype, have been shown to enhance immunity against tumors. For instance, fusion of GM-CSF to the C_H3 domain of a humanized monoclonal antibody comprised of hIgG1 plus the V_{H+L} region of the murine 38C13 B cell tumor sIg, enhanced antibody production against the tumor immunoglobulin and significantly protected mice from a lethal tumor challenge (61, 62). Fusion between the cytokine and antigen domain was necessary because tumor immunity was not enhanced by pre-treatment with the humanized monoclonal antibody (hmAb) alone, hmAb plus GM-CSF as separate molecules and hmAb fused to a carrier protein (61, 62). The adjuvant effect of cytokine – antigen fusion proteins were not known, but the requirement for covalent linkage between the cytokine and antigen domains suggested a role for cytokine mediated targeting of the B cell tumor antigen to specific cell subsets (61, 62).

To develop a therapy for EAE, our hypothesis was to fuse the encephalitogenic peptide of MBP to anti-inflammatory cytokines or cytokine antagonists in order to inhibit autoreactive T cells and promote antigen-specific tolerance. Laboratory members previously designed and studied fusion proteins comprised of the encephalitogenic domain of guinea pig MBP (NAg) fused to IL-2, IL-4, IL1-RA, IL-10, IL-13, IL-16 and IFNβ (28, 63-65). IL-2 was chosen for its requirement to maintain self tolerance (66) while IL-4, IL-10 and IL-13 were chosen to promote the switch from a pathogenic Th1 response to a nonpathogenic Th2 response (28, 63-65). IL-10 was additionally postulated to drive a regulatory T cell phenotype. IFNβ was selected because of the therapeutic benefit to some MS patients and IL1-RA was chosen because it is a receptor

antagonist of IL-1, a potent inflammatory cytokine in EAE that when blocked by IL1-RA, reduced EAE severity (67). IL-16 was studied for its association in reducing T cell proliferation and for a possible role in promoting chemotaxis (68, 69).

Genetic constructs encoding the various cytokine - NAg fusion proteins were covalently linked by PCR, expressed in baculoviral expression systems, purified by affinity chromatography and found to be biologically active at the cytokine domain and / or NAg domain. Pre-treatment and treatment experiments with cytokine – NAg fusion proteins in the Lewis rat model of EAE revealed the following rank order of tolerogenic activity: NAg-IL16 > IL2-NAg > IL1RA-NAg, IL13-NAg ≥ IL10-NAg, intact guinea pig MBP and NAg (65). In a separate experiment, pre-treatment and treatment regimens of IL2-NAg were shown to have greater tolerogenic activity than IL4-NAg; the tolerogenic activity of IL4-NAg was comparable to the NAg and GPMBP controls (64). Pre-treatment and treatment regimens of IFNβ-NAg were also found to be more tolerogenic than individual regimens of IFNβ and NAg (28). Overall, NAg-IL16 and IL2-NAg were the most potent tolerogens at reducing paralytic disease in the Lewis rat model of EAE.

The tolerogenic activity of NAg-IL16 and IL2-NAg were dependent on covalent linkage between the cytokine and neuroantigen domains. Rats pretreated with IL2-NAg or NAg-IL16 were protected from the development of paralytic disease when compared to rats pretreated with a combination of cytokine and NAg domains as separate molecules (64, 65). Furthermore, IL2-NAg or NAg-IL16 treatment during disease onset prevented severe EAE when compared to rats treated with the cytokine and NAg domains as separate molecules. The requirement for covalent linkage suggested that the tolerogenic nature of the fusion proteins was not due to inhibitory effects of the cytokine alone. The tolerogenic effect was most likely due to cytokine mediated

targeting of the NAg domain to antigen presenting cell subsets, increasing NAg presentation to responding T cells.

In vitro data suggested that the cytokine domains of NAg-IL16 and IL2-NAg targeted NAg to activated / blastogenic T cells, expressing MHC II, and promoted RsL.11 (NAg specific) T cell responses (64, 65). These data suggested that the tolerogenic mechanism of T cell presentation in vivo may be the result of T cell fratricide and subsequent elimination of autoreactive T cell clones. In other words activated, encephalitogenic T cells presenting NAg on MHC II would be killed upon recognition by another NAg specific T cell. Research supporting this hypothesis showed that adoptive transfer of MBP-loaded, MHC II$^+$ T cells prior to encephalitogenic challenge reduced EAE severity in Lewis rats (70). Furthermore, data indicated that NAg specific T cell responders induced apoptosis in T cells presenting MBP (71).

The tolerogenic mechanism of IFNβ-NAg differed from the mechanism associated with NAg-IL16 and IL2-NAg because the effects of IFNβ-NAg were not dependent on covalent linkage between the cytokine and NAg domains (28). Pre-treatment or treatment with IFNβ-NAg diminished EAE severity comparable to IFNβ plus NAg concurrently administered as separate molecules. These data suggested that cytokine mediated targeting of NAg to APC subsets was not likely part of the tolerogenic mechanism of IFNβ-NAg. In vitro analyses examining T cell fratricide revealed that the tolerogenic effect of IFNβ-NAg may be due to the independent actions of IFNβ and NAg. In other words NAg and IFNβ concurrently promoted killing of T cells due to the cytotoxicity of IFNβ and T cell fratricide of T cells presenting MBP. Data also showed that IFNβ was cytotoxic to select T cell clones, suggesting that the clinical effectiveness of IFNβ may be dependent on subsets of encephalitogenic T cells (28).

1.6 THE CONCEPT OF DESIGNING FUSION PROTEINS WITH GM-CSF AND M-CSF CYTOKINE DOMAINS

In this study, cytokine-NAg fusion proteins were designed with GM-CSF and M-CSF cytokine domains to potentially target NAg to dendritic cell and macrophage APC in order to subsequently modulate NAg specific T cell responses. GM-CSF and M-CSF have been shown to suppress T cell responses *in vivo* through a mechanism associated with dendritic cell and macrophage antigen presenting cells. Dendritic cells have been identified as the fundamental APC that mediates tolerance induction, however the role for macrophages in tolerance induction has recently come to fruition and cannot be ruled out as a significant mediator of T cell tolerance.

GM-CSF and M-CSF are traditionally classified as hematopoietic growth factors but have additional effects on mature myeloid populations (72). GM-CSF expression typically requires stimulation by LPS, TNF or IL-1 and is produced by activated T cells, endothelial cells, polymorphonuclear cells, mast cells, macrophages and bone marrow stromal cells (73). M-CSF on the other hand is constitutively expressed by macrophages, fibroblasts, endothelial cells and bone marrow stromal cells (72). Cells that respond to these cytokines are largely the same cells that secrete them. For instance monocytes, macrophages and polymorphonuclear cells respond to GM-CSF, while monocytes and macrophages respond to M-CSF. Generally, GM-CSF and M-CSF have been shown to increase cell survival and proliferation, cell differentiation, chemotaxis and activation of responder cells (72).

A number of dendritic cell subsets have been identified that vary in origin, tissue distribution and function (74). Dendritic cells originate from lymphoid or myeloid precursors and respectively differentiate into plasmacytoid dendritic cells (CD11c$^-$ CD123$^+$) or Langerhans (CD11c$^+$ CD1a$^+$; located in epidermis), interstitial (CD11c$^+$ CD1a$^-$; located in the dermis and

tissues) and CD14$^+$ monocyte-derived (CD11c$^+$ CD1a$^-$) dendritic cells. Immature dendritic cells, irrespective of origin, have been shown to induce peripheral T cell tolerance, known as the steady state hypothesis. The idea being that immature dendritic cells are unable to efficiently present antigen to T cells due to low expression of MHC II and B7 co-stimulatory molecules. Immature DC are thought to drive antigen-specific T cells to become anergic, to be deleted, or to acquire a regulatory T cell phenotype (74).

Targeting antigen to dendritic cells *in vivo* resulted in CD4$^+$ and CD8$^+$ T cell tolerance (75, 76). DEC205, a lectin receptor expressed highly on CD11$^+$ DC, but not B cell or T cells, was used to target antigen to steady state dendritic cells *in vivo* via an anti-DEC205 antibody. Anti-DEC205-Ag fusion proteins activated antigen-specific T cells *in vivo*, however the T cells were unresponsive to antigen when reactivated *in vitro*. The authors suggested this antigenic tolerance was associated with T cell anergy or deletion, based on bioassays and flow cytometry respectively (75, 76). In the EAE model, anti-DEC205-MOG fusion proteins targeted MOG to CD11$^+$ dendritic cells *in vivo*, presumably in the steady state, as determined by MOG specific bioassays. Pre-treatment of mice with anti-DEC205-MOG seven days before challenge diminished severe EAE and reduced the number of CD4$^+$ T cells in the spinal cord when compared to mock treated mice. Tolerance was suggested to be the result of T cell anergy that was associated with the expression of CD5, a negative regulator of T cell activation (77).

Additional support for dendritic cells as mediators of tolerance was evident when adherent, bone marrow derived dendritic cells loaded with MBP induced tolerance, compared to an unpulsed dendritic cell control, after administration as a pre-treatment in the Lewis rat model of EAE (78, 79). Antigen loaded dendritic cells were not found to be encephalitogenic during a four week evaluation period. Furthermore, adherent, bone marrow derived dendritic cells from

EAE rats mediated tolerance when adoptively transferred as a pre-treatment to naïve rats four weeks before encephalitogenic challenge. The authors suggested that MBP specific T cell clones were deleted via apoptosis, as shown by flow cytometry, and the apoptotic mechanism was correlated with increased nitric oxide and IFNγ production by blood mononuclear cells (78, 79).

In experimental autoimmune thyroiditis, another autoimmune disease model, GM-CSF and dendritic cells were shown to synergistically expand FoxP3$^+$ regulatory T cells that specifically inhibited anti-thyroglobulin immune responses *in vitro* and *in vivo* (80). CD11$^+$ CD8$^-$ dendritic cells isolated from GM-CSF treated mice expanded FoxP3$^+$CD4$^+$CD25$^+$ regulatory T cells from transgenic CD4$^+$ T cells *in vitro*. These derived regulatory T cells were capable of suppressing thyroglobulin specific T cells *in vitro*. The CD11$^+$ CD8$^-$ dendritic cells isolated from GM-CSF treated mice suppressed autoimmune thyroiditis when administered three days before a subsequent challenge with thyroglobulin in CFA. Overall, GM-CSF acting through CD11$^+$ CD8$^-$ dendritic cells mediated suppression in the experimental autoimmune thyroiditis model, as well as the NOD diabetic model of type 1 diabetes, and was associated with increased number of CD4$^+$ T cells expressing a regulatory phenotype (80, 81).

M-CSF was tested for the ability to drive tolerogenic dendritic cells because of its overlapping functions with GM-CSF (82). Human monocytes cultured in the presence of M-CSF and IL-4 yielded a dendritic cell phenotype characterized by expression of cell surface markers, CD14^{low} CD64^{low} HLA-DR^{high}, and endocytosis of FITC-dextran. Immature (not activated with LPS) MCSF-DC induced a regulatory T cell phenotype when compared to mature (LPS activated) dendritic cells. These T cells were capable of suppressing a mixed lymphocyte reaction between naïve CD4$^+$ T cells and allogeneic stimulators. The tolerogenic mechanism was associated with IL-10 production by MCSF-DC that potentially drove a regulatory T cell

response. These results indicated a tolerogenic role for M-CSF through the differentiation of monocyte derived dendritic cells (82). Support for this observation was found when administration of M-CSF increased graft survival via a mechanism associated with decreased $CD14^+$ monocytes and TNF production (83).

In EAE, peritoneal macrophages treated with M-CSF and MOG reduced MOG specific transgenic T cell proliferation *in vitro* with respect to controls (84). A pre-treatment regimen of M-CSF + MOG peritoneal macrophages significantly protected mice from developing severe EAE when compared to peritoneal macrophages individually treated with M-CSF or MOG. The tolerogenic mechanism was associated with the capacity of MCSF + MOG treated peritoneal macrophages to induce $CD4^+$ ($CD25^+FoxP3^+$) and $CD8^+$ ($CD122^+$) regulatory T cells *in vitro* when compared to macrophage controls treated individually with M-CSF or MOG. $CD4^+$ and $CD8^+$ T cells, isolated from EAE donor mice pretreated with MCSF + MOG peritoneal macrophages, conferred tolerance to EAE in recipient mice when adoptively transferred three days post encephalitogenic challenge. Splenocytes from the recipient mice exhibited diminished T cell proliferation upon restimulation with antigen *in vitro*. Additional support for the monocyte / macrophage lineage and T cell tolerance came from *in vitro* assays with myeloid suppressor cells (85). Splenic $CD11b^+$ cells isolated from EAE mice, 10 days post-challenge, were capable of suppressing $CD4^+$ T cells activated with antibodies against CD3 and CD28. Cells of this monocyte lineage were further characterized as $CD11b^+$ $Gr-1^+$, specifically $CD11b^+$ $Ly6-C^{high}$ $Ly6-G^-$, and were capable of inducing T cell apoptosis in association with nitric oxide production by the myeloid suppressor cells (85). Overall, these data suggested that M-CSF and macrophages are a potential therapeutic target for the induction of antigen-specific tolerance in EAE (84).

1.7 RESEARCH PROPOSAL

The objective of this project was to design a platform to study and develop novel therapies in the Lewis rat model of EAE for the ultimate treatment of multiple sclerosis. We hypothesized that the GM-CSF and M-CSF cytokines could potentially be used to target NAg to dendritic cell and macrophage antigen presenting cells, in order to modulate NAg specific T cell responses and induce tolerance to myelin self antigens. GM-CSF and M-CSF were chosen for their ability to act on cells of the monocyte and macrophage lineage in addition to their ability to suppress T cell responses *in vivo*. We proposed that GM-CSF and M-CSF fused to NAg could potentially influence T cell responses by targeting NAg specifically to those antigen presenting cells bearing the cytokine receptor and by the biological activity of the cytokine domain.

Signaling through the cytokine-receptor complex can influence T cell responses in our model by regulating expression of co-stimulatory molecules on antigen presenting cells and by increasing antigen uptake and presentation of antigen on MHC II via enhanced cytokine-receptor mediated endocytosis. In more detail, GM-CSF and M-CSF binding to their respective receptors, GM-CSF receptor ($\alpha\beta_c$) and M-CSF receptor (CSF-1R homodimer), would result in autophosphorylation of tyrosine residues and subsequent activation of downstream signaling cascades including MAPK, PI3-K and JAK-STAT (73, 86). Signaling through these pathways may lead to the upregulation of HLA-II, and other surface molecules following the addition of M-CSF or GM-CSF (87, 88). GM-CSF and M-CSF receptor endocytosis and degradation is the means by which receptor signaling is controlled. Receptors are downregulated following receptor activation (i.e., phosphorylation of tyrosine residues) whereby the cytoplasmic domains, containing the tyrosine residues, are ubiquitinated and degraded. The truncated receptor-ligand complex is subsequently endocytosed and degraded in the lysosomal compartment where, in our

22

model, NAg can be processed and loaded onto MHC class II for subsequent presentation to NAg specific T cells (73, 86).

The objectives of this dissertation were as follows: <u>AIM 1</u> included generation of the GMCSF-NAg and MCSF-NAg fusion proteins, assessment of their biological activity and necessity of the fusion between the cytokine and NAg domains to modulate antigenic T cell proliferation *in vitro*; <u>AIM 2</u> was designed to determine which antigen presenting cell subsets (macrophages, dendritic cells, B cells or T cells) were targeted by the cytokine-NAg fusion proteins and to determine the ability of targeted subsets to modulate antigenic T cell responses *in vitro*; and <u>AIM 3</u> was designed to evaluate the ability of GMCSF-NAg and MCSF-NAg to modulate the cell mediated and humoral immune responses in the Lewis rat model of experimental autoimmune encephalomyelitis. This research showed that GMCSF-NAg and MCSF-NAg were biologically active and that fusion between the cytokine and NAg domains were required to enhance antigenic T cell responses *in vitro*. *In vivo*, pre-treatment and treatment regimens of GMCSF-NAg and MCSF-NAg promoted antigen-specific tolerance, preventing the development of severe paralytic EAE. Covalent linkage between the cytokine and NAg domains was required for the induction of tolerance, *in vivo*, through a mechanism that was associated with the GM-CSF and M-CSF cytokine domains targeting the tethered NAg to dendritic cell and macrophage antigen presenting cells.

CHAPTER 2

MATERIALS AND METHODS

2.1 ANIMALS AND REAGENTS

Lewis rats were bred and maintained at East Carolina University Brody School of Medicine (Greenville, NC.). Animal care and use were performed in accordance with the guidelines set forth by the East Carolina University Institutional Animal Care and Use Committee. Injections were administered to Lewis rats while under isoflurane (Abbott Laboratories, Chicago, IL.) anesthesia. Guinea pig myelin basic protein (GPMBP) was purified from the spinal cords of guinea pigs (Rockland, Gilbertsville, PA.). The synthetic peptide GP69 - 88 (Y-G-S-L-P-Q-K-S-Q-R-S-Q-D-E-N-P-V-V-H-F) was purchased from Quality Controlled Biologicals, Inc. (Hopkinton, MA.). Mouse anti-rat B cell hybridoma supernatants containing the OX-6 anti-I-A (RT1B) IgG1 mAb, OX-33 anti-CD45 (B cell form) IgG1 mAb, OX-8 anti-CD8-alpha IgG1, OX-1 anti-CD45 (rat leukocytes) IgG1, W3 / 25 anti-CD4 IgG1 were concentrated by ultrafiltration through Amicon spiral wound membranes with a 100 kDa size exclusion (Millipore, Billerica, MA.). Hybridomas were obtained from the European Collection of Cell Cultures (Health Protection Agency Culture Collections, Salisbury, UK). Mouse anti-rat CD11c (MCA1441) IgG2a was purchased from AbD Serotec (Raleigh, NC). Mouse anti-rat B7.1 (3H5) IgG1, anti-B7.2 (24F) IgG1, anti-CD161a (10 / 78) IgG1, and anti-CD3 (G4.18) IgG3 monoclonal antibodies were purchased from PharMingen (San Diego, CA). FITC-conjugated goat anti-mouse IgG1 and PE-conjugated goat anti-mouse IgG2a (Southern Biotechnology Associates, Birmingham, AL) were used as secondary staining reagents to detect

primary antibody. B cells were FACS sorted with PE conjugated goat anti-rat IgG + IgM (H+L) (Southern Biotechnology Associates, Birmingham, AL.) to label surface Ig and FITC-goat anti-mouse IgG1 (Southern Biotechnology Associates) was used as a secondary staining reagent to stain OX33-labeled B cells. Indirect ELISA was performed with the secondary antibody goat anti-rat IgG + IgM (H+L) conjugated to alkaline phosphatase (Southern Biotechnology Associates).

2.2 CELL LINES AND CULTURE CONDITIONS

The RsL.11 MBP-specific T cell clone was a primary, IL-2 dependent line derived from Lewis rats sensitized with rat MBP in CFA (71). The R1T T cell clone was a blastogenic, IL-2 dependent clone derived from the Lewis rat T cell clone GP2.E5 / R1 derived from rats sensitized with guinea pig MBP (89). R1T constitutively expressed high levels of the IL2 receptor CD25, MHC class II glycoproteins (MHCII), B7.1, and B7.2 (90). CTLL T cells were an IL-2 dependent line of murine T cells (American Type Culture Collection, Manassas, VA.). The aforementioned T cell lines were propagated in complete RPMI {10% heat-inactivated fetal bovine serum, 2 mM glutamine, 100 μg / ml streptomycin, 100 U / ml penicillin (Whittaker Bioproducts, Walkersville, MD), 50 uM 2-ME (Sigma-Aldrich)} supplemented with recombinant rat IL-2, 0.4% v / v Sf9 supernatant (91). IL-6 specific T1165 plasmacytoma cell line was a generous donation from Richard Nordan and Michael Potter (National Cancer Institute, Bethesda, MD.). T1165 mouse plasmacytoma cells were propagated in complete RPMI supplemented with recombinant rat IL6-NAg (0.4% v / v Sf9 supernatant). BW5147 thymoma cells, derived from an AKR / J mouse T cell lymphoma (American Type Tissue Culture Collection, Manassas, VA.), were propagated in complete RPMI. Sf9 (*Spodoptera frugiperda*)

insect cells were cultured with Sf-900 II SFM (Invitrogen, Carlsbad, CA.) in the absence of antibiotics and serum.

2.3 STRUCTURE AND DESIGN OF RECOMBINANT PROTEINS

Two GM-CSF based fusion proteins (GMCSF-NAg and GM-CSF, Table 2.1) were used in this study. The GMCSF-NAg fusion protein was designed with the mature rat GM-CSF domain (126 amino acids) at the N-terminus and the major encephalitogenic 68-87 epitope of GPMBP (i.e., the NAg domain) plus 6 histidine residues (6 his-tag) at the C-terminus. The numbering system for GPMBP was based on accession number P25188 (www.ncbi.nlm.nih.gov). The GM-CSF fusion protein was designed with the mature rat GM-CSF domain at the N-terminus and a 7 his-tag at the C-terminus. The rat GM-CSF domain of both fusion proteins was based on a partial Lewis rat mRNA sequence (accession number U00620) that encoded the mature rat cytokine, but not the rat signal sequence. The signal sequence of mouse GM-CSF was inserted by standard PCR cloning procedures, prior to my joining the laboratory, in order to ensure proper processing and secretion of the fusion protein. The rat GM-CSF signal sequence, made available later, contained an AGT-TTC sequence that encoded S^{15}-F^{16}, while the mouse signal sequence contained an AGC-CTC sequence encoding S^{15}-L^{16}. The mouse GM-CSF signal sequence supported efficient expression of rat GM-CSF fusion proteins in Sf9 insect cells, despite the one amino acid sequence difference.

Two M-CSF fusion proteins (MCSF-NAg and M-CSF, Table 2.1) were also used in this study and were based on the Brown Norway rat M-CSF sequence (accession number NM_023981). The N-terminal domain of both fusion proteins contained the 220 amino acid N-terminal domain of M-CSF, which forms the secreted, biologically-active homodimer, and the

26

native rat 33 amino acid M-CSF signal sequence. The M-CSF domain lacked the transmembrane and cytoplasmic domains of full-length M-CSF. The C-terminal domain of the MCSF-NAg fusion protein contained the major encephalitogenic 68-87 epitope of GPMBP plus a 6 his-tag. The C-terminal domain of the M-CSF fusion protein was designed with a 7 his-tag in the absence of the encephalitogenic peptide. These M-CSF fusion proteins lacked the transmembrane and cytoplasmic domains of full-length M-CSF.

Two additional fusion proteins were generated during this experiment, IL6-NAg and IL2-NAg-GFP (Table 2.1). The IL6-NAg fusion protein was designed with the native rat IL-6 signal sequence and the mature rat IL-6 domain (221 amino acids) at the N-terminus. The C-terminus contained the major encephalitogenic 68-87 epitope of GPMBP plus a 6 his-tag. The rat IL-6 domain was based on the Brown Norway rat mRNA sequence (accession number NM_012589). The IL2-NAg-GFP fusion protein was designed with IL2-NAg (Mannie, 2007) at the N-terminus and cycle 3 GFP plus an 8 his-tag at the C-terminus.

Several additional cytokine-NAg fusion proteins (Table 2.1) were used in this study, including IL1RA-NAg, IL2-NAg, IL4-NAg, IL10-NAg, IL13-NAg (63), and IFNβ-NAg (28). These fusion proteins contained the respective rat cytokine as the N-terminal domain linked to a C-terminal domain that included the 73-87 encephalitogenic peptide (P-Q-K-S-Q-R-S-Q-D-E-N-P-V-V-H). The aforementioned fusion proteins had a C-terminal 6 his-tag to facilitate purification. An additional fusion protein, NAgIL-16 (65), was comprised of a N-terminal 7 his-tag, the 69-87 encephalitogenic peptide of MBP, and the rat IL-16 cytokine C-terminus.

Table 2.1: Cytokine-NAg Fusion Constructs		
Name	**N-to C- terminal domain structure**	**Mutations**
GMCSF-NAg	native signal sequence-GMCSF-(GP68-87)-6 his tag	-
MCSF-NAg	native signal sequence-MCSF-(GP68-87)-6 his tag	-
IL1RA-NAg	native signal sequence-IL1RA-EK-(GP73-87)-6 his tag	-
IL2-NAg	native signal sequence-IL2-(GP73-87)-6 his tag	-
IL4-NAg	native signal sequence-IL4-(GP73-87)-6 his tag	-
IL6-NAg	native signal sequence-IL6-(GP68-87)-6 his tag	-
IL10-NAg	native signal sequence-IL10-EK-(GP73-87)-6 his tag	-
IL13-NAg	native signal sequence-IL13-EK-(GP73-87)-6 his tag	-
NAg-IL16	honey bee mellitin signal sequence-7 his tag-(GP69-87)-IL16	-
GM-CSF	native signal sequence-GMCSF-7 his tag	-
M-CSF	native signal sequence-MCSF-7 his tag	-
IL2-NAg-GFP	native signal sequence-IL2-(GP73-87)-GFP-8 his tag	-
<u>Native signal sequence</u>, specific rat cytokine signal sequence; <u>EK</u>, enterokinase linker domain; <u>his</u>, histidine, <u>GP73-87, GP69-87</u>, encephalitogenic sequence of guinea pig myelin basic protein		

2.4 GENERATION OF CYTOKINE - NAg PLASMID CONSTRUCTS

The gene encoding GP68-87 was digested from the Lag3-GP68-87.5.10 pFastBac-1 plasmid using Spe I and Dpn I restriction endonucleases (Invitrogen, Carlsbad, CA.). Dpn I was used to liberate the GP68-87 gene because Dpn I sites flank the gene. Spe I was used to digest the remainder of the pFastBac-1 plasmid at various Spe I sites. The reaction mix included 1.0 μg of Lag3-GP68-87 plasmid, 1.0 unit of Dpn I, 1.0 unit of Spe I, and 1x React Buffer 4 (Invitrogen, Carlsbad, CA.) in a final volume of 10 μl. The digestion was performed at 37°C for 6 hours followed by heat inactivation of the enzymes at 75°C for 20 minutes. Concentration of the DNA was determined by absorbance at 260 nm {absorbance x 50 (μg / ml) / absorbance x dilution factor}.

GP68-87 was fused to the GM-CSF, M-CSF and IL-6 genes by a two step, overlap and extension polymerase chain reaction. In step 1, GP68-87 was amplified from the Lag3-GP68-87 digest using fusion primers (Invitrogen Custom Primers, Carlsbad, CA.) with specificity to the GM-CSF, M-CSF or IL-6 sequences and / or GP68-87 (Table 2.2). The upstream GMCSF-NAg

primer 19F02 encoded for 10 amino acids of the rat GM-CSF C-terminus (single underlined) and 8 amino acids of the GP68-87 N-terminus. The downstream GMCSF-NAg primer 17H03 consisted of a CTT buffer sequence, a Kpn I restriction enzyme site (double underlined), a stop codon, a 6 histidine sequence (bold) and the sequence encoding 7 amino acids of the GP68-87 C-terminus. The upstream MCSF-NAg primer 19F04 encoded for 10 amino acids of the rat M-CSF C-terminus (single underlined) and 8 amino acids of the GP68-87 N-terminus. The upstream IL6-NAg primer 19F03 encoded for 10 amino acids of the rat IL-6 C-terminus (single underlined) and 8 amino acids of the GP68-87 N-terminus. The downstream primers for MCSF-NAg 17H01 and IL6-NAg primer 17H02 were identical to the downstream GMCSF-NAg primer 17H03. The PCR mix included 1.0 nM of the Lag3-GP68-87 digest, 0.5 µM of the forward primer (19F02, 19F03, 19F04), 0.5 µM of the reverse primer (17H01, 17H02, 17H03), 1.0 mM MgSO$_4$, 0.3 mM dNTP, sterile molecular grade water, 1.3 units Platinum *Pfx* DNA polymerase, and 1x *Pfx* amplification buffer (Invitrogen) in a final volume of 50 µL. The molar concentration of DNA used in the restriction digest was determined for future use with PCR {(µg / µL) x (10^6 µL / L) x 1 µmole / (# base pairs x 660 µg)}. Thermocycler (Bio-Rad, Hercules, CA.) conditions for the amplification of GP68-87 included an initial denaturation step of 95°C for 3 minutes, followed by an amplification cycle of 30 seconds at 95°C, 30 seconds at 59°C, and 30 seconds at 68°C for 30 cycles, followed by an extension step of 68°C for 10 minutes. Platinum *Pfx* DNA polymerase provided a hot start reaction due to the presence of an antibody bound to the polymerase, which was released during a 94°C denaturation step.

In the second PCR step, the amplified GP68-87 products served as extension primers to covalently link GP68-87 to GM-CSF, M-CSF, or IL-6. The amplicons encoded the specific cytokine sequence provided by the GM-CSF (19F04), M-CSF (19F02), or IL-6 (19F03) primers,

the entire NAg domain, histidine tag, stop codon, Kpn I restriction enzyme site, and CTT buffer sequence. The GP68-87 amplicons served as extension primers due to their ability to overlap the cytokine sequences encoded by pFastBac-1 plasmids. The PCR mix included 300 ng to 450 ng of plasmid template, 10 μL of the respective GP68-87 amplicon, 1.0 mM MgSO$_4$, 0.3 mM dNTP, sterile molecular grade water, 1.3 units Platinum *Pfx* DNA polymerase, and 1x *Pfx* amplification buffer (Invitrogen, Carlsbad, CA.) in a final volume of 50 μL. The PCR Enhancer solution (Invitrogen) was additionally used in the IL-6 extension reaction at a final 1x concentration to aid this problematic extension reaction.   Thermocycler conditions for the extension reaction included an initial denaturation step of 94°C for 3 minutes, followed by an amplification cycle of 1 minute at 94°C, 30 seconds at 60°C, and 7 minutes at 68°C for 39 cycles, followed by an extension step of 68°C for 10 minutes.   Concentrations of the pFastBac-1 plasmids were determined by absorbance at 260 nm.

2.5 GENERATION OF THE IL2 - NAg - GFP PLASMID CONSTRUCT

In order understand the mechanism of cytokine targeting to APCs, we proposed to detect localization of the cytokine-NAg fusion proteins to particular APC subsets by means of flow cytometry. We designed cytokine-NAg fusion proteins with a GFP tag to facilitate detection by flow cytometry.   The cycle 3 GFP domain was provided by the pcDNA-DEST53 vector (Invitrogen, Carlsbad, CA.).   GFP was fused to IL2Ekdel.1 (IL2-NAg) by a two step, overlap and extension polymerase chain reaction.   In step 1, GFP was amplified from the TorA3D5scFvGFP.6 pFastBac-1 plasmid using fusion primers (Invitrogen Custom Primers, Carlsbad, CA.) with specificity to the sequences encoding GFP and / or NAg (Table 2.2).   The upstream NAg-GFP primer (2850) encoded for 11 amino acids of the GP73-87 C-terminus (no

underline) and 9 amino acids of the GFP N-terminus (single underline). The downstream NAg-GFP primer (2852) consisted of a sequence that complimented 6 amino acids of the pFASTBac-1 plasmid, a stop codon, a sequence that complimented the 8 his-tag (bold), and a sequence that complimented 8 amino acids at the GFP C-terminus (single underline). The PCR mix included 0.7 nM of the TorA3D5scFv-GFP.6 pFASTBac-1 plasmid, 0.5 μM of the forward primer (2850), 0.5 μM of the reverse primer (2852), 1.0 mM $MgSO_4$, 0.3 mM dNTP, sterile molecular grade water, 1.3 units Platinum *Pfx* DNA polymerase, and 1x *Pfx* amplification buffer (Invitrogen, Carlsbad, CA.) in a final volume of 50 μL. The thermocycler conditions for the amplification of GFP included an initial denaturation step of $95^{o}C$ for 3 minutes, followed by an amplification cycle of 30 seconds at $95^{o}C$, 30 seconds at $59^{o}C$, and 30 seconds at $68^{o}C$ for 30 cycles, followed by an extension step of $68^{o}C$ for 10 minutes.

In step 2, the amplified GFP product served as the extension primer to covalently link GFP to IL2-NAg. The amplicon encoded the C-terminus of GP73-87, the entire GFP domain, the histidine tag, stop codon, and a portion of the pFastBac-1 sequence. The PCR mix included 1 μL of IL2-NAg plasmid template, 5 μL of the respective GFP amplicon, 1.0 mM $MgSO_4$, 0.3 mM dNTP, sterile molecular grade water, 1.3 units Platinum *Pfx* DNA polymerase, 1x *Pfx* amplification buffer (Invitrogen), and 1x PCR Enhancer solution in a final volume of 50 μL. Thermocycler conditions for the extension reaction included an initial denaturation step of $94^{o}C$ for 3 minutes, followed by an amplification cycle of 1 minute at $94^{o}C$, 30 seconds at $60^{o}C$, and 7 minutes at $68^{o}C$ for 39 cycles, followed by an extension step of $68^{o}C$ for 10 minutes.

Table 2.2: Primer Design	
Primer Name	**Primer Sequence 5' – 3'**
pFastBac (8B08)	TATTCCGGATTATTCATACC
pFastBac (56E12)	TGTGGTATGGCTGATTATGATCCTC
GMCSF-NAg (19F02)	<u>CCTTTTGACTGCTGGAAGCCGGTCCAGAAA</u>/TATGGCTCCCTGCCCCAGAAGTCG
GMCSF-NAg (17H01)	CTT<u>GGTACC</u>TTA**GTGATGGTGATGGTGATG**/GTGGACTACAGGGTTTTCATC
MCSF-NAg (19F04)	<u>GAGGACCCAGGCAGTGCTAAGCAGCGACCG</u>/TATGGCTCCCTGCCCCAGAAGTCG
MCSF-NAg (17H03)	CTT<u>GGTACC</u>TTA**GTGATGGTGATGGTGATG**/GTGGACTACAGGGTTTTCATC
IL6-NAg (19F03)	<u>AAGGTCACTATGAGGTCTACTCGGCAAACC</u>/TATGGCTCCCTGCCCCAGAAGTCG
IL6-NAg (17H02)	CTT<u>GGTACC</u>TTA**GTGATGGTGATGGTGATG**/GTGGACTACAGGGTTTTCATC
NAg-GFP (2850)	CAGCGGTCCCAAGATGAAAACCCTGTAGTCCAC<u>ATGGCCAGCAAAGGAGAAGAACTTTTC</u>
NAg-GFP (2852)	CGACAAGCTTGGTACCTTA**GTGATGGTGATGGTGATGGTGATG**<u>TTTGTAGAGCTCATCCATGCCATG</u>

Single underlined sequences highlighted respective cytokine or GFP domains. Restriction enzyme sites are accentuated by a double underline. Bold sequences encoded for histidine residues.

2.6 PURIFICATION AND SEQUENCING OF CYTOKINE-NAg CONSTRUCTS

Parental plasmids (GM-CSF, M-CSF, IL-6, and IL2-NAg pFastBac-1) were digested from the GMCSF-NAg, MCSF-NAg, IL6-NAg, and IL2-NAg-GFP extension products with the Dpn I restriction enzyme in Buffer 4 (Invitrogen, Carlsbad, CA.). First, MicroCon YM100 Centrifugal Filter Devices (Millipore, Billerica, MA.) were used to wash the extension reactions in sterile molecular grade water according to manufacturer's instructions. MicroCon YM100 were used to remove salt and small molecular weight fragments; the devices had a 125 base pair cut off for double-stranded DNA and a 100 kDa cut off for proteins. Desalting the extension reactions was necessary to prepare the DNA for restriction enzyme digestion. The restriction enzyme digest contained 2 units of Dpn I, Buffer 4 (diluted 1 / 10) and 1.0 – 5.0 µg DNA from the extension reaction. Parental DNA was digested for 6 hours at 37°C, followed by a heat inactivation of Dpn I at 75°C for 20 minutes. Parental DNA was digested in order to increase transformation efficiency of the pFastBac-1 plasmids encoding GMCSF-NAg, MCSF-NAg, IL6-NAg, and IL2-NAg-GFP. Plasmid DNA was transformed into electrocompetent Top10 *E. coli* (Invitrogen) by means of the Micropulser Electroporator (BioRad, Hercules, CA.). 2 µL of the restriction enzyme digest was mixed with 40 µL of Top 10 *E. coli* and then subjected to a 1.8 kilovolt pulse. Immediately after electroporation, *E. coli* were mixed with 500 µL of S.O.C. media (super optimal broth with catabolite repression) {2% w / v bacto-tryptone, 0.5% w / v bacto-yeast extract, 10 mM NaCl, 2.5 mM KCl, 10 mM MgCl, 20 mM glucose, pH 7.0} and then cultured at 37°C with agitation for 1 hour. Bacterial cultures were subsequently diluted and cultured on LB - ampicillin plates {200 µg / mL ampicillin in Luria – Bertani broth} at 37°C for 24 hours. Transformants were selected in ampicillin because pFastBac-1 encodes for β-lactamase, an enzyme that can hydrolyze and inactivate β-lactam antibiotics such as ampicillin.

Colonies selected in the presence of ampicillin were PCR screened for the respective cytokine-NAg fusion construct. First, individual colonies were grown in a 100 µL mini-culture of LB – ampicillin at 37°C for 4 hours. The culture was generated to provide a crude template for the PCR screening. The PCR mix included 2.5 µL of culture, 0.5 µM of the reverse primer 17H03 (NAg - plasmid specific) or 2852 (GFP - plasmid specific), 0.5 µM of the forward primer 19F02 (GM-CSF specific), 19F03 (IL-6 specific), 19F04 (M-CSF specific), or 2850 (NAg-GFP specific), 1.5 mM MgCl$_2$, 0.2 mM dNTP, sterile molecular grade water, 1.5 units Platinum Taq DNA polymerase, and 1x PCR buffer (Invitrogen) in a final volume of 50 µL. Thermocycler conditions included an initial denaturation step of 94°C for 2 minutes, followed by an amplification cycle of 30 seconds at 94°C, 30 seconds at 62°C, and 30 seconds at 72°C for 39 cycles, followed by an extension step of 72°C for 10 minutes.

The 100 µL mini-cultures were also used to inoculate cultures for the isolation of plasmid DNA. 10 µL of the mini-culture was used to inoculate a 3 mL LB – ampicillin culture. The Marligen MiniPrep Kit (Marligen, Rockville, MD.) was used to lyse *E. coli* {200 mM NaOH, 1% SDS, 20mg / ml Rnase A} and purify plasmid DNA according to manufacturer instructions. Absorbance at 260 nm was used to determine the concentration of plasmid DNA {absorbance x 50 (µg / ml) / absorbance x dilution factor}. Plasmids (1.0 – 3.0 µg) were sequenced at the Genomics Core Facility (East Carolina University, Greenville, NC.). The sequencing primers 8B08 (forward primer) and 56E12 (reverse primer) were complimentary to sites on the pFastBac-1 plasmid that flanked the cytokine-NAg construct. Sequencing primers were used at a concentration of 5.0 µM.

2.7 PROTEIN EXPRESSION AND PLAQUE PURIFICATION OF BACULOVIRUS

Recombinant proteins were expressed by means of Bac-to-Bac baculovirus expression systems (Invitrogen, Carlsbad, CA.). Ultimately the cytokine constructs were translocated from pFastBac-1 plasmids into a baculovirus (bacmid) shuttle vector. Baculovirus encoding the designated constructs were used to infect Sf9 cells (Spodoptera frugiperda army worm). Sf9 cells expressed and secreted fusion proteins into the culture media such that the proteins were readily available for purification by affinity chromatography.

In the first step, purified pFastBac-1 plasmids were transformed into electrocompetent DH10Bac *E. coli* to facilitate site-specific transposition of the fusion constructs into the baculoviral vector. Plasmids encoding GMCSF-NAg, MCSF-NAg, IL6-NAg, and IL2-NAg-GFP were transformed into electrocompetent DH10Bac *E. coli* by means of the Micropulser Electroporator (BioRad, Hercules, CA.). 2 μL of the purified plasmid were mixed with 40 μL of DH10Bac *E. coli* and then subjected to a 1.8 kilovolt pulse. Immediately after electroporation, *E. coli* were mixed with 500 μL of S.O.C. (super optimal broth with catabolite repression) media and then cultured at 37°C with agitation for 1 hour. Cultures were subsequently diluted and cultured on LB Select plates {10 μg / mL tetracycline, 50 μg / mL kanamycin, 7 μg / mL gentamicin, 100 μg / mL Bluo-Gal, and 40 μg / mL IPTG, in Luria – Bertani broth} at 37°C for 24 hours. Transformants were selected on LB Select plates because of the antibiotic resistance genes carried by the transformed DH10Bac. The pFastBac-1 plasmid encoded for gentamicin resistance, the bacmid plasmid (bMON14272) encoded for kanamycin resistance and the helper plamid (pMON7124) encoded the transposase and tetracycline resistance genes.

Site-specific transposition was mediated by the Tn7 transposase (DDE transposase) encoded within the helper plasmid. Tn7 translocated cytokine constructs from the pFastBac

plasmid to the bacmid DNA via a cut and paste mechanism. The cytokine construct (i.e., the transposon) was flanked by the inverted repeats Tn7R and Tn7L, which were recognized and cut by the Tn7 transposase generating a linear, excised transposon. Tn7 facilitated the insertion of the cytokine construct into the bacmid vector between two staggered nicks at the mini-attTn7 site (Curcio, 2003). The mini-attTn7 site was positioned within the gene encoding LacZα. Transposition at the mini-attTn7 site lead to disruption of the lacZα gene resulting in the lack of β-galactosidase (a tetramer of two LacZα and LacZΩ proteins). β-galactosidase activity was visualized as a blue colony that resulted form the cleavage of Bluo-gal into galactose and an insoluble blue product. Bluo-gal cleavage was possible only in the presence of IPTG, which repressed the constitutively active LacZ repressor (LacI). Transposition was indicated by the presence of white colonies on the LB Select plates. White colonies were cultured in order to purify bacmid plasmid DNA. In the case of IL6-NAg and IL2-NAg-GFP, white colonies were additionally PCR screened for the presence of cytokine constructs as discussed previously.

DH10Bac bacmid DNA was purified according to the Bac-to-Bac Baculovirus Expression System (Invitrogen) protocol. Briefly, white colonies were cultured in 5 mL of LB Select media (in the absence of Bluo-Gal and IPTG) overnight at 37°C with agitation. Cultures were lysed in a solution containing 15 mM Tris-HCl (pH 8.0), 10 mM EDTA, 100 μg / ml RNase A, 1% SDS, and 0.2 N NaOH. Proteins in the lysate were precipitated with 3 M potassium acetate (pH 5.5). The soluble DNA fraction was removed from the protein and precipitated in isopropanol. The DNA pellet was washed in 70% ethanol and ultimately resuspended in sterile molecular grade water. DNA concentrations were determined by spectrophotometry at 260 nm.

Purified bacmid DNA was transiently transfected into Sf9 insect cells according to manufacturer's instructions. Briefly, 5 μL of bacmid DNA was mixed with 100 μL of SFM (Invitrogen, Carlsbad, CA.) and immediately combined with a mixture of 6 μL CellFectin Reagent (lipid suspension) plus 100 μL of SFX. The DNA-lipid mixture was added to 1×10^6 Sf9 cells and incubated for 5 hours at 27°C. After the incubation, the media was changed and Sf9 cultures were monitored for signs of baculovirus infection. Bacmid DNA encoded viral particles that would establish a visible infection throughout the Sf9 culture in 3-7 days.

Single viruses were isolated by limiting dilution of baculovirus (i.e., plaque purification) stock from the Sf9 transfection supernatant. Sf9 insect cells (10^4 cells / well) were infected with a limiting dilution of baculovirus (10^{-5} - 10^{-8}) in SFM. On day 9 of infection, supernatants from individual wells were tested to determine the biological activity of the fusion proteins encoded by individual baculoviruses. Biological activity of the NAg domain was tested using an assay comprised of irradiated splenic APC (5×10^5 cells / well), NAg-specific RsL.11 T cells (2.5×10^4 cells / well), cRPMI, and supernatant from wells of the Sf9 plaque purification. Cultures were pulsed with [^{3}H]thymidine (1 μCi / well, Perkin Elmer, Waltham, MA.) on day 2 of a 3-day culture in order to quantitate RsL.11 proliferation. [^{3}H]thymidine incorporation into DNA was measured by use of a Wallac 1450 Microbeta Plus liquid scintillation counter. M-CSF and GM-CSF cytokine activity was assessed through a bioassay comprised of peritoneal exudate cells (4×10^3 cells / well), cRPMI, and supernatant from the wells of the Sf9 plaque purification. 10 days later, cultures were pulsed with 10 μL of MTS / PMS (Promega, Madison, WI) for at least 6 hours. Reduction of MTS by dehydrogenase in metabolically active cells generates an insoluble formazan product that can be quantitated at 490 nm. GFP fluorescence of IL2-NAg-GFP

infected Sf9 cells was detected by flow cytometry seven days post-transfection. GFP fluorescence was excited at 488 nm and detected with the FITC filter set at 530 nm.

2.8 PROTEIN EXPRESSION AND PURIFICATION

Individual baculoviruses encoding for M-CSF, GM-CSF, MCSF-NAg, GMCSF-NAg, IL6-NAg, and IL2-NAg-GFP were expanded in order to generate viral stocks for protein expression. Baculovirus from transfection supernatants (10 µL) were expanded in Sf9 cells (10 x 10^6) cultured in 20 mL of SFM plus 5 % heat inactivated newborn calf serum for seven days. Only 10 µL were expanded so as to prevent the expansion of replication defective virus particles. Supernatant and cells were harvested and frozen at -25°C until used in protein expression cultures. Proteins were expressed in 4-day cultures of Sf9 cells (40 x 10^6) plus 1.0 mL of the respective baculovirus expansion supernatant in 20 mL of SFM. After 4 days, supernatant and cells were harvested and cells were clarified from the supernatant by centrifugation (1000 rpm x 8 minutes). Clarified supernatants were stored at -25°C until they were processed for protein purification.

Proteins in the clarified supernatant were concentrated to an approximate 20 mL volume in pressurized Amicon Stir Cells (Millipore, Billerica, MA.). A YM10 Ultrafiltration Membrane (Millipore) with a cut off of 10,000 kDa was used, during concentration, to remove low molecular weight proteins. The sizes of the recombinant proteins were between 15.4 to 55.1 kDa. Protein concentrates were hard spun (3,000 rpm for 20 minutes) and sterile filtered with 0.22 µm bottle top filter in order to remove insoluble material.

GM-CSF, M-CSF, GMCSF-NAg, MCSF-NAg, and IL2-NAg-GFP were purified via two affinity chromatography steps using resins with specificity for the C-terminal his-tag. Proteins

were initially purified with a chitin column composed of an anti-histidine monoclonal antibody (scFv, single chain variable domain) that was immobilized on chitin beads (New England BioLabs, Ipswich, MA.). The monoclonal antibody (see below) was a recombinant protein comprised of an N-terminal scFv monoclonal antibody domain ($V_H + V_L$) fused by a linker to two, tandem chitin-binding domains (CBD) at the C-terminus (Blank 2002). Chitin columns were washed with 8.0 mL TBST buffer {50 mM Tris-HCl (pH 8.0), 1M NaCl, 0.1 mM EDTA, 1% Triton X} and equilibrated with 8.0 mL MBS buffer {20 mM MES, 500 mM NaCl, 0.1 mM EDTA, pH 6.5} prior to the addition of the sterile filtered protein concentrate. Following the addition of concentrate, the column was washed with 12.0 mL MBS buffer. Proteins were subsequently eluted from the column in a 4 mL fraction with CAPS elution buffer {50 mM CAPS, 500 mM NaCl, 500 mM EDTA, pH 10.0}. Proteins were eluted from the chitin column under basic pH in order to disrupt the noncovalent bonds between the antibody and C-terminal histidine tag.

The scFv-CBD fusion protein was encoded by the *E. coli* K12 strain SB536 transformed with the pKB2scFvCBD plasmid (a generous gift from the laboratory of Dr. Andreas Pluckthun). SB536 were cultured in 3 mL of SB media {20 g / L tryptone, 10 g / L yeast extract, 5 g / L NaCl, 50 mM K_2HPO_4} plus 30 μg / mL chloramphenicol at 37°C with agitation. Expression of scFv-CBD was induced with 1 mM IPTG when bacteria reached an optical density of 1.5 at 550 nm. Protein expression occurred over 3 hours before cultures were harvested (5,500 rpm for 15 minutes at 4°C) and bacterial pellets resuspended in TBST (1.0 mL / 1.0 gram pellet weight). Bacteria were subsequently lysed in order to liberate the scFv-CBD fusion proteins. Bacterial pellets were first treated with PMSF {100 mM PMSF in DMSO} and DNase I {1 mg / mL in glycerol}. PMSF (Sigma-Aldrich, St. Louis, MO.) is a serine protease inhibitor required to

reduce protein lysis and DNase I (Roche Diagnostics, Palo Alto, CA.) was required to reduce viscosity, resulting from the liberated DNA, of the bacterial lysates. Bacterial lysates were generated by French press lysis at 10,000 psi. Insoluble material was removed in two steps, centrifugation (11,000 rpm for 30 minutes) at 4°C and sterile filtration with a 0.22 μm bottle top filter. Sterile filtered lysates were incubated with chitin beads overnight at 4°C with agitation. Chitin beads plus scFv-CBD were moved to a BioRad PolyPrep column (BioRad, Hercules, CA.), washed in TBST and stored in a TBST plus 0.02% NaN$_3$ buffer.

After elution from the chitin column, GM-CSF, M-CSF, GMCSF-NAg, and MCSF-NAg (not IL2-NAg-GFP) were subjected to a final affinity chromatography step using Ni-NTA agarose columns (Qiagen, Valencia, CA.). The Ni-NTA agarose binds with high affinity to the imidazole ring in each residue of the 6 his-tag. The nickel ion can simultaneously bind two imidazole rings. Ni-NTA columns were equilibrated with 10.0 mL wash buffer {50 mM NaH$_2$PO$_4$ (monobasic and anhydrous), 500 mM NaCl, 10.0 mM imidazole, pH 8.0} before the addition of the chitin elution fraction. Low levels of imidazole were added to the wash buffer in order to reduce / disrupt non-specific binding of native proteins comprised of random histidine residues. Following the addition of the chitin elute, the Ni-NTA column was washed with 8.0 mL wash buffer and protein was subsequently eluted in 6 x 1.0 mL fractions with IMAC elution buffer {50 mM NaH$_2$PO$_4$ (monobasic and anhydrous), 500 mM NaCl, 250 mM imidazole, pH 8.0}. Proteins were eluted in the presence of a high imidazole concentration in order to compete away fusion proteins with a histidine tag.

Protein purity was shown by SDS-PAGE. Ni-NTA elution fractions (10.0 μL) were diluted 1:2 in loading buffer {100 mM Tris-HCl, 4% SDS, 0.2% bromophenol blue, 20% glycerol, 200 mM beta-mercaptoethanol} before being denatured at 95°C for 5 minutes. After

heat denaturation, the samples were added to SDS-PAGE gels with a 5% stacking layer and a resolving gel that ranged from 10% - 15% acrylamide, depending on the respective protein size. Gels were made with the following reagent stocks, 30% bisacrylamide, Tris-HCl (pH 6.8 or 8.8), 10% SDS, 10% ammonium persulfate, TEMED, and MilliQ water. The Benchmark Pre-stained protein ladder (Invitrogen, Carlsbad, CA.) was loaded as a molecular weight standard. Samples were run through the stacking gel at approximately 15 milliamps until the samples were stacked on top of the resolving gel. Protein was run through the resolving gel at approximately 22 milliamps. Gels were subsequently fixed in a solution of 50% methanol and 8% acetic acid for 30 minutes before being washed and stained overnight in Gel Code Blue Stain Reagent (Thermo-Fisher Scientific, Rockford, IL.), a coomassie-based dye. After excess Gel Code was removed, the gel was incubate in storage buffer {10% glycerol and 20% ethanol in water} for 30 minutes before sealing the gel in cellophane (Research Products International, Mount Prospect, IL.) for long term storage.

Ni-NTA protein elution fractions were concentrated (3690 rpm for 35 minutes) and then diafiltrated (sterile MilliQ water: IL6-NAg, MCSF-NAg, and M-CSF or sterile PBS: GMCSF-NAg and GM-CSF) in Amicon Ultra-15 centrifugal filter devices (Millipore, Billerica, MA.). Proteins were diafiltrated at least 3 times in order to dilute the total imidazole concentration to less than 0.05 mM. Imidazole was diluted to circumvent an immune response against imidazole contaminants in our protein preparations. IL2-NAg-GFP was concentrated in chitin elution buffer and not diafiltrated because this fusion protein was to be used for diagnostic purposes only.

Total purified protein was quantified via BCA (bicinchoninic acid) assay (Thermo-Fisher Scientific, Rockford, IL.) or absorbance at 280 nm. The BCA assay took advantage of the Cu

41

(II) ion to deprotonate peptide bonds and generate a Cu (I) ion complex under alkaline conditions. Cu (I) could then be bound by two molecules of BCA resulting in a colored product that could be detected at 560nm. A standard curve was used to assess the concentration of our protein samples. The BSA standard was serially diluted from 1124 μg / mL to 11 μg / mL by a factor of 1.78. The mixed BCA solution was added at 200 μL / well to the standard curve and the protein samples before being incubated at $37^{\circ}C$ for 30 minutes. The BCA solution was mixed at a ratio of 50:1 Reagent A (BCA in an alkaline solution): Reagent B (cupric sulfate). Optical density was read at 562 nm using the Ultraspec 2000 spectrophotometer (Pharmacia Biotech). The standard curve was plotted and the linear portion of the curve was used to obtain the concentration of our protein samples. As an alternative to the BCA assay, protein concentrations were determined by absorbance {A_{280} x absorbance coefficient (mg / mL)} using the NanoDrop ND 1000 spectrophotometer (NanoDrop Technologies, Wilmington, DE.).

2.9 MYELOID, B CELL AND NK CELL APC

Bone marrow cells were obtained from the tibias and femurs of Lewis rats in order to isolate myeloid-derived DC or macrophages. An 18G needle filled with Hanks Buffered Saline Solution {HBSS (Sigma-Aldrich) plus 0.35 g $NaHCO_3$, pH 7.4} was used to liberate and break up the bone marrow. Cells were washed two times in HBSS (1,000 rpm for 10 minutes) and insoluble material was removed. Bone marrow cells were cultured in cRPMI in the presence or absence of 0.1% v / v GM-CSF or M-CSF baculovirus supernatant or 50 nM of purified GMCSF-NAg or MCSF-NAg for at least 7 days. Fresh media and cytokine supplements were added after 3 days of culture. Adherent populations were detached from plastic surfaces by

incubation in 3 mM EDTA-HBSS and were used as a source of dendritic cells or macrophages. Enriched cells were either used as APC in bioassays or analyzed by flow cytometry.

Cell surface markers for the dendritic cell and macrophage derived lines were analyzed by flow cytometry. Cells (1×10^5 cells / tube) were initially incubated with 5% heat inactivated normal rat serum for 20 minutes at 4^oC in order to block Fc receptors. Afterward, cells were stained with the respective primary antibody at 4^oC for 45 minutes. Cells were stained with the following primary antibody combinations: anti-CDllc (2.5 μg / mL) alone, no primary antibody, or anti-CDllc in combination with purified monoclonal antibodies anti-B7.1 (2.5 μg / mL) and anti-B7.2 (2.5 μg / mL), or anti-CDllc in combination with OX-1, OX-6, OX-8, or W3 / 25 hybridoma supernatant diluted 1:20. Cells were washed twice in HBSS-1% fetal bovine serum and then blocked with 5% heat inactivated normal rat serum prior to the addition of secondary antibodies. FITC conjugated anti-IgG1 (2.5 μg / mL) and PE conjugated anti-IgG2a (2.5 μg / mL) secondary antibodies were incubate with the cells for 45 minutes at 4^oC and then washed twice prior to analysis by flow cytometry. All washes were performed at 4^oC. Data were acquired with a Becton Dickinson FACScan (San Jose, CA) flow cytometer and analyzed with CellQuest software. Dead cells were excluded by forward versus side scatter profiles. All experimental conditions were compared to isotype control, i.e., cells that were incubated with secondary but not primary antibody.

OX33$^+$ or OX33$^+$Ig$^+$ B cell APC were purified from Lewis rat splenocytes by fluorescence activated cell sorting. The spleen was harvested and made into a single cell suspension by passing the organ through a wire mesh. Red blood cells were removed using density gradient centrifugation (Histopaque, Sigma-Aldrich). Cells (100×10^6) were washed two times in HBSS (1,000 rpm for 10 minutes) and then blocked with 5% heat inactivated normal rat

serum. Cells were labeled with the primary antibody OX-33 (1:200 dilution of hybridoma supernatant) for 45 minutes at 4°C. Cells were then washed 2 times in HBSS-1% fetal bovine serum prior to incubation with the secondary antibodies FITC-conjugated goat anti-mouse IgG1 (2.5 μg / mL) and / or R-PE conjugated goat anti-rat IgG + IgM (H+L) (2.5 μg / mL) for 45 minutes at 4°C. Cells were then washed twice prior to sorting with Beckton Dickinson FACSVantage flow cytometer (San Jose, CA). Purified B cells were greater than 95% pure. Dead cells were excluded from the sort by forward versus side scatter patterns.

NK cells were purified from Lewis rat splenocytes. The spleen was made into a single cell suspension by passing the spleen through a wire mesh. Red blood cells were removed using density gradient centrifugation. Cells (40×10^6) were washed two times in HBSS (1,000 rpm for 10 minutes) and then blocked with 5% heat inactivated normal rat serum. Cells were labeled with primary antibodies anti-CD161a (2.5 μg / mL) and anti-CD3 (2.5 μg / mL) for 45 minutes at 4°C. CD161 is a marker for NK cells and T cells, therefore anti-CD3 was used to distinguish T cells from NK cells. Cells were washed twice in HBSS-1% fetal bovine serum and then blocked with 5% heat inactivated normal rat serum before the addition of secondary antibodies. Cells were stained with 2.5 μg / mL of the secondary antibodies RPE-conjugated goat anti-mouse IgG1 and FITC conjugated goat anti-rat IgG3 for 45 minutes at 4°C. Cells were washed twice with HBSS-1% fetal bovine serum prior to sorting with Beckton Dickinson FACSVantage flow cytometer (San Jose, CA). Purified NK cells were greater than 96% pure. Dead cells were excluded from the sort by forward versus side scatter patterns.

2.10 MEASUREMENT OF CYTOKINE SPECIFIC RESPONSES

Biological activities of the GM-CSF, M-CSF, GMCSF-NAg, MCSF-NAg, and IL6-NAg cytokine domains were tested with specific indicator cells. Biological activity of the GM-CSF and M-CSF domains were assessed with Lewis rat bone marrow cells (10^5 cells / well) or splenocytes (5×10^5 cells / well) plus designated concentrations of purified protein (100 nM – 10 fM) or baculovirus supernatant (10^{-2} - 10^{-7}). Bone marrow and splenocytes were harvested and directly added to bioassay wells. Each data point was performed in triplicate or quadruplicate. Cultures were pulsed with [^{3}H]thymidine (1 μCi / well, Perkin Elmer, Waltham, MA.) on day 2 of a 3-day culture. Cultures were harvested onto filters by use of a Tomtec Mach III harvester and [^{3}H]thymidine incorporation into DNA was measured with the Wallac 1450 Microbeta Plus liquid scintillation counter. These data were representative of at least two experiments. IL-6 specific T1165 hybridoma cells (10^4 cells / well) were cultured with serially diluted IL6-NAg baculoviral supernatants (10^{-2} - 10^{-8}). Each data point was performed in triplicate. This experiment was performed once. IL-2 specific CTLL indicator cells (10^4 cells / well) were cultured with purified IL2-NAg-GFP or IL2-NAg titrated on a log scale from 100 nM – 10 fM. This experiment was performed once an each data point was performed in triplicate. Cultures were pulsed with MTS / PMS after 48 hours and MTS reduction was quantitated by spectrophotometry at 492 nm.

2.11 MEASUREMENT OF NEUROANTIGEN-SPECIFIC RESPONSES

Biological activity of the NAg domain was measured by antigenic proliferation of NAg specific T cell clone (RsL.11). To measure antigen-specific proliferation, RsL.11 T cell responders (2.5×10^4 / well) were cultured with irradiated splenic APC (3000 rads, 2.5×10^5 /

well), myeloid APC (1.5 x 10^4 / well), or purified B cells (2.5 x 10^5 / well) in the presence of designated antigen concentrations. Cultures were pulsed with 1 μCi / well of [^{3}H]thymidine (Perkin Elmer, Waltham, MA.) during the last 24 hours of a 3-day culture. Cells were harvested onto filter mats and DNA incorporation of [^{3}H]thymidine was measured by a scintillation counter. IL-2 production by RsL.11 T cells was measured after 24 hours of culture in the aforementioned conditions. 24 hour supernatants (20 μl) were incubated with the IL-2 dependent T cell clone CTLL. IL-2 bioactivity was measured by the ability of the supernatant to support the viability and growth of CTLL cells over 3 days. Prior to the set up of the IL-2 bioassays, CTLL cells were washed 2 times in HBSS (1,000 rpm x 8 minutes). Cultures were pulsed with 10 μL of MTS / PMS (Promega, Madison, WI) on day 2 of the 3-day culture. CTLL viability was measured by the reduction of MTS / PMS (Promega, Madison, WI) into a colored product that was measured at 290 nm. Error bars represented standard deviations of triplicate sets of wells.

RsL.11 responses in the presence of T cell APC were measured by a T cell killing assay. In this assay, T cell APC (R1T) that presented NAg on MHC II were killed by RsL.11 T cells (Mannie, 2007). Prior to assay setup, R1T cells were cultured for 24 hours in complete RPMI (without IL-2) to allow the clearance of IL-2 from cell surface receptors. This was necessary to allow binding of IL2-NAg to IL-2 receptors without hindrance. R1T cells (2.5 x 10^4 / well) were then cultured with irradiated (1,000 rads; 5.0 x 10^4 / well) RsL.11 T cells in the presence of designated concentrations of antigen. After 4 hours of culture, IL-2 (0.4% v / v IL-2 baculovirus supernatant) was added to all wells because this assay measured IL-2 dependent proliferation of R1T cells unless they were killed by irradiated RsL.11 responders (71). In the absence of IL-2, R1T would die independently of RsL.11 mediated killing. Cultures were pulsed with

46

[^{3}H]thymidine on day 2 of a 3-day culture. Cells were harvested and DNA incorporation of [^{3}H]thymidine was measured by a scintillation counter. Error bars represented standard deviations of triplicate sets of wells.

Sorted CD161$^+$CD3$^-$ NK cells (96% pure population; 4.3×10^4 / well) were cultured with 100nM of designated fusion proteins (IL4-NAg was mistakenly added at 230 nM) for 72 hours. Next, RsL.11 T cells (5×10^4 cells / well) were stained with 1 μM CFSE (Invitrogen, Carlsbad, CA.) at 37°C for 15 minutes plus agitation. CFSE stained RsL.11 were washed and subsequently co-cultured with NK cells for an additional 72 hours. RsL.11 antigenic proliferation was measured with a Becton Dickinson FACScan flow cytometer and analyzed with CellQuest software (San Jose, CA.). RsL.11 T cells were stained with CFSE according to the manufacturer's protocol. This experiment was performed one time.

2.12 INDUCTION AND ASSESSMENT OF EAE

EAE was induced in Lewis rats by the subcutaneous injection of an emulsion comprised of 50 μg of DHFR-NAg fusion protein in a total 100 μL volume of Complete Freund's Adjuvant {200 ug of *Mycobacterium tuberculosis* in Incomplete Freund's Adjuvant (Difco, Detroit, MI.)}. Two injections of 50 μl were administered on either side of the base of the tail. DHFR-NAg consisted of an N-terminal mouse dihydrofolate reductase domain and a C-terminal encephalitogenic peptide (GP69-87) domain (63-65). The GM-CSF-based and M-CSF-based fusion proteins were tested for tolerogenic activity by subcutaneous injection in saline without adjuvant according to designated schedules and doses listed in the results section. EAE was monitored by disease severity and weight loss. The following scale was used to score clinical signs of EAE: distal limp tail (0.25), limp tail (0.5), ataxia (1.0), partial hind limb paralysis

47

(2.0), and full hind limb paralysis (3.0). Partial hind limb paralysis was defined as the retention of some voluntary ambulatory movement in the hind limbs without the ability to ambulate upright. Full hind limb paralysis manifested as complete flaccid hind limb paralysis. Weight loss was measured by placing the rats on a Sartorius balance (Goettingen, Germany).

The mean cumulative group score was calculated by summing the daily scores for each rat and then averaging the cumulative scores within a group. The mean maximal group score was calculated by averaging the most severe EAE score for each rat within a group. Weight loss was calculated as a percent daily weight divided by the maximal weight for each rat. The group mean percent weight loss was calculated by averaging the percent weight loss for each rat within a group. Group mean values were reported with the standard deviation. Severe EAE was defined as the incidence of ataxia (A; 1.0), hind-leg paralysis (EP; 2.0) or full hind-limb paralysis (P; 3.0). Compiled data from three replicate experiments (Tables 3.2 and 3.3) were used to assess differences in the mean cumulative score, mean maximal score, and the mean number of days with severe EAE between treatment groups from the three experiments. Significance of the compiled data was analyzed by parametric two-way ANOVA (experiment versus treatment group) based on ranked data. The median cumulative scores and median maximal scores, of the compiled data, were listed as the median values for all rats in a treatment group and significance was measured by nonparametric two-way ANOVA based on ranked data. Differences among treatment groups within one experiment (Table 3.1 and experiment 1 of Table 3.3) were analyzed by one-way parametric ANOVA for the categories of mean cumulative score, mean maximal score, and the mean number of days with severe EAE; the significance of mean cumulative and mean maximal scores were based on ranked data. The median cumulative scores and median maximal scores, of experiment 1 of Table 3.3, were listed as the median values for all rats within

a treatment group. Daily scores and percent weight loss among treatment groups (Figure 3.16) were respectively analyzed by parametric one-way ANOVA. Daily scores and daily percent weight loss (Figures 3.17 and 3.18) were analyzed by nonparametric and parametric two-way ANOVA. ANOVA analyses were analyzed with the Bonferroni Post-Hoc Test. The incidence of severe EAE was analyzed pair-wise with the Fisher's Exact Test. Statistical analyses were performed with SPSS software (Chicago, IL.)

2.13 SERUM REACTIVITY TO NAg

Serum samples were obtained from Lewis rats by a terminal intracardiac puncture at the conclusion of the experiment. Lewis rats were anesthetized with isoflurane during the intracardiac puncture with a 20G1" needle. Rats were immediately euthanized following the terminal bleed. Blood samples were left to clot inside the syringe for at least one hour at room temperature. Serum was removed from the clot and centrifuged (2,000 rpm 15 minutes) to separate residual blood cells. Serum samples were stored at -80°C until analyzed by ELISA.

ELISA were performed to detect serum reactivity to NAg in Lewis rats treated with GMCSF-NAg, GMCSF + NAg, GM-CSF, MCSF-NAg or NAg either before or after encephalitogenic challenge. 5.0 μg / mL of GP69-88 peptide antigen was covalently linked to Nunc Immobilizer Amino plates (Rochester, NY.) in the presence of sodium carbonate buffer {100 mM Na_2CO_3 in MilliO water, pH 9.6} for at least 1 hour at 37°C. Wells were then washed with PBST {PBS plus 0.05% Tween} before diluted serums ($10^{-1} - 10^{-5}$) were added to the plate. Tween was added to the wash in order to block exposed plastic where the peptide did not bind. Next, serum antibodies were incubated with the covalently bound peptide for 2 hours at 37°C. Unbound serum was washed away with PBST before the addition of the secondary antibody goat

anti-rat IgM + IgG (H + L) conjugated to alkaline phosphatase. The secondary antibody (diluted 1:2000 in PBS) was incubated with the primary antibody for 2 hours at 37°C. Wells were washed 3 times with PBS before incubation with the chromophore substrate p-nitrophenylphosphate {3 mM pNPP, 50 mM Na_2CO_3, 0.5 M $MgCl_2$} at room temperature for 1 hour. Color changes were recorded at 405 nm with the Thermo Multiskan Ex plate reader plus Ascent software (Thermo-Fisher Scientific, Rockford, IL.). Statistical analyses were performed with parametric, one-way ANOVA and Bonferroni post-hoc tests.

2.14 SPECIFICITY OF IL2-NAg-GFP

IL2-NAg-GFP was assessed as a flow cytometry tool to detect expression of the IL-2 receptor on the cell surface of splenocytes and purified T cell clones. R1T (1 x 10^5 / well) and BW5147 (1 x 10^5 / well) were plated overnight in a 96 well plate (Corning, Lowell, MA.) in cRPMI. R1T were cultured overnight in cRPMI (without IL-2) in order to empty the IL-2 receptors prior to the addition of IL2-NAg-GFP. The next day, 100 nM of IL2-NAg-GFP were incubated with the cells for one hour at 37°C before analysis by flow cytometry. Cells were not washed after the addition of IL2-NAg-GFP.

When Lewis rat splenocytes were used, the splenocytes were activated with 2.5 mg / ml Concanavalin A (Sigma-Aldrich, St. Louis, MO.) and 10.0 mg / ml lipopolysaccharide (List Biologicals, Campbell, CA.) for 24 hours. Concanavalin A and lipopolysaccharide served as mitogens for T cells and B cells, respectively. Red blood cells were depleted from leukocytes by density centrifugation. After activation, splenocytes were washed and cultured overnight in cRPMI without IL-2. Splenocytes (1 x 10^5 / well) were pretreated with 100 nM of GM-CSF, M-CSF, IL-4, IL-2 or no cytokine for 3 hours at 37°C. After the pre-treatment, 100 nM of IL2-

NAg-GFP was added to the splenocyte cultures for 1 hour at 37°C. Cells were not washed after the addition of IL2-NAg-GFP. The Becton Dickinson LSRII flow cytometer (San Jose, CA.) was used to detect GFP fluorescence. GFP fluorescence was excited at 405 nm and detected with the AmCyan filter at 530 / 30 nm. Cells were stained with 2.0 μg / ml of propidium iodide to discern the dead cell population by flow cytometry. Propidium iodide fluorescence was excited at 488 nm and detected with the PE-Cy5 filter at 660 / 20 nm. Data were analyzed with the FLOWJO software program (Ashland, OR.). All experimental conditions were performed in duplicate.

CHAPTER 3

RESULTS

3.1 GENERATION OF THE CYTOKINE - NAg CONSTRUCTS

The main hypothesis of this dissertation was that NAg targeted to dendritic cells could regulate NAg specific T cell responses in EAE. This hypothesis was formed in light if the role of dendritic cells in the induction of tolerance. We chose to generate cytokine-NAg fusion proteins with the GM-CSF and M-CSF cytokines in order to target NAg to myeloid APC. IL-6 was additionally used as a cytokine domain because of its ability to target activated B cells. GMCSF-NAg, MCSF-NAg, and IL6-NAg fusion proteins were constructed by covalently linking the genes encoding GM-CSF, M-CSF, and IL-6 with NAg (the encephalitogenic peptide of guinea pig myelin basic protein). All cytokines were covalently linked to a C-terminal 6 his-tag. The DNA encoding NAg was fused to the GM-CSF, M-CSF, and IL-6 genes (encoded in pFastbac-1 plasmids) by a two-step, overlap and extension PCR. The overlap and extension PCR was performed with cytokine-NAg fusion primers. The sequences of the upstream fusion primers (54 base pairs in length) contained a 5' end complimentary to the C-terminus of the cytokine domain and a 3' end complimentary to the N-terminus of the NAg domain. The downstream primer (51 base pairs in length) was composed of a 5' – 3' sequence that complimented the pFastBac-1 plasmid sequence, a stop codon, a 6 his-tag and the NAg C-terminus. Ultimately, the upstream and downstream fusion primers converged at the NAg domain. In the first PCR step, NAg was amplified from the Lag3 plasmid (encoding NAg) using the GMCSF-NAg (19F04), MCSF-NAg (19F02), or IL6-NAg (19F03) upstream fusion primers plus the downstream fusion primer. The predicted amplification product of the first step

PCR was 117 base pairs, which ran just above the 100 base pair standard on the agarose gel (Figure 3.1).

In the second PCR step, the amplified NAg PCR product, from Figure 3.1, served as the extension primer. The NAg PCR product encoded a stop codon, a 6-histidine tag, and the entire NAg domain (amino acids 68 – 88) covalently linked to the specified cytokine sequence provided by the GM-CSF (19F04), M-CSF (19F02), or IL-6 (19F03) primer. The NAg PCR product was extended into the parental pFastBac-1 plasmids encoding GM-CSF, M-CSF, and IL-6. The resulting products were 5.2–5.5 kilobases in length and fell well above the 2027 base pair Hind III fragment (Figures 3.2 and 3.3).

Parental plasmids remaining from the extension reaction were digested with DpnI prior to transformation. The digestion was performed to increase transformation efficiency of the cytokine-NAg extension product into electrocompetent Top10 *E. coli* by digesting away the parental plasmid. Restriction enzyme digestion of the extension product did not result in visible digest products of the parental plasmid, presumably due to the low level of contaminating parental plasmid. Therefore positive and negative controls, i.e. parental plasmid in the presence or absence of restriction enzyme, were run to test for enzyme efficacy.

Top10 *E. coli* transformed with pFastBac-1 plasmids that encoded GMCSF-NAg, MCSF-NAg, or IL6-NAg were selected in ampicillin, and screened by PCR for the presence of NAg (Figure 3.4). Colonies were screened with the downstream NAg primer and the upstream GM-CSF (19F04), M-CSF (19F02), or IL-6 (19F03) primer. Colonies that were positive for GMCSF-NAg, MCSF-NAg, or IL6-NAg yielded an amplicon of approximately 117 base pairs. Plasmids were isolated from the NAg positive colonies and subsequently sequenced. Point

mutations were not identified in the GMCSF-NAg, MCSF-NAg, and IL6-NAg fusion constructs.

Asterisks denoted the colonies that contained cytokine-NAg constructs without point mutations.

Figure 3.1: PCR amplification of the NAg using cytokine-NAg fusion primers. Cytokine-NAg fusion proteins were generated by a 2-step overlap and extension PCR process. In the first PCR step, NAg was amplified the Lag3 plasmid using designated cytokine-NAg fusion primers. The upstream primers contained a 5' end complimentary to the C-terminus of the cytokine domain IL-6 (primer 19F03, Lane 2), M-CSF (primer 19F02, Lane 3), or GM-CSF (primer 19F04, Lane 4), and a 3' end complimentary to the N-terminus of the NAg domain. The downstream primer was composed of a 5' end that complimented the plasmid DNA, a stop codon, and 6 his-tag plus a 3' end that complimented the C-terminus of the NAg domain. Lane 1 contained the 100-base pair ladder. Ultimately, the upstream and downstream fusion primers converged at the NAg domain. The predicted amplification product of the first step PCR was 117 base pairs, which ran just above the 100 base pair standard on the 1.0 % agarose gel.

Figure 3.2: PCR Extension of NAg into the pFastBac-1 plasmids encoding GM-CSF and M-CSF. Cytokine-NAg fusion proteins were generated by a 2-step PCR process. In the second PCR step, the amplified NAg PCR product, from Figure 3.1, served as the extension primer. The NAg PCR product encoded a portion of the pFastBac-1 plasmid, a stop codon, a 6 his-tag, and the entire NAg domain covalently linked to the specified cytokine sequence provided by the upstream primer. The NAg PCR product complimented the cytokine sequence within the respective pFastBac-1 plasmid encoding M-CSF (Lane 2) and GM-CSF (Lane 3), resulting in the high molecular weight products of MCSF-NAg (5.5 kilobases) and GMCSF-NAg (5.2 kilobases). Methylated parental plasmids (without the NAg insert) were digested from the extension reaction with the Dpn I restriction enzyme to increase downstream transformation efficiency of plasmids encoding the cytokine-NAg constructs. Lanes 4 and 5 showed the DpnI digest products from the GMCSF-NAg (Lane 4) and MCSF-NAg (Lane 5) extension reactions. The M-CSF parental plasmid digested with Dpn I (Lane 6) in addition to the M-CSF parental plasmid in the absence of Dpn I (Lane 7) served as controls for the restriction enzyme digest. Lane 1 contained the 100 base pair standard on the 1.0 % agarose gel. The high molecular weight bands of GMCSF-NAg and MCSF-NAg appeared as high molecular weight bands above the 2027 base pair standard.
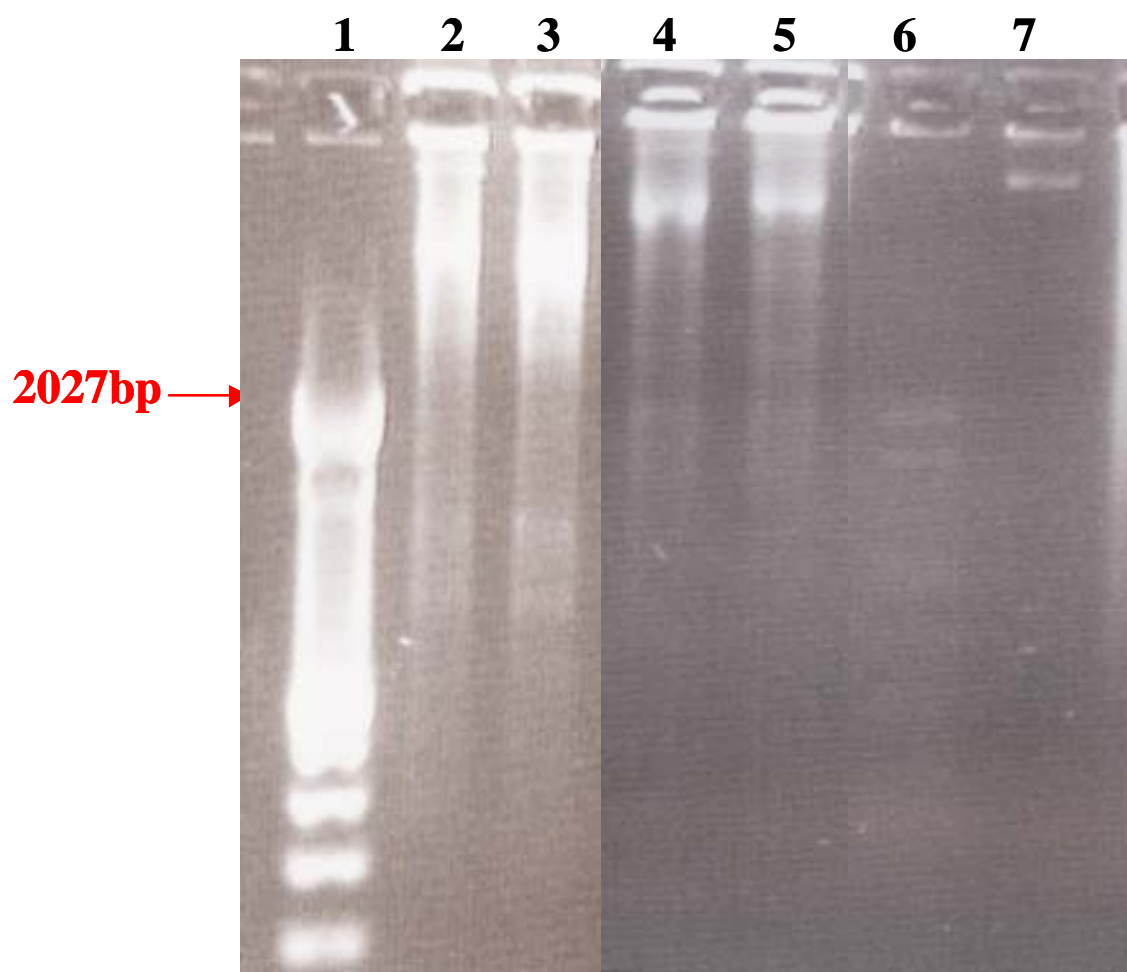
Figure 3.3: PCR Extension of NAg into the pFastBac-1 plasmid encoding IL-6. Cytokine-NAg fusion proteins were generated by a 2-step PCR process. In the second PCR step, the amplified NAg PCR product, from Figure 3.1, served as the extension primer. The NAg PCR product (Figure 3.1) encoded a portion of the pFastBac-1 plasmid, a stop codon, a 6 his-tag, and the entire NAg domain covalently linked to the specified cytokine sequence provided by the upstream primer. NAg was extended into the pFastBac-1 plasmid encoding IL-6 (Lane 2) as shown by generation of IL6-NAg, a high molecular weight product of ~ 5.4 kilobases. Methylated parental plasmids (without the NAg insert) were digested from the extension reaction with the Dpn I restriction enzyme to increase downstream transformation efficiency of plasmids encoding the IL6-NAg construct. Lane 4 shows the Spe I and Dpn I digest product from the IL6-NAg (Lane 4) extension reaction. The IL-6 parental plasmid was digested with Spe I and DpnI (Lane 5) as a positive control for the restriction enzyme digest. Lanes 1 and 3 contained 100 base pair standard on the 1.0 % agarose gel. The high molecular weight band IL6-NAg appeared as high molecular weight band above the 2027 base pair standard.
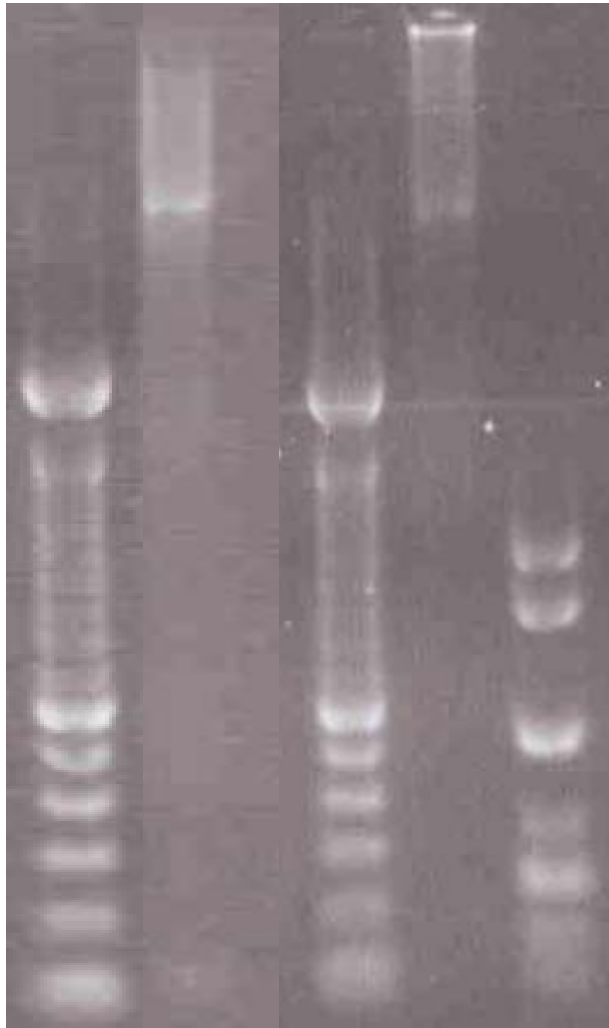
**Figure 3.4: PCR screen on *E. coli* transformed with pFastBac-1 plasmids encoding MCSF-NAg, GMCSF-NAg, or IL6-NAg.** Top 10 *E. coli* were transformed with pFastbac-1 plasmids that encoded MCSF-NAg, GMCSF-NAg, or IL6-NAg. Colonies were selected for ampicillin resistance encoded by the pFastBac-1 plasmid. Colonies were screened with the downstream NAg primer and the respective upstream cytokine fusion primer, M-CSF fusion primer (primer 19F02, Lanes 1-7), GM-CSF fusion primer (primer 19F04, Lanes 8-15), and IL-6 fusion primers (primer 19F03, Lanes 16-18). Colonies that exhibited bands around 117 base pairs were considered positive for transformation. A positive transformation yielded a band located above the 100 base pair standard. PCR products were run on a 1.0 % agarose gel. Asterisks denote those positive colonies that contained no point mutations.
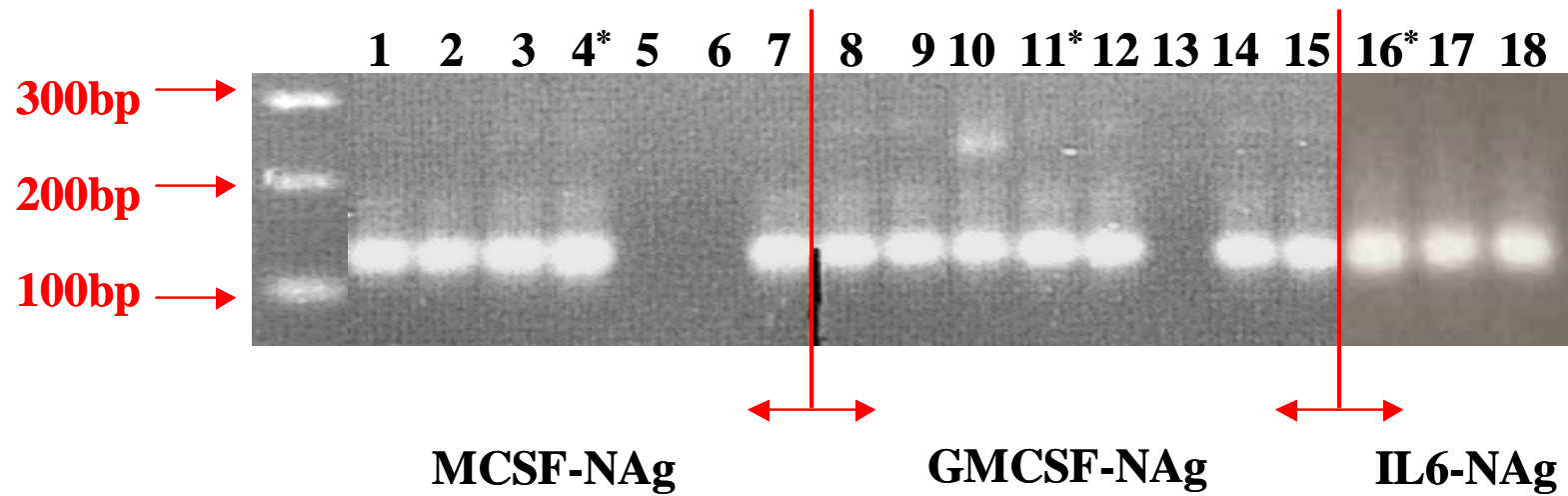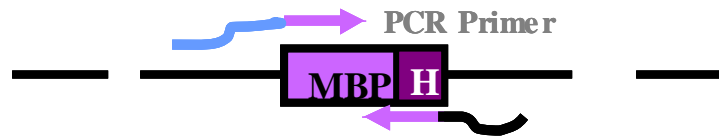
3.2 GENERATION OF BACULOVIRAL EXPRESSION SYSTEMS

The DNA encoding GMCSF-NAg, MCSF-NAg, IL6-NAg, GM-CSF without NAg, or M-CSF without NAg were transposed from pFastBac-1 into a baculoviral vector within DH10Bac *E. coli*. First, pFastBac-1 plasmids were electroporated into DH10Bac *E. coli*. Site-specific transposition was mediated by the Tn7 transposase encoded in a helper plasmid within DH10Bac *E. coli*. The transposase Tn7 translocated the cytokine fusion protein constructs (flanked by mini-Tn7 sequences) from pFastBac-1 into the bacmid DNA vector (containing a mini-*att*Tn7 site). Colonies that had undergone transposition were detected through blue and white screening in the presence of Bluo-Gal and the LacI repressor IPTG. White colonies were likely positive for baculoviral vectors encoding GMCSF-NAg, MCSF-NAg, IL6-NAg, GM-CSF, or M-CSF because transposition at the bacmid *att*Tn7 site disrupted the lacZα gene, such that β-galactosidase was not present. In the absence of β-galactosidase, white colonies were generated because Bluo-gal could not be cleaved into an insoluble blue product. Transformed DH10Bac colonies were selected in the presence of kanamycin, gentamicin, and tetracycline.

The baculoviral vectors encoding GM-CSF, M-CSF, GMCSF-NAg, MCSF-NAg, or IL6-NAg were transfected into Sf9 insect cells. Baculoviruses were released into the media after establishing a lytic infection within the Sf9 culture. Individual viruses encoding designated fusion proteins were isolated by plaque purification. In other words, individual viruses were isolated by co-culturing Sf9 insect cells with limiting dilutions of baculovirus supernatant. Viruses were selected based on their ability to promote a strong lytic infection and generate protein. Fusion proteins were designed to be secreted into the supernatant of infected Sf9 cultures in order to make the fusion proteins readily available for biological testing. Bioassays were performed on plaque assay supernatants in order to assess the biological activity of the

cytokine or NAg protein domains. RsL.11 T cells were co-cultured with irradiated, Lewis rat splenic APC plus supernatant from the plaque purification assay (Figures 3.5A - C) in order to assess biological activity of the NAg domain. Antigenic proliferation of RsL.11 T cells was detected by [^{3}H]thymidine incorporation into the DNA. Cultures were pulsed with [^{3}H]thymidine on day 2 of a 3-day culture. Fusion protein supernatants were tested for cytokine bioactivity (Figures 3.5D and 5E) using Lewis rat peritoneal exudate cells as indicator cells. Peritoneal exudate cells were cultured with supernatant from the plaque assay. The growth and survival of peritoneal exudate cells, as evaluated by MTS reduction, showed that GM-CSF and M-CSF were biologically active. On day 10 of culture, peritoneal exudate cells were pulsed with MTS / PMS and color production read at 492 nm. Highlighted data represented the individual baculoviruses selected for virus expansion (Figure 3.5). M-CSF.1.B5 was chosen based on visual observations.

Figure 3.5: Plaque purification of baculovirus encoding GMCSF-NAg, GM-CSF, MCSF-NAg, M-CSF, or IL6-NAg. Individual baculovirus encoding GMCSF-NAg, GM-CSF, MCSF-NAg, M-CSF, or IL6-NAg were plaque purified. (A - E) Sf9 insect cells (10^4 / well) were infected with a limiting dilution of designated baculovirus (10^{-5} - 10^{-8}). On day 9 of infection, supernatants from individual wells were tested for biological activity or the NAg or cytokine domains. Fusion proteins were secreted into the supernatant of baculoviral infected Sf9 insect cells and therefore readily available for biological testing by either a NAg or cytokine specific bioassay. (A - C) Irradiated splenic APC (5×10^5 / well) and NAg-specific RsL.11 T cells were cultured with supernatant from wells of the plaque purification assay. Cultures were pulsed with [^{3}H]thymidine on day 2 of a 3-day culture, in order to assess RsL.11 proliferation. (D - E) Peritoneal exudate cells (4×10^3 / well) were cultured with supernatant from wells of the plaque purification assay. Cultures were pulsed 10 days later with MTS / PMS. Reduction of MTS resulted in a color change that was read at 492 nm. Growth and survival of the peritoneal exudate cells indicated GM-CSF and M-CSF bioactivity. (A - E) Shaded wells designate the baculoviruses chosen for expansion. M-CSF.1.B5 was chosen based on visual observations.

A

GMCSF-NAg.4.2					
Dilution 10^{-7}			Dilution 10^{-8}		
129331	122879	1303	636	193280	870
11739	190182	214588	624	216	384
180	336	161647	402	108	156
555	246	132	170845	408	786
142411	203898	3506	210	102	636
149992	86401	432	246	228	492
25155	170202	162455	324	126	630
666	105530	510	1134	852	1110

B

MCSF-NAg.9.2					
Dilution 10^{-7}			Dilution 10^{-8}		
168	145272	156	444	132	1086
107432	270	140158	104494	114	168
204	84767	79406	103645	132	360
71751	216	103313	87342	174	53961
312	101127	36	240	30	354
76453	264	408	432	234	174
13374	109861	372	252	268	522
516	85609	93594	216	684	90

C

IL6-NAg.7					
Dilution 10^{-7}			Dilution 10^{-8}		
185	164	14164	147	169	99
355	184	16520	142	188	186
319	16314	264	266	231	16242
9289	15917	4767	13305	175	140
227	8672	1847	197	165	92
284	217	257	244	171	162
14570	165	186	179	122	229
13300	230	10595	157	158	68248

D

G-MCSF.8					
Dilution 10^{-5}			Dilution 10^{-6}		
0.741	0.738	0.702	0.79	0.748	0.919
0.826	0.749	0.936	1.51	0.861	1.211
0.486	0.796	0.801	1.442	1.366	1.094
0.807	0.755	1.159	1.342	0.929	1.34
0.742	0.924	0.91	1.072	0.438	1.679
0.482	0.888	1.019	1.305	0.96	1.338
0.928	0.749	0.263	0.722	0.927	1.051
0.622	0.835	0.758	0.876	0.69	0.81

E

M-CSF.1					
Dilution 10^{-5}			Dilution 10^{-6}		
1.175	0.666	1.271	1	0.838	0.7
0.682	0.694	1.27	0.993	0.779	0.981
0.724	1.202	0.731	1.072	0.728	1.06
0.806	1.114	1.274	0.798	1.042	1.014
0.819	0.82	0.646	1.004	0.687	1.103
1.217	0.657	0.841	0.814	1.057	0.769
1.255	0.593	0.74	0.712	1.164	1.011
0.951	0.678	0.661	1.033	0.962	1.053

3.3 PURIFICATION OF FUSION PROTEINS

Plaque purified baculoviruses were expanded in Sf9 cells for 6-8 days to generate viral stocks for future protein expressions. Proteins were expressed in large-scale Sf9 cultures that were infected with baculovirus for four days. On day four of culture, supernatants were harvested and clarified of Sf9 cells. Supernatants were ultimately concentrated and purified by two affinity chromatography steps. All proteins were engineered with a C- terminal 6 his-tag for protein purification. The first affinity column contained an immobilized single-chain antibody against the C-terminal histidine tag, and the second column consisted of immobilized nickel ions. SDS-PAGE was run on the GMCSF-NAg, MCSF-NAg, IL6-NAg, M-CSF, and GM-CSF elutions from the nickel column in order to check for protein purity and size (Figure 3.6). Mature GMCSF-NAg (17.5 kDa) and GM-CSF (15.4 kDa) are estimated to have one N-linked glycosylation site, while MCSF-NAg (27.9kDa) and M-CSF (25.8 kDa) are estimated to have three N-linked glycosylation sites. Conversely, the SDS-PAGE showed that GM-CSF and M-CSF fusion proteins exhibited two and four bands respectively. The banding pattern did coincide with the number of N-linked glycosylation (N x S, or N x T) sites in the cytokine domain of the fusion protein; the NAg domain did not contain N-linked glycosylation sites. Protein expression overwhelms the Sf9 cells, resulting in incomplete glycosylation. We postulate that when the Sf9 system became overwhelmed by protein production, incomplete glycosylation would result in bands representing the glycosylated and unglycosylated forms of the protein. For instance, we postulated that GMCSF-NAg exhibited two bands because one band represented the glycosylated form of GMCSF-NAg while the other band represented the unglycosylated form. IL6-NAg (24.8kDa) had no potential N-linked glycosylation sites, and therefore has only one band. Importantly, SDS-PAGE indicated that the fusion proteins had minimal contaminants.

Protein purity is essential to prevent lymphocyte reactivity to contaminants during *in vitro* and *in vivo* experimentation.

Figure 3.6: The purity of GMCSF-NAg, MCSF-NAg, M-CSF, GM-CSF, and IL6-NAg was determined by SDS-PAGE. Recombinant fusion proteins were expressed in large-scale Sf9 insect cell cultures. Supernatants were concentrated and subsequently purified by means of a 6 his-tag engineered at the C-terminus of all fusion proteins. Two affinity chromatography matrices were used to purify the proteins. The first affinity column contained an immobilized single-chain Fv antibody against the C-terminal histidine tag, and the second column was comprised of immobilized nickel ions. Purified GMCSF-NAg, MCSF-NAg, M-CSF, GM-CSF, and IL6-NAg were analyzed on 10% - 15% SDS-PAGE. Mature GMCSF-NAg (17.5 kDa) and GM-CSF (15.4 kDa) have one N-linked glycosylation site, while MCSF-NAg (27.9kDa) and M-CSF (25.8 kDa) have 3 N-linked glycosylation sites. The banding pattern coincided with the number of N-linked glycosylation sites. We postulated that the Sf9 system became overwhelmed by protein expression and resulted in glycosylated and unglycosylated forms of the fusion proteins, yielding two or four bands respectively. IL6-NAg (24.8kDa) had no potential N-linked glycosylation sites and therefore exhibited only one band. SDS-PAGE indicated that the fusion proteins had minimal contaminants. Protein bands were visualized after staining the SDS-PAGE gels in Gel Code, a coomasie-based protein stain.
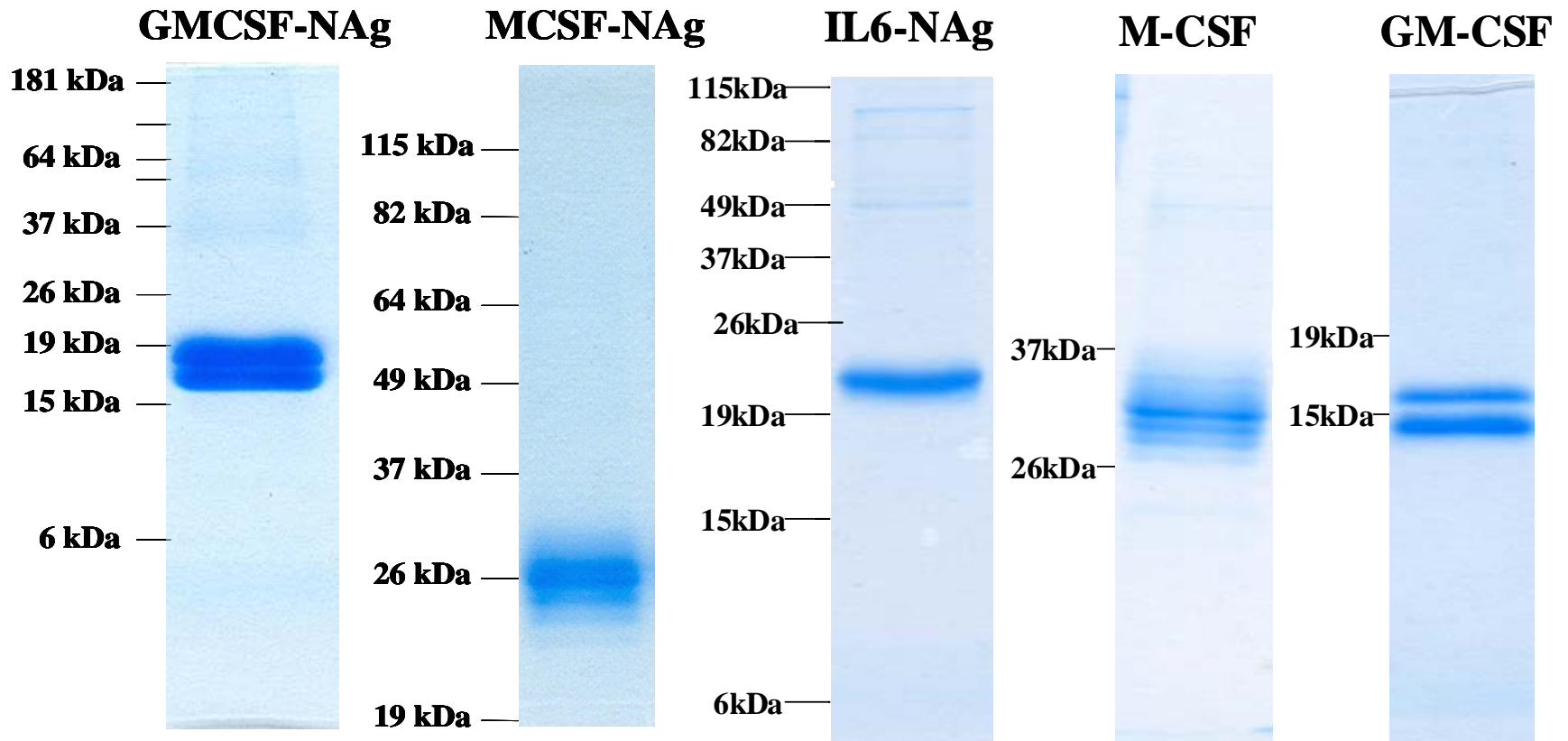
3.4 BIOLOGICAL ACTIVITY OF THE CYTOKINE DOMAINS

Purified proteins were assessed for biological activity of the cytokine domain prior to use with *in vitro* and *in vivo* experiments. The cytokine domains of purified GMCSF-NAg, MCSF-NAg, GM-CSF, and M-CSF were shown to be biologically active by facilitating the survival and growth of bone marrow progenitors (Figure 3.7A). Lewis rat bone marrow cells were cultured with purified proteins titrated on a log scale from 100 nM – 10 fM. Cultures were pulsed with [^{3}H]thymidine on day 2 of a 3-day culture. The biological activities of GMCSF-NAg and MCSF-NAg exhibited a bell shaped curve of growth. The biological activity of GM-CSF and GMCSF-NAg titrated to a concentration of 1 pM, while M-CSF and MCSF-NAg titrated to a concentration of 100 pM. Proteins containing the GM-CSF cytokine were at least 10 fold more potent than proteins containing the M-CSF cytokine. High concentrations of GM-CSF and M-CSF diminished bone marrow cell viability, presumably due to activation of myeloid APC and subsequent release of cytotoxic mediators. Fusion of NAg to either GM-CSF or M-CSF did not diminish biological activity of the cytokine. For instance, the cytokine domain of GM-CSF or M-CSF exhibited similar response curves to GMCSF-NAg or MCSF-NAg respectively. Similarly, the cytokine activity of IL-6 was not abolished by fusion to NAg, as shown by the sigmoidal survival curve of the IL-6 dependent T1165 hybridoma cell line (Figure 3.7B). T1165 hybridoma cells were cultured with serially diluted IL6-NAg baculoviral supernatants from plaque purified viruses C12 and D10. Cultures were pulsed with MTS / PMS after 48 hours and the color production was read at 492 nm. IL6-NAg activity was present when diluted 100,000 fold. Peak survival of T1165 was seen when IL6-NAg baculoviral supernatants were diluted 10,000 fold. Overall, the cytokine domains of GMCSF-NAg, MCSF-NAg, GM-CSF, M-CSF, and IL6-NAg exhibited biological activity.

An alternative way to assess cytokine bioactivity was to test the specificity of GM-CSF and M-CSF to act as growth factors for immature APC. Therefore the effects of GM-CSF and M-CSF were compared between immature bone marrow APC and mature splenic APC (Figure 3.8). Lewis rat bone marrow cells or splenocytes were cultured with designated concentrations of M-CSF (Figure 3.8A) and GM-CSF (Figure 3.8B) baculoviral supernatant, or purified MCSF-NAg (Figure 3.8C) and GMCSF-NAg (Figure 3.8D). Cultures were pulsed with [^{3}H]thymidine on day 2 of a 3-day culture. The cytokine domains of GM-CSF, GMCSF-NAg, M-CSF, and MCSF-NAg facilitated a specific proliferative effect on bone marrow cells, but not splenic APC. Proteins containing GM-CSF (Figure 3.8B and D) were at least 10 fold more potent than those proteins containing M-CSF (Figure 3.8A and C). For instance, purified GMCSF-NAg exhibited a half maximal proliferative effect around 100 pM and MCSF-NAg around 1 nM. Overall, these results are consistent with the fact that GM-CSF and M-CSF proteins act as survival and growth factors for hematopoietic progenitors that express the cytokine receptors.

The cytokine domains of GMCSF-NAg and MCSF-NAg supported the differentiation of distinct APC subsets (Figure 3.9). Bone marrow cells were cultured with 50 nM GMCSF-NAg (left panel) and 50 nM MCSF-NAg (right panel) for ten days. Surface markers of adherent APC were analyzed by flow cytometry. CD11c$^+$ myeloid APC derived with GMCSF-NAg had higher surface concentrations (approximately 10 fold) of MHC class II, B7.1, CD4, and CD8 as compared to APC derived with MCSF-NAg. Both GMCSF-NAg and MCSF-NAg derived APC exhibited similar levels of CD45 and B7.2. NAg alone did not promote survival or differentiation of bone marrow cells (data not shown). Furthermore, the NAg domain of GMCSF-NAg or MCSF-NAg did not interfere with the ability of the GM-CSF or M-CSF domain to drive differentiation of distinct APC subsets. These data are consistent with the idea

that GM-CSF and M-CSF would promote differentiation pathways to respectively generate dendritic cell and macrophage lineages, and that dendritic cells may serve as better APC than macrophages.

Figure 3.7: Cytokine bioassay to assess the cytokine activity of the fusion proteins. The cytokine domain of GMCSF-NAg, MCSF-NAg, and IL6-NAg exhibited biological activity. (A) Lewis rat bone marrow cells (10^5 / well) were cultured with titrated of GMCSF-NAg, MCSF-NAg, GM-CSF, M-CSF, 100 nM – 10 fM (x-axis). Cultures were pulsed with [^{3}H]thymidine on day 2 of a 3-day culture. Biological activity of the cytokine domains facilitated survival and growth of bone marrow progenitors. Fusion of NAg to either GM-CSF or M-CSF did not diminish biological activity of the cytokine. (B) IL-6 specific T1165 hybridoma cells (10^4 / well) were cultured with serially diluted IL6-NAg baculoviral supernatants (10^{-2} to 10^{-8}) from viruses C12 and D10. Cultures were pulsed with MTS / PMS after 48 hours and color production, generated by MTS reduction, was read at 492 nm. Cytokine activity of IL-6 was not abolished by fusion of IL-6 to NAg, as shown by the sigmoidal survival response curve of T1165 hybridoma cell line. This experiment was performed one time.
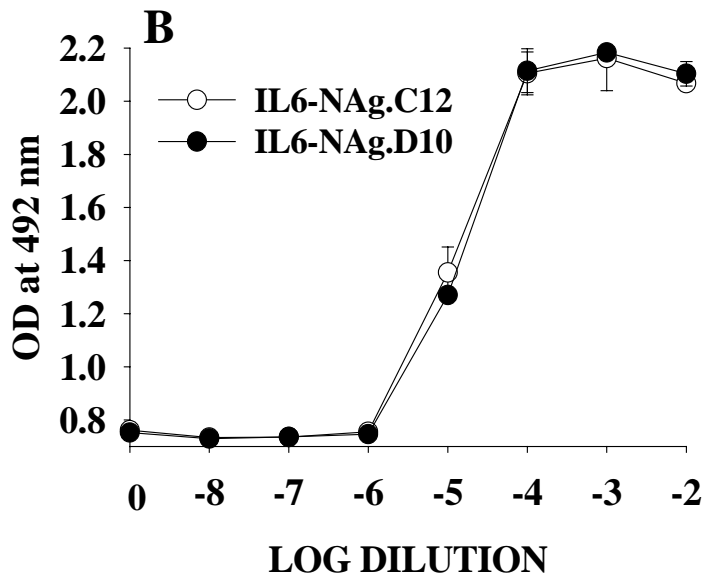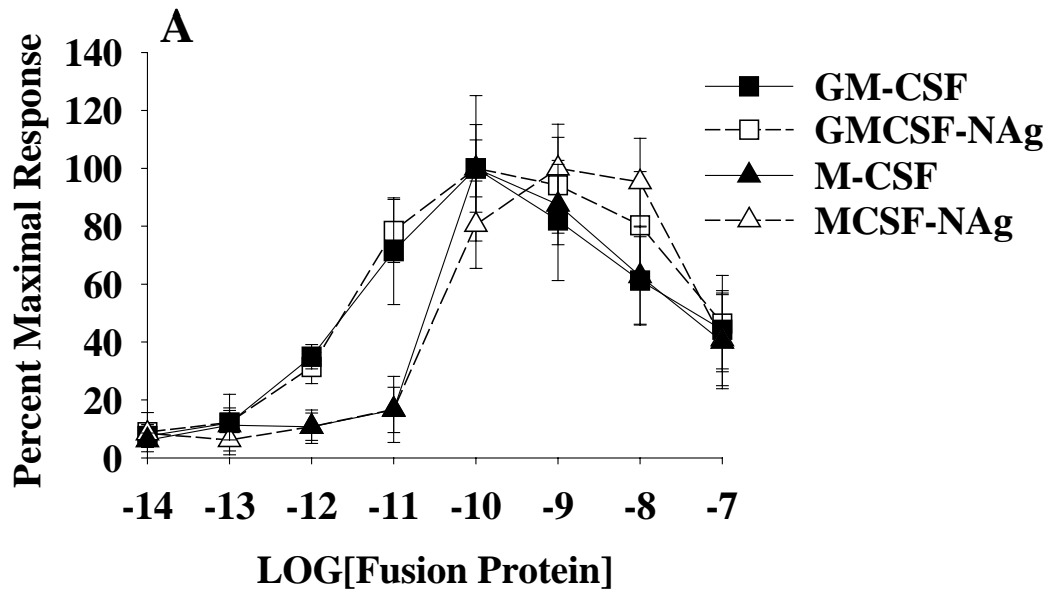
Figure 3.8: Cytokine bioassay to assess the activity of fusion proteins on immature bone marrow APC versus mature splenic APC. The cytokine domains of GM-CSF, GMCSF-NAg, M-CSF, and MCSF-NAg facilitated a specific proliferative effect on bone marrow and not splenic APC. These data indicated that GM-CSF and M-CSF acted specifically as growth factors for immature APC and not mature APC. This was consistent with the fact that GM-CSF and M-CSF proteins act as survival and growth factors for hematopoietic progenitors that express the cytokine receptors. (A-D) Lewis rat bone marrow cells (10^5 / well) or splenocytes (5×10^5 / well) were cultured with serially diluted M-CSF (A) and GM-CSF (B) baculoviral supernatant (10^{-2} to 10^{-8}, x-axis), or purified MCSF-NAg (C) and GMCSF-NAg (D) titrated on a log scale from 100 nM to 1 pM. Cultures were pulsed with [^{3}H]thymidine on day 2 of a 3-day culture. These data are representative of at least two experiments.
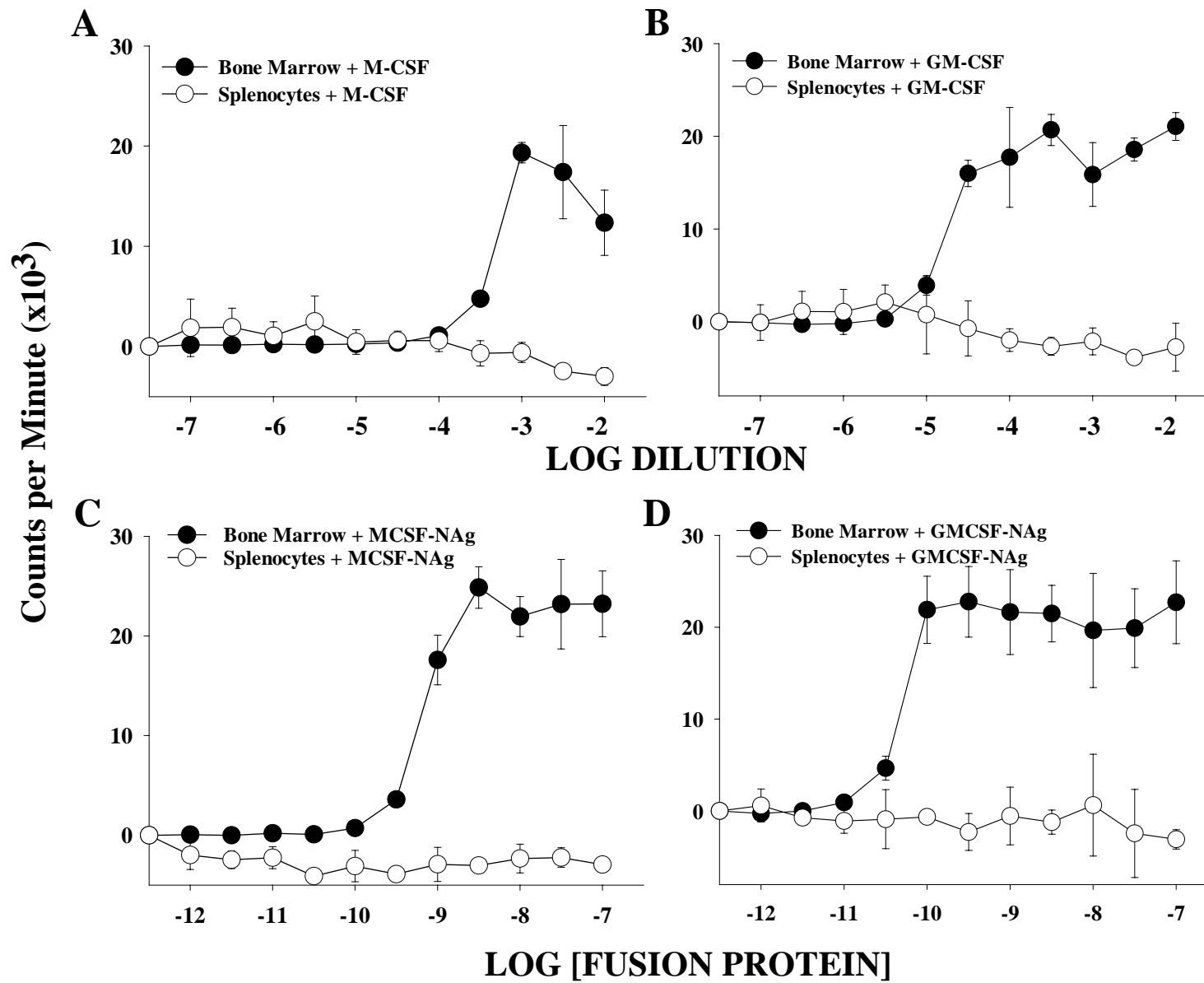
Figure 3.9: Characterization of the cell surface markers expressed on APC subsets that were derived with GMCSF-NAg and MCSF-NAg. The cytokine domains of GMCSF-NAg and MCSF-NAg supported differentiation of two distinct APC subsets. Bone marrow cells were cultured with 50 nM GMCSF-NAg (left panels) or 50 nM MCSF-NAg (right panels) for 10 days. Surface markers of adherent APC were analyzed with the Becton Dickinson FACScan flow cytometer along with the CELLQuest analysis software. CD11c$^+$ myeloid APC derived with GMCSF-NAg had higher surface concentrations (approximately 10 fold) of MHC class II, B7.1, CD4, and CD8 as compared to APC derived with MCSF-NAg. Both GMCSF-NAg and MCSF-NAg derived APC exhibited similar levels of CD45 and B7.2. These data are consistent with the idea that GM-CSF and M-CSF would promote differentiation pathways to respectively generate the dendritic cell and macrophage lineages. These data are representative of three experiments.

GMCSF-NAg   MCSF-NAg

CD45

CD11c

MHC
class II

B7.1

B7.2

CD4

CD8

Cells Per Channel

Fluorescence
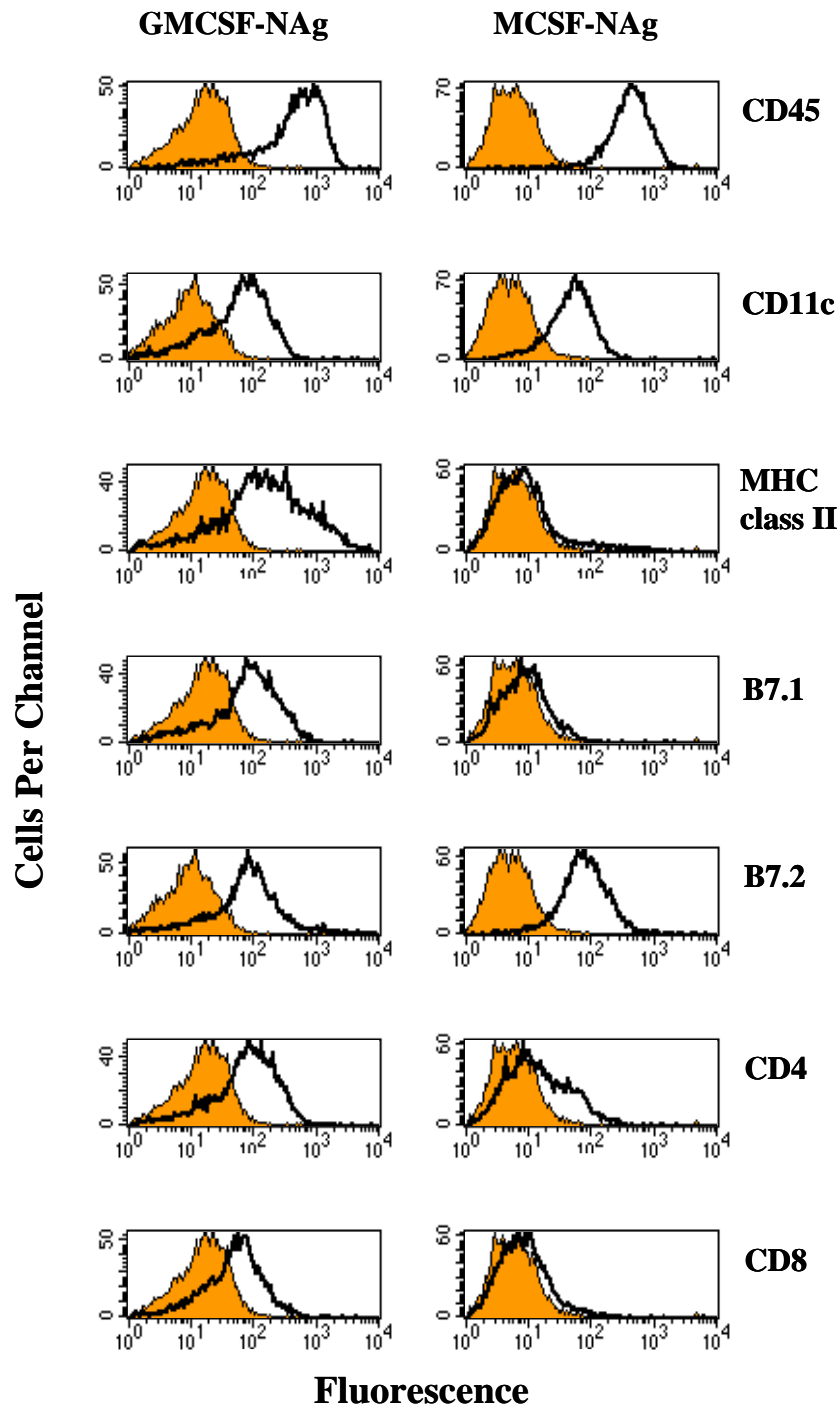
3.5 BIOLOGICAL ACTIVITY OF THE NAg DOMAINS

Purified proteins were assessed for biological activity of the NAg domain prior to use for *in vitro* and *in vivo* experiments. The NAg domains of GMCSF-NAg and MCSF-NAg were shown to be biologically active. *In vitro* proliferative assays measured the antigenic response of NAg-specific RsL.11 T cell clones by tritiated thymidine incorporation (Figure 3.10). Irradiated Lewis rat splenic APC and NAg-specific RsL.11 T cells were co-cultured with titrated GMCSF-NAg, MCSF-NAg, NAg alone, or NAg in the presence or absence of 100 nM GM-CSF or 100 nM M-CSF. Cultures were pulsed with [^{3}H]thymidine on day 2 of a 3-day culture. Data revealed that the cytokine domains of GMCSF-NAg and MCSF-NAg enhanced RsL.11 proliferative response greater than NAg alone. GMCSF-NAg and MCSF-NAg respectively enhanced the half maximal proliferative response at least 1,000 fold and 10 fold greater than NAg alone. Furthermore, NAg activity of the GMCSF-NAg and MCSF-NAg fusion proteins titrated to 1 pM and 10 pM concentrations, respectively. These data indicated that the GM-CSF and M-CSF cytokine domains did not hinder NAg presentation by MHC class II; in fact the cytokine domains enhanced antigenic proliferation of RsL.11 T cells.

IL-2 production was monitored as an additional endpoint of RsL.11 T cell activation. In Figure 3.11, irradiated splenic APC and NAg-specific RsL.11 T cells were cultured with titrated GMCSF-NAg, MCSF-NAg, or GPMBP. Assay supernatants were collected after 24 hours of culture and tested for IL-2 production. IL-2 dependent CTLL T cells served as indicators of IL-2 production. CTLL T cells were cultured in the presence of 20 μl of the 24-hour supernatant, and then pulsed with MTS / PMS on day two of culture. Viability of the CTLL T cells was determined via MTS reduction. Data revealed that RsL.11 activation resulted in IL-2 production that mirrored the [^{3}H]thymidine incorporation data seen in Figure 3.10. In other words, the rank

order of potency (GMCSF-NAg > MCSF-NAg > NAg) as seen by the RsL.11 proliferative response was reflected by the strength of the IL-2 response. GMCSF-NAg and MCSF-NAg respectively enhanced CTLL proliferation 1,000 fold and at least 10 fold greater than GPMBP. The potentiated antigenic responses induced by GMCSF-NAg and MCSF-NAg was likely due to enhanced uptake of NAg through the cytokine receptors.

The hypothesis of enhanced NAg uptake through cytokine-receptor mediated endocytosis was supported by the data of Figure 3.10. The data showed that covalent linkage between the cytokine and NAg domains was required to potentiate the RsL.11 antigenic response. MCSF-NAg potentiated the RsL.11 half maximal proliferative response at least 10 fold greater than NAg + M-CSF as separate molecules. Likewise, GMCSF-NAg potentiated the proliferative response at least 1,000 fold greater than NAg + GM-CSF as separate molecules. The potency of GMCSF-NAg and MCSF-NAg could not be explained by the independent actions of the cytokine or NAg domains on either the APC or T cell responders. These data suggested that cytokine-receptor mediated uptake of NAg significantly increased the amount of NAg presented by APC, enhancing the T cell proliferative response.

An inhibition assay was performed in order to address the hypothesis of cytokine-receptor mediated endocytosis of NAg. This assay was designed such that the GM-CSF or M-CSF receptors on splenic APC were saturated or "inhibited" prior to the addition of GMCSF-NAg or MCSF-NAg. Receptor saturation would hypothetically prevent cytokine-receptor mediated uptake of GMCSF-NAg and MCSF-NAg, resulting in a diminished RsL.11 proliferative response to the tethered NAg. Co-cultures of irradiated splenic APC with RsL.11 T cells were pretreated with GM-CSF or M-CSF for 4 hours before the addition of GMCSF-NAg, MCSF-NAg, or NAg, respectively (Figure 3.12). GM-CSF pre-treatment diminished the RsL.11

proliferative response to GMCSF-NAg by approximately 1,000 fold, from a half maximal concentration of 10 nM to 10 pM (Figure 3.12A). M-CSF pre-treatment did not inhibit antigenic proliferation in the presence of GMCSF-NAg. M-CSF pre-treatment did diminish the RsL.11 proliferative response to MCSF-NAg by approximately 10 fold, from a half maximal concentration of 10 nM to 1 nM (Figure 3.12B). RsL.11 proliferation in the presence of MCSF-NAg was not inhibited by GM-CSF pre-treatment. Pre-treatment with GM-CSF or M-CSF did not alter the RsL.11 proliferative response to NAg (Figure 3.12C). These data supported the hypothesis that GMCSF-NAg and MCSF-NAg potentiated the RsL.11 proliferative response by cytokine-receptor mediated uptake. Cytokine targeting was specific because the RsL.11 proliferative response to MCSF-NAg or GMCSF-NAg was only inhibited when co-cultures were pre-treated with M-CSF or GM-CSF respectively.

Figure 3.10: Bioassay to assess the biological activity of the NAg domain and to determine the importance of the cytokine-NAg linkage. Cytokine domains of GMCSF-NAg and MCSF-NAg strongly promoted NAg-specific RsL.11 T cell reactivity to the covalently linked NAg. (A-B) Irradiated Lewis rat splenic APC ($5x10^5$ / well) and NAg-specific RsL.11 T cells ($2.5x10^4$ / well) were cultured with titrated GMCSF-NAg, MCSF-NAg, or NAg in the presence or absence of an additional 100 nM GM-CSF or 100 nM M-CSF. Cultures were pulsed with [^{3}H]thymidine on day 2 of a 3-day culture. Data revealed that the cytokine domains of GMCSF-NAg and MCSF-NAg enhanced RsL.11 proliferative response greater than NAg alone and enhanced potentiation was due to covalent linkage of the cytokine and NAg domains. These data are representative of three experiments.
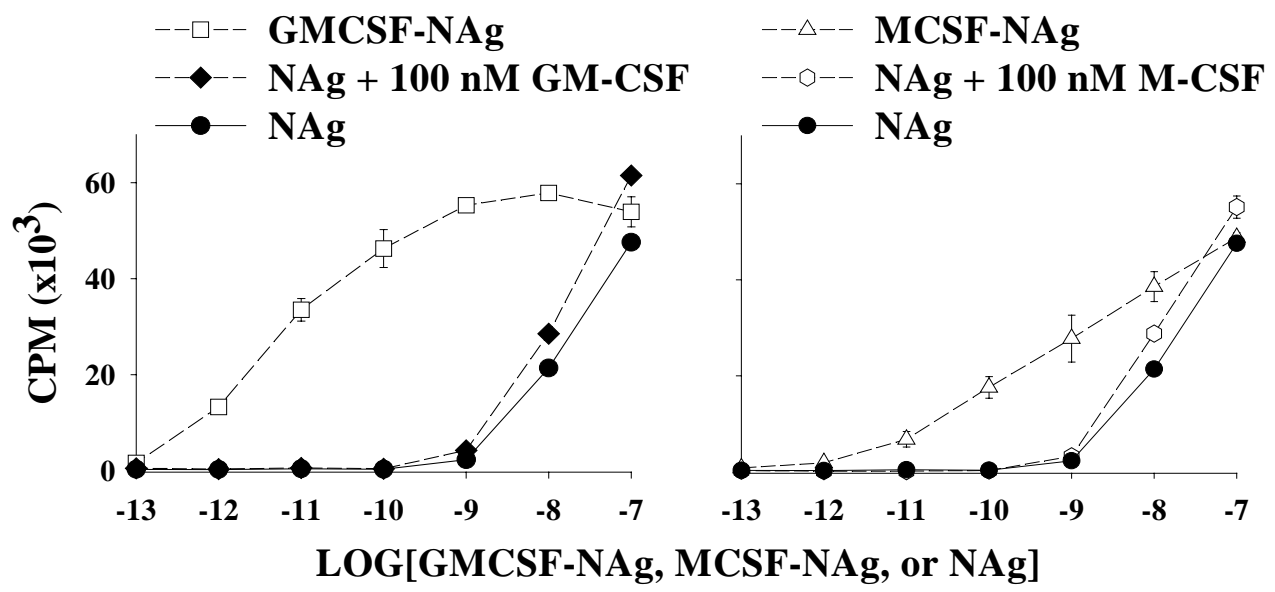
Figure 3.11: GMCSF-NAg and MCSF-NAg potentiated the RsL.11 IL-2 response greater than NAg alone. The cytokine domains of GMCSF-NAg and MCSF-NAg strongly enhanced RsL.11 T cell activation to the covalently linked NAg. Irradiated Lewis rat splenic APC (5×10^5 / well) and NAg-specific RsL.11 T cells (2.5×10^4 / well) were cultured with titrated GMCSF-NAg, MCSF-NAg, or GPMBP from 100 nM to 10 fM. Supernatants were collected after 24 hours of culture and tested for IL-2 production using CTLL T cells (10^4 / well) as indicators. CTLL cultures were pulsed with MTS / PMS after 48 hours and color production was read at 492 nm. The rank order of potency (GMCSF-NAg > MCSF-NAg > NAg) as seen by the RsL.11 proliferative response (Figure 3.10) was mirrored by the strength of the IL-2 response. These data are representative of at least three experiments.
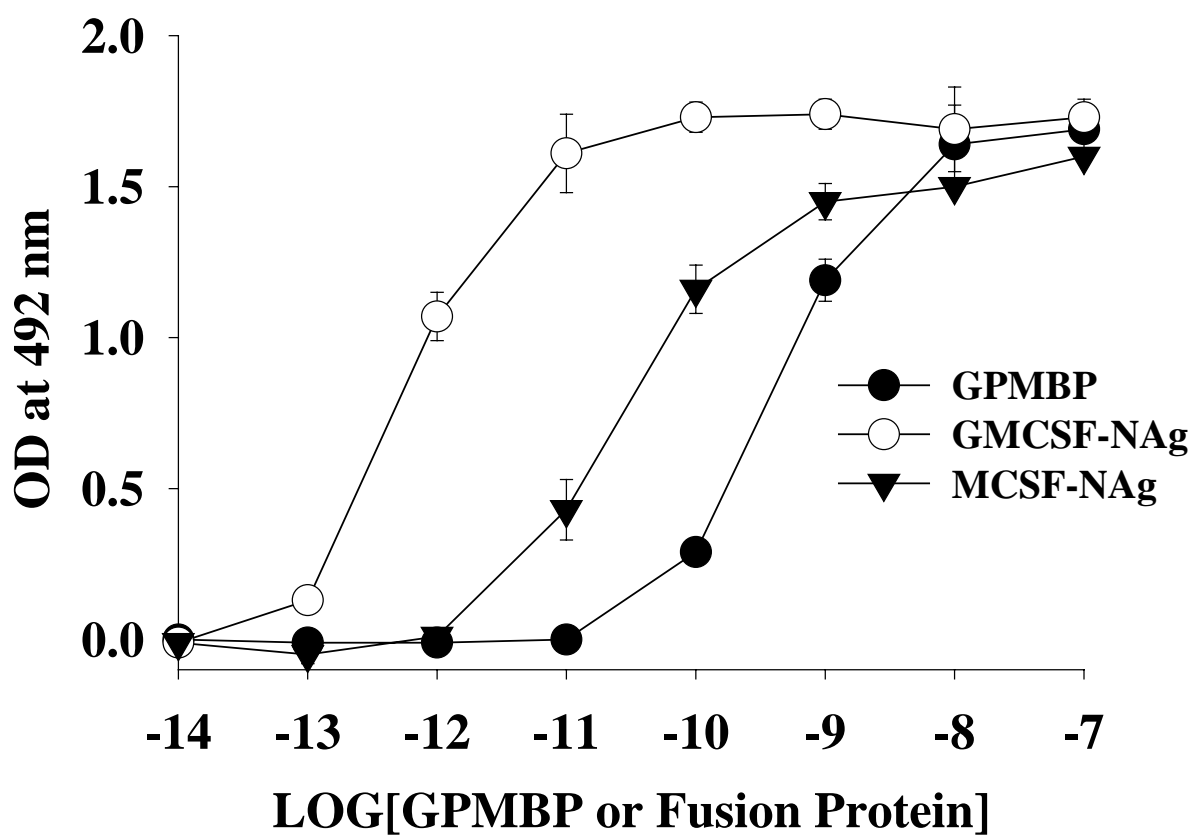
Figure 3.12: The cytokine domains of GMCSF-NAg and MCSF-NAg enhanced antigenic reactivity to NAg by a mechanism that was competitively blocked by the respective cytokine. An inhibition assay was performed in order to address the hypothesis that potentiation of the T cell proliferative response was due to cytokine-receptor mediated uptake of NAg. This assay was designed such that the GM-CSF or M-CSF receptors on splenic APC were saturated or "inhibited" prior to the addition of GMCSF-NAg or MCSF-NAg. Receptor saturation would hypothetically prevent cytokine-receptor mediated uptake of GMCSF-NAg and MCSF-NAg, resulting in a diminished RsL.11 proliferative response. (A-C) Irradiated Lewis rat splenic APC and RsL.11 T cells were cultured with 100 nM of GM-CSF, 100 nM M-CSF, or no cytokine 4 hours before the addition of titrated GMCSF-NAg (A), MCSF-NAg (B), or NAg (C) (x-axis). Cultures were pulsed with [^{3}H]thymidine on day 2 of a 3-day culture. These data are representative of three experiments.

60

CPM (x10^3)

40

20

0

-13 -12 -11 -10 -9 -8 -7
LOG[GMCSF-NAg]

-12 -11 -10 -9 -8 -7
LOG[MCSF-NAg]

▽--- 100 nM M-CSF
◇--- 100 nM GM-CSF
⬡— No addition

-12 -11 -10 -9 -8 -7
LOG[NAg]
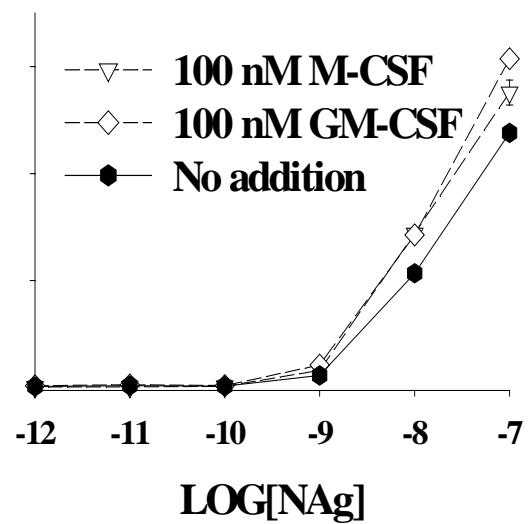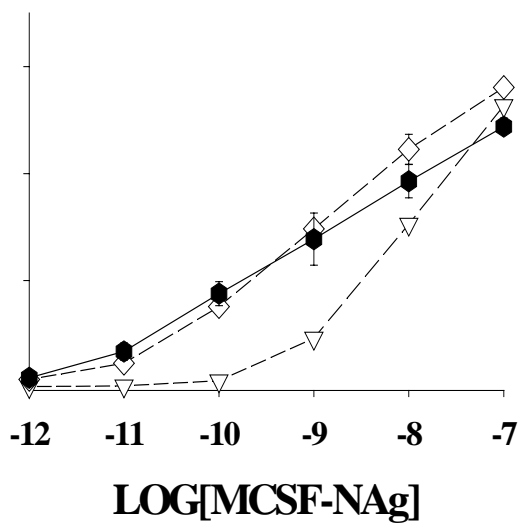
3.6 THE CYTOKINE DOMAIN TARGETS NAg TO VARIOUS APC SUBSETS

We hypothesized that RsL.11 antigenic potentiation was dependent on specific APC subsets bearing the cytokine receptor based on 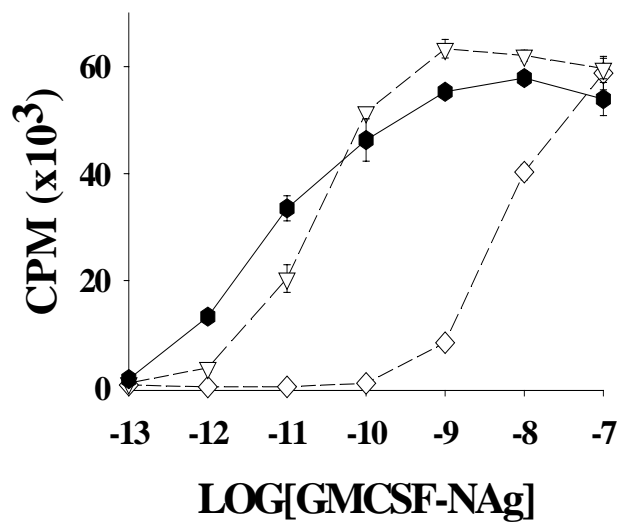the previous data. Therefore, individual APC subsets (dendritic cell, macrophage, B cell and T cell APC) were cultured with cytokine-NAg fusion proteins to determine the ability of the APC to influence antigenic proliferation of RsL.11 T cells. Macrophage and dendritic cell APC were respectively derived from Lewis rat bone marrow cells cultured for 7 days with 0.1% M-CSF (Figure 3.13A) or GM-CSF (Figure 3.13B) baculovirus supernatant. Bone marrow derived APC were co-cultured with RsL.11 T cells and purified fusion proteins titrated on a log scale. Aminoguanidine, a specific iNOS inhibitor, was added to macrophage and dendritic cell assays to circumvent nitric oxide production, because increasing concentrations of GMCSF-NAg and MCSF-NAg resulted in nitric oxide production (data not shown). Cultures were pulsed with [^{3}H]thymidine on day 2 of a 3-day culture.

The cytokine domains of GMCSF-NAg and MCSF-NAg effectively targeted NAg to macrophage and dendritic cell APC (Figure 3.13 A and B). The cytokine domains of GMCSF-NAg, MCSF-NAg, and IL4-NAg targeted NAg to macrophages and respectively potentiated the proliferative response at least 320 fold, 32 fold and 10 fold greater than GPMBP alone (Figure 3.13A). Specifically, the half maximal antigenic response of RsL.11 T cells to GMCSF-NAg, MCSF-NAg, IL4-NAg, and GPMBP were approximately 1 pM, 10 pM, 32 pM and 320 pM, respectively. IL10-NAg, IFNβ-NAg, IL2-NAg, and IL1Rα-NAg cytokine domains did not target NAg to macrophages. In fact these cytokines had lower antigenic potentiation than GPMBP, suggesting these cytokines may interfere with antigen processing and presentation by macrophages. The cytokine domains of GMCSF-NAg, MCSF-NAg, and IL4-NAg targeted the tethered NAg domain to dendritic cells (Figure 3.13B). GMCSF-NAg, MCSF-NAg and IL4-

NAg respectfully potentiated the RsL.11 proliferative response at least 320 fold, 100 fold and 10 fold greater than GPMBP alone. Specifically, the half maximal antigenic response of RsL.11 T cells to GMCSF-NAg, MCSF-NAg, IL4-NAg, and GPMBP were approximately 10 pM, 32 pM, 320 pM and 3.2 nM, respectively. IL2-NAg, IL1Rα-NAg and IFNβ-NAg cytokine domains did not target NAg to dendritic cells. It is important to note that the response curves of Figures 3.13A and 3.13B exhibited a bell shape, marked by diminished T cell responses at the higher antigen concentrations. This suggests that APC activation by antigen-stimulated T cells prompted the production of alternative inflammatory mediators (ie, IFNγ and TNF) other than nitric oxide. Overall, these data indicate that GMCSF-NAg and MCSF-NAg can target NAg to myeloid APC and as a result, significantly enhance antigen presentation to NAg specific T cells. The ability of GMCSF-NAg and MCSF-NAg to target NAg to macrophages and dendritic cells is specific because other cytokine-NAg fusion proteins, such as IL2-NAg, IL1Rα-NAg and IFNβ-NAg did not efficiently target NAg to these APC subsets.

GMCSF-NAg and MCSF-NAg were also tested for their ability to target NAg to B cell APC. Splenic OX33$^+$ B cells (Figure 3.13C) and OX33$^+$Ig$^+$ B cells (Figure 3.13D) were FACS sorted and co-cultured with RsL.11 T cells plus titrated protein. Cultures were pulsed with [^{3}H]thymidine on day 2 of a 3-day culture. IL4-NAg targeted NAg to FACS sorted B220$^+$ B cells and B220$^+$ / surface Ig$^+$ B cells at least 1,000 fold greater than NAg alone. Specifically, the half maximal antigenic response of RsL.11 T cells to IL4-NAg, and NAg were approximately 3.2 pM and 10 nM in the presence of B220$^+$ B cells or B220$^+$ / surface Ig$^+$ B cells respectively. GMCSF-NAg and MCSF-NAg did not efficiently target NAg to FACS sorted B220$^+$ B cells. Alternatively, GMCSF-NAg, IL2-NAg, and IL6-NAg along with IL4-NAg targeted NAg to FACS sorted B220$^+$ / surface Ig$^+$ B cells. Specifically, the half maximal antigenic response of

90

RsL.11 T cells to IL4-NAg, IL2-NAg, GMCSF-NAg, IL6-NAg and NAg were approximately 3.2 pM, 100 pM, 320 pM, 1 nM and 10 nM. The sorting of $B220^+$ / surface Ig^+ B cells potentially activated the B cell population through cross-linking of the surface Ig receptors, because $B220^+$ / surface Ig^+ B cells exhibited a distinct targeting profile from $B220^+$ B cells. Certain cytokines, including IL10-NAg, IFNβ-NAg, IL1Rα-NAg, and MCSF-NAg cytokine domains did not target NAg to $B220^+$ B cells or $B220^+$ / surface Ig^+ B cells. Overall, these data showed that the cytokine domains of GMCSF-NAg and MCSF-NAg effectively targeted NAg to myeloid APC subsets and not to B cell APC. Furthermore, the activation status of APC subsets can play a role in the targeting efficiency of cytokine-NAg fusion proteins.

The specificity of GMCSF-NAg and MCSF-NAg to target macrophages and dendritic cells is supported by the inability of these fusion proteins to target NAg to MHC class II^+ T cell APC (Figure 3.14). This conclusion was revealed by a T cell killing assay, where irradiated RsL.11 T cells kill R1T cells (blastogenic MHC class II^+ T cells) that present NAg on MHC class II. In this assay, R1T cells were cultured for 24 hours in complete RPMI without IL-2 to allow clearance of IL-2 from cell surface receptors. R1T cells were then cultured with irradiated RsL.11 T responders in the presence of titrated fusion protein or the NAg peptide. After 4 hours, 0.4% IL-2 baculovirus supernatant was added to all wells, because R1T cells were highly IL-2 dependent and die upon IL-2 deprivation. Therefore, this assay measured IL-2 dependent proliferation of R1T cells unless the R1T cells were killed upon antigen presentation to irradiated RsL.11 responders. Cultures were pulsed with [^{3}H]thymidine on day 2 of a 3-day culture. IL2-NAg enhanced RsL.11 mediated T cell killing 1,000 fold greater than NAg alone with a half maximal killing response of 3.2 pM versus 3.2 nM respectively (Figure 3.14A). IFNβ-NAg and

IL4-NAg equally enhanced T cell killing 100 fold greater than NAg alone. MCSF-NAg and GMCSF-NAg did not target NAg to R1T APCs when compared to NAg.

RsL.11 mediated killing of R1T cells was dependent on NAg presentation by MHC class II expressed on R1T cells (Figure 3.14B). Co-cultures of R1T, irradiated RsL.11 responders, and antigen were grown in the presence or absence of the anti-RT1B mAb (OX6; anti-I-A). After 4 hours, 0.4% IL-2 baculovirus supernatant was added to all wells. Again, this assay measured IL-2 dependent proliferation of R1T cells unless the R1T cells were killed upon antigen presentation. Cultures were pulsed with [^{3}H]thymidine on day 2 of a 3-day culture. The monoclonal antibody against MHC class II blocked the RsL.11 mediated killing of R1T cells in the presence of NAg, IL2-NAg, and IL4-NAg (Figure 3.14B). This is shown by greater R1T proliferation (i.e., reduced R1T killing) in the presence of OX6. On the other hand, RsL.11 mediated killing of R1T cells in the presence of IFNβ-NAg was dependent on the cytokine itself and not the NAg presentation. Specifically, there was no difference between the RsL.11 mediated killing of R1T cells in the presence or absence of OX6. Overall, these data indicated that various cytokine-NAg fusion proteins could be used to target certain APC subsets and not others. GMCSF-NAg was the most efficient fusion protein for targeting NAg to DC and macrophage lineages, while IL4-NAg and IL2-NAg were the most efficient for targeting NAg to B cell and T cell APC respectively.

Cytokine-fusion proteins were also tested for their ability to target NAg to NK cells, because NK cells are postulated to regulate adaptive immune responses. Sorted CD161$^+$CD3$^-$ NK cells were cultured with 100 nM of NAg-IL16, IL2-NAg, MCSF-NAg, GMCSF-NAg, IL4-NAg, or GPMBP for 72 hours. After 72 hours, CFSE stained NAg-specific RsL.11 T cell clones were added to each culture. RsL.11 antigenic proliferative responses were analyzed by flow

cytometry after an additional 2 days of culture. CFSE (carboxyfluorescein succinimidyl ester) is a colorless dye that passively diffuses into cells and is cleaved by intracellular esterases to form a fluorescent product. Fluorescent CFSE is retained in cells by forming fluorescent conjugates with cellular amines. CFSE conjugates are vertically transferred through cell division, meaning that there is a successive loss of fluorescence with each cell division. In other words, cells that have divided will exhibit weaker fluorescence than those cells that have not undergone division. In this experiment, the antigenic response of RsL.11 T cells was measured by a successive loss of fluorescent CFSE upon each cell division. The peaks represent daughter cell populations of varying fluorescent intensities.

Cytokine-NAg fusion proteins were found to differentially target NAg to NK cells. Our data showed that NK cells could present NAg on MHC class II (Figure 3.15), which is contrary to the belief that NK cells do not function as antigen presenting cells. The RsL.11 proliferative response, represented by consecutive peaks of decreasing fluorescence, was potentiated by GMCSF-NAg, IL4-NAg, and NAg-IL16 in comparison to GPMBP. Specifically, in the presence of GMCSF-NAg and IL4-NAg, the RsL.11 proliferation profile was predominantly shifted to populations with lower fluorescence intensity, in comparison to GPMBP. Furthermore, the GPMBP profile exhibited 5 fluorescent peaks with intensities between 80 and 1000, while the GMCSF-NAg and IL4-NAg profile exhibited 3 fluorescent peaks with intensities ranging from 80 to 300. These data indicated that the majority of the CSFE labeled parental cells had undergone antigenic proliferation in the presence of GMCSF-NAg and IL4-NAg, but not in the presence of GPMBP. Note that the IL4-NAg data may be misleading because the fusion protein was added at 230 nM instead of 100 nM. NAg-IL16 exhibited only a slightly higher number of lower fluorescent intensity peaks than GPMBP, but exhibited a similar profile to GPMBP. IL2-

NAg and MCSF-NAg had a similar RsL.11 proliferation profile to GPMBP, represented by 5 fluorescent peaks with intensities between 80 and 1000. The potentiated NAg response by NAg-IL16, GMCSF-NAg, and IL4-NAg suggested that IL-16, GM-CSF, and IL-4 receptors mediated NAg uptake and presentation by NK cells. These data are significant because it reveals that NK cells should not be ignored when dissecting the mechanism of antigen-specific tolerance induced by GMCSF-NAg in our EAE models.

Figure 3.13: The cytokine domains of GMCSF-NAg and MCSF-NAg efficiently targeted NAg to myeloid APC subsets. Individual APC subsets (dendritic cell, macrophage, B cell and T cell APC) were cultured with cytokine-NAg fusion proteins to determine the ability of the APC to influence antigenic proliferation of RsL.11 T cells. Bone marrow cells were cultured with M-CSF (A) or GM-CSF (B) baculovirus supernatants (0.1% v / v) for 7 days and were used as APC. Bone marrow derived APC (15 x 10^3 / well) were cultured with RsL.11 T cells and 2.5 mM aminoguanidine in the presence of titrated proteins 100 nM - 100 fM. Aminoguanidine, a specific iNOS inhibitor, was added to circumvent nitric oxide production by macrophage and dendritic cell populations. (C & D) Splenic OX33$^+$ B cells (C) and OX33$^+$Ig$^+$ B cells (D) were FACS sorted and cultured (2.5 x 10^4 / well) with RsL.11 T cells plus titrated fusion proteins or NAg 100 nM - 100 fM. B cells sorted with surface Ig potentially activated the B cell population, resulting in a distinct targeting profile between B220$^+$ / surface Ig$^+$ B cells and B220$^+$ B cells. These data are representative of three experiments.
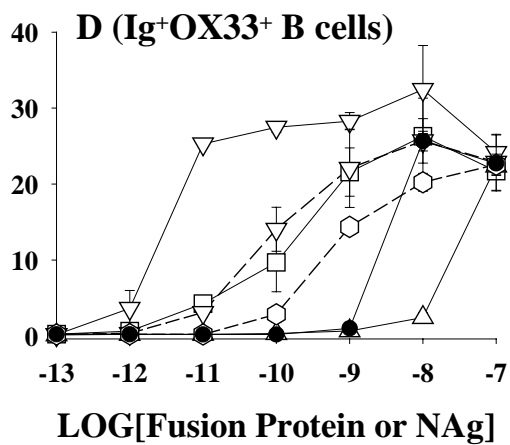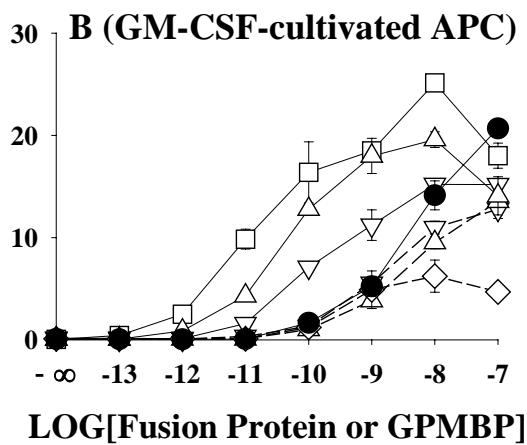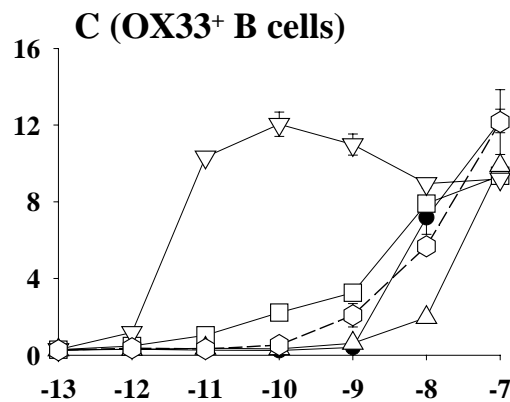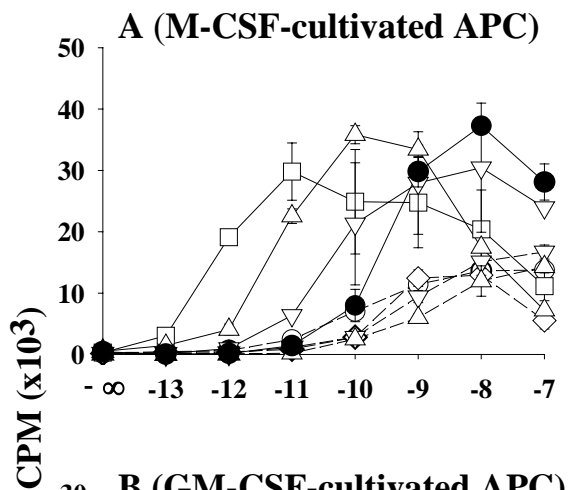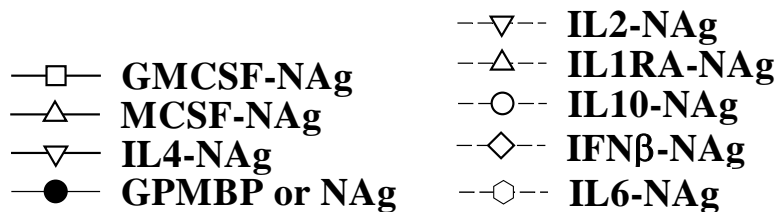
Figure 3.14: The cytokine domains of IL2-NAg and IL4-NAg efficiently targeted NAg to R1T T- cell APC. The specificity of GMCSF-NAg and MCSF-NAg to target macrophages and dendritic cells was supported by the inability of these fusion proteins to target NAg to MHC class II$^+$ T cell APC. This was revealed through a T cell killing assay, where irradiated RsL.11 T cells kill R1T cells (blastogenic MHC class II$^+$ T cells) that present NAg on MHC class II. (A & B) R1T cells were cultured for 24 hours in complete RPMI without IL-2 to allow clearance of IL-2 from cell surface receptors. R1T cells were then cultured with irradiated RsL.11 T responders in the presence of fusion protein or NAg that were titrated from 100 nM to 10 fM concentrations. After 4 hr, IL-2 (0.4% v / v IL2 bv supernatant) was added to all wells. This assay measured IL-2 dependent proliferation of R1T cells unless these T cell APC were killed upon antigen presentation to irradiated RsL.11 responders. Cultures were pulsed with [^{3}H]thymidine at 48 hours of a 3-day culture. (B) R1T, irradiated RsL.11 responders, and antigen were cultured in the presence or absence of the anti-RT1B mAb (OX6) (anti-I-A mAb). OX6 blocked RsL.11 mediated killing of R1T cells in the presence of NAg, IL2-NAg, and IL4-NAg. RsL.11 mediated killing of R1T in the presence of IFNβ-NAg was dependent on the cytokine itself and not the presentation of NAg. These data are representative of three experiments.

Legend:
- □— GMCSF-NAg
- △— MCSF-NAg
- ▽— IL4-NAg
- ●— GPMBP or NAg
- ▽-- IL2-NAg
- ◇-- IFNβ-NAg

A & B (MHCII⁺CD25⁺ T cells)

A

LOG[Fusion Protein or NAg]

B

- Fusion protein or NAg plus OX6
- Fusion protein or NAg

No antigen
IL2-NAg
IL4-NAg
IFNbeta-NAg
NAg

CPM (x10³)
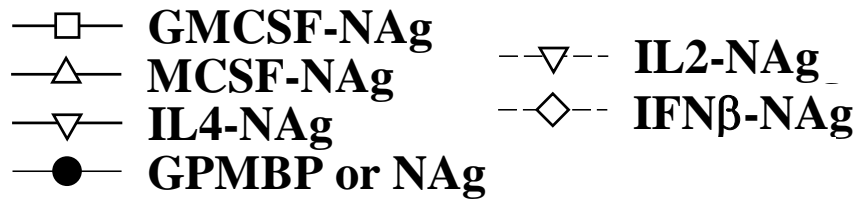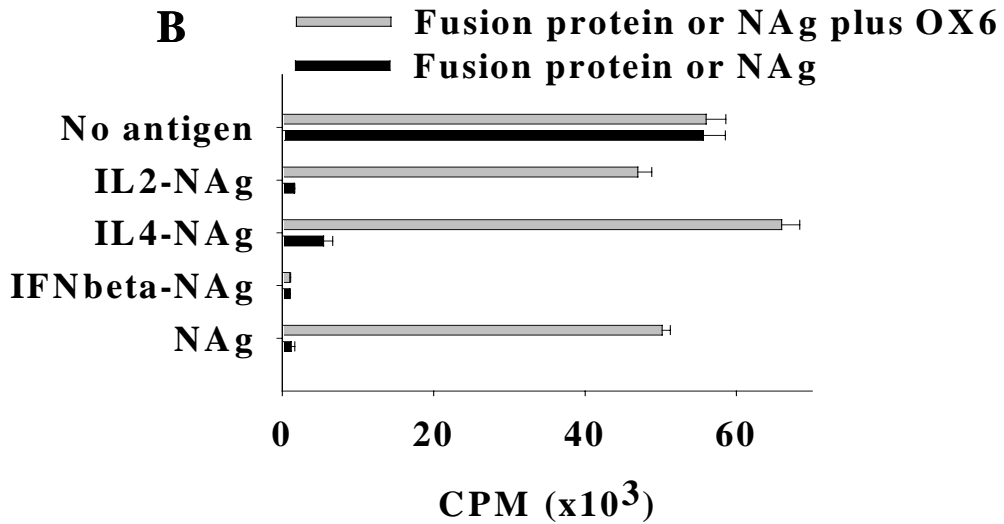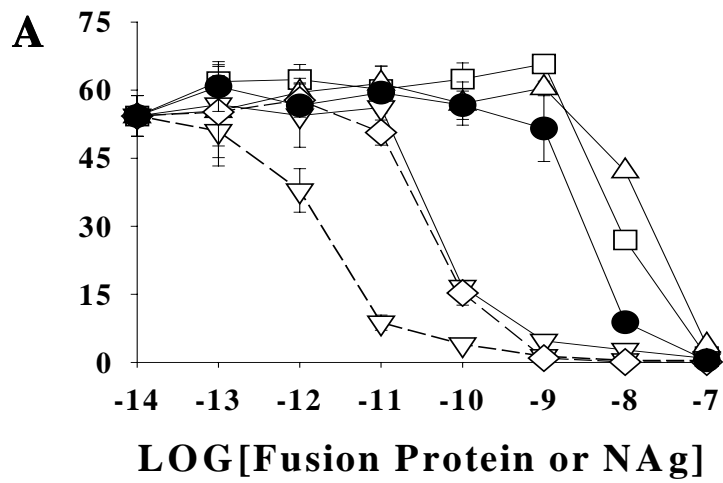
Figure 3.15: GMCSF-NAg enhanced antigenic proliferation of RsL.11 T cells by targeting NAg to NK cells. Our data showed that NK cells could present NAg on MHC class II and that cytokine-NAg fusion proteins were found to differentially target NAg to NK cells. Sorted CD161$^+$CD3$^-$ NK cells (96% pure population; 4.3x10^4 / well) were cultured with 100 nM of NAg-IL16, IL2-NAg, MCSF-NAg, GMCSF-NAg, IL4-NAg (IL4-NAg was mistakenly added at 230 nM instead of 100 nM), or GPMBP for 72 hours. After 72 hours, CFSE stained NAg-specific RsL.11 T cell clones (5x10^4) were added per well. RsL.11 antigenic proliferative responses were analyzed by flow cytometry after an additional 72 hours. CFSE (carboxyfluorescein succinimidyl ester) conjugates are transferred only through cell division, so cells that divide will exhibit weaker fluorescence than those cells that have not undergone cell division. CFSE was excited at 492 nm and emission was captured at 517 nm. This experiment was performed one time.
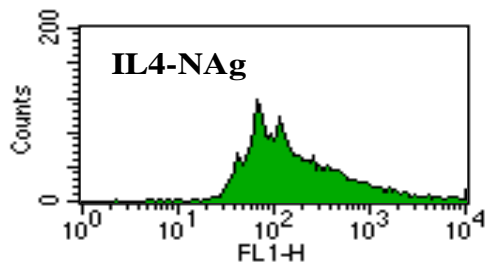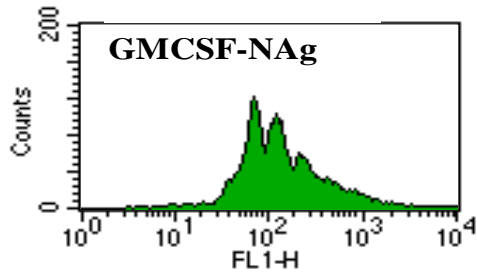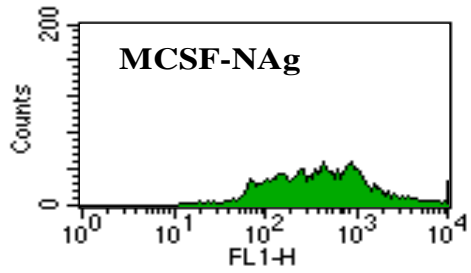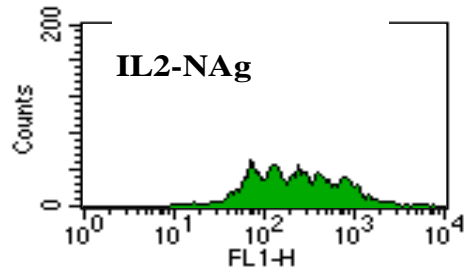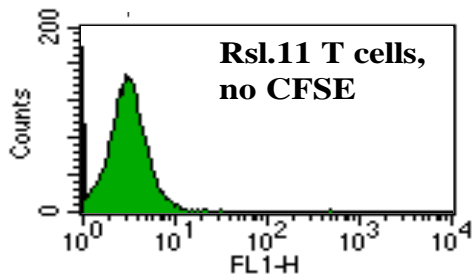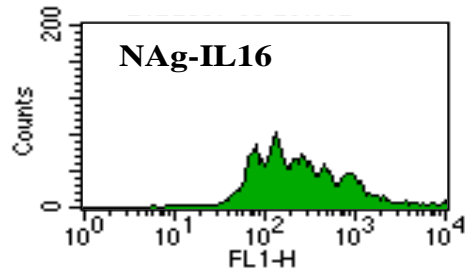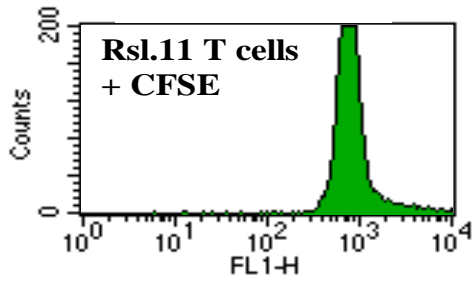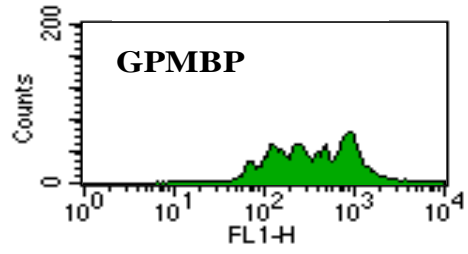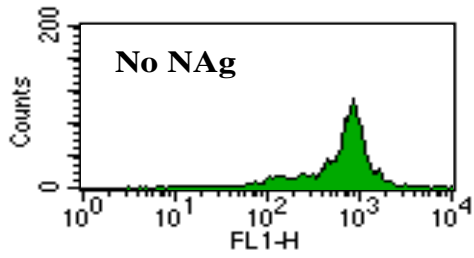
3.7 GMCSF-NAg AND MCSF-NAg PRE-TREATMENT REGIMENS WERE TOLEROGENIC IN EAE

EAE is the animal model for multiple sclerosis. EAE is a CD4$^+$ T cell mediated disease marked by inflammation in the CNS, resulting in demyelination and paralytic symptoms. EAE does not spontaneously occur in Lewis rats, and is therefore induced through subcutaneous immunization with an emulsion of NAg and complete Freund's adjuvant (incomplete Freund's adjuvant plus *Mycobacterium*). In Lewis rats, EAE presents as a monophasic disease characterized by an acute, paralytic disease from which the rats fully recover. EAE is marked by weight loss during disease onset and disease progression. EAE progression typically develops in the following order, distal limp tail, full limp tail, ataxic gait, partial hind limb paralysis, and full hind limb paralysis. Forelimb paralysis is not common. Relapses are rare, and if a relapse does occur it is typically mild, i.e. a distal limp tail or a full limp tail.

For safety concerns it was important to demonstrate that the cytokine domains of GMCSF-NAg and MCSF-NAg did not act as an adjuvant to induce EAE in the absence of CFA. Initially 1.5 nmole of GMCSF-NAg, MCSF-NAg, or IL6-NAg fusion proteins were administered to Lewis rats in the absence of CFA to assess whether the fusion proteins alone could induce EAE. GMCSF-NAg, MCSF-NAg, and IL6-NAg did not induce EAE in the absence of CFA (data not shown). We thoroughly tested the encephalitogenic potential of GMCSF-NAg and MCSF-NAg via a number of manipulations, such as increasing the administered concentration of GMCSF-NAg or MCSF-NAg from 1.5 nmoles to 8.0 nmoles, administering four boosters of GMCSF-NAg or MCSF-NAg at concentrations of either 1.5 nmoles or 8.0 nmoles, or injecting 8.0 nmoles of GMCSF-NAg and 8.0 nmoles of MCSF-NAg concurrently. Furthermore, we examined whether a subcutaneous versus intravenous delivery route of GMCSF-NAg or MCSF-

NAg (1.5 nmoles) influenced EAE development. Despite the manipulations, GMCSF-NAg, MCSF-NAg, or the combination of GMCSF-NAg and MCSF-NAg were unable to induce EAE in the absence of CFA (data not shown).

Moreover, it was important to determine if GMCSF-NAg and MCSF-NAg fusion proteins were on the cusp of being encephalitogenic in Lewis rats. If this were the case, then alternative adjuvants (other than CFA) might drive GMCSF-NAg and MCSF-NAg to become encephalitogenic. The encephalitogenic potentials of GMCSF-NAg and MCSF-NAg were examined in the presence of several adjuvants, including 400 ng alum (adjuvant approved for human use), 1.5 nmoles IL-2 (T cell growth factor), and 0.15 nmoles IL1-α (cytokine mediator of EAE). Pertussis toxin (200 ng and 500 ng) was also tested as an adjuvant with GMCSF-NAg and MCSF-NAg, for the reason that pertussis toxin is required, as an adjuvant, for the induction of EAE in mice. We also examined whether a subcutaneous versus an intraperitoneal delivery route of pertussis toxin (200 ng) influenced EAE development in the Lewis rat. Despite the aforementioned manipulations, alternative adjuvants did not drive GMCSF-NAg or MCSF-NAg to induce EAE in the absence of CFA (data not shown).

Next, we tested the potential of GMCSF-NAg in CFA and MCSF-NAg in CFA to induce EAE in comparison to NAg in CFA (Table 3.1). We hypothesized that GMCSF-NAg in CFA and MCSF-NAg in CFA could potentiate EAE due to the ability of GMCSF-NAg and MCSF-NAg to potentiate T cell responses *in vitro*. Lewis rats were challenged with 0.5 nmoles of GMCSF-NAg, MCSF-NAg, or NAg in CFA and monitored daily for symptoms of EAE. Rats challenged with GMCSF-NAg in CFA and MCSF-NAg in CFA exhibited less severe disease as compared to the rats that received NAg in CFA. For instance, 50% of the rats challenge with GMCSF-NAg developed EAE in comparison to the rats challenged with MCSF-NAg and NAg

in CFA, which exhibited full incidence of EAE. Furthermore, only 25% of the GMCSF-NAg challenged rats developed severe EAE as compared to the MCSF-NAg and NAg challenged rats that exhibited 75% and 100% incidence of severe EAE, respectively. Compared with NAg, GMCSF-NAg ($P \leq 0.001$ for all comparisons) and MCSF-NAg ($P \leq 0.038$ for all comparisons) significantly diminished mean cumulative scores, maximal scores and the number of days rats exhibited severe EAE. Overall, GMCSF-NAg emerged as a strong inhibitor of EAE, even more so than MCSF-NAg. The data from this experiment provided the first indication that GMCSF-NAg and MCSF-NAg could be tolerogenic. Furthermore, these data complimented the observations that GMCSF-NAg and MCSF-NAg do not induce EAE.

To further explore the tolerogenic potential of GMCSF-NAg and MCSF-NAg, the fusion proteins were administered to Lewis rats as a pre-treatment regimen prior to the induction of EAE. Rats were pretreated with 4.0 nmoles of NAg, MCSF-NAg or GMCSF-NAg on days 21, 14 and 7 before challenge with 50 µg DHFR-NAg in CFA on day 0. Rats were monitored daily for clinical manifestations of EAE, which included disease severity and weight loss. The NAg pre-treatment control group exhibited a typical disease progression characterized by severe EAE (ataxia, partial or full hind limb paralysis) on days 11.5 – 15 and significant weight loss (defined as a 10 - 20% weight loss) between days 14 and 23 (Figure 3.16). The daily group EAE scores and the daily percent maximal weight loss (Figure 3.16) showed that GMCSF-NAg (EAE scores: $P \leq 0.037$ for days 12 – 14; Weight loss: $P \leq 0.035$ for days 11 - 28) and MCSF-NAg (EAE scores: $P \leq 0.017$ for days 10.5, 12 – 13; Weight loss: $P \leq 0.042$ for days 15 - 22) pre-treatment regimens significantly reduced EAE severity when compared to the NAg pre-treatment group. GMCSF-NAg was significantly more protective than MCSF-NAg with respect to EAE scores ($P \leq 0.029$ on day 14) and EAE associated weight loss ($P \leq 0.029$ for days 16 - 23). More

specifically, GMCSF-NAg ($P \leq 0.001$) and MCSF-NAg ($P \leq 0.008$) pre-treatment groups exhibited considerably less severe EAE than the NAg pre-treatment group with respect to cumulative and maximal disease scores, incidence and duration of disease, and percentage weight loss (Table 3.2, combined experiments 1-3). GMCSF-NAg presented as a more profound inhibitor of EAE than MCSF-NAg ($P \leq 0.013$) with respect to cumulative and maximal disease scores, and percentage weight loss (Table 3.2, combined experiments 1-3). Overall, analysis of the pre-treatment regimens indicated that GMCSF-NAg was more effective than MCSF-NAg and NAg at inhibiting the development of severe EAE.

Next we examined whether the tolerogenic mechanism of GMCSF-NAg and MCSF-NAg, in Lewis rats, was dependent on the covalent linkage between cytokine and NAg domains. Rats were pretreated with 4.0 nmoles of NAg, MCSF-NAg, 'MCSF + NAg' as separate molecules, GMCSF-NAg or 'GM-CSF + NAg' as separate molecules on days 21, 14 and 7 before challenge with 50 μg DHFR-NAg in CFA on day 0. EAE severity and weight loss were assessed daily. As previously mentioned, the NAg pre-treatment control group exhibited a typical disease progression characterized by severe EAE (ataxia, partial or full hind limb paralysis) on days 11.5 – 15 and significant weight loss (10 - 20% weight loss) between days 14 and 23 (Figure 16). The 'GM-CSF + NAg' pre-treatment group exhibited significant weight loss between days 11 and 18, and a notable early onset of severe EAE beginning on day 9.5 and continuing through day 13. The 'M-CSF + NAg' group exhibited a more typical progression of EAE characterized by severe EAE on days 11.5 – 13.5 and significant weight loss on days 12 - 20 (Figure 3.17).

The tolerogenic mechanism of the GMCSF-NAg and MCSF-NAg pre-treatment regimens required covalent linkage between the cytokine and NAg domains (Figure 3.17 an

Table 3.2). Analysis of the daily group EAE scores and the daily percent maximal weight loss revealed that GMCSF-NAg was a significantly better tolerogen than the 'GMCSF + NAg' (EAE scores: $P \leq 0.002$ for days 9 - 12; Weight loss: $P \leq 0.029$ for days 9 - 19) and 'MCSF + NAg' (EAE scores: $P \leq 0.003$ for days 9,5, 11 − 13.5; Weight loss: $P \leq 0.012$ for days 12 - 21) pre-treatment regimens (Figure 3.17). In more detail, groups that received the GMCSF-NAg pre-treatment regimen exhibited significantly less severe disease than those that received 'GM-CSF + NAg' ($P \leq 0.001$) and 'M-CSF + NAg' ($P \leq 0.001$), regarding cumulative and maximal disease scores, incidence and duration of disease, and percentage weight loss (Table 3.2, combined experiments 1-3). Furthermore, the groups that received the MCSF-NAg pre-treatment regimen exhibited significantly less severe disease than those that received 'MCSF + NAg' ($P \leq 0.033$) and 'GMCSF + NAg' ($P \leq 0.008$) with respect to maximal disease scores, incidence and duration of disease, and percentage weight loss (Table 3.2, combined experiments 1-3). MCSF-NAg was additionally more tolerogenic than 'GM-CSF + NAg' ($P \leq 0.008$) with respect to the overall cumulative disease score. Analysis of the daily scores and weight changes (Figure 3.17) confirmed that MCSF-NAg was a significantly better tolerogen than 'GMCSF + NAg' (EAE scores: $P \leq 0.007$ for days 9 − 10.5; Weight loss: $P \leq 0.017$ for days 9 − 10, 12) and 'MCSF + NAg' (EAE scores: $P \leq 0.016$ on day 9.5). Altogether, these data showed that the tolerogenic nature of GMCSF-NAg and MCSF-NAg required covalent linkage between the cytokine and NAg domains, and was not due to the intrinsic activity of the cytokine alone.

Table 3.1: GMCSF-NAg and MCSF-NAg in CFA promoted a tolerogenic response when compared to NAg in CFA. We tested the potential of GMCSF-NAg in CFA and MCSF-NAg in CFA to induce EAE when compared to NAg in CFA. Lewis rats were challenged with 0.5 nmoles GMCSF-NAg, MCSF-NAg, or NAg in CFA. Rats were scored at daily for 4 weeks. Severe EAE was defined as the incidence of partial paralysis or full hind-limb paralysis. Rats challenged with GMCSF-NAg in CFA and MCSF-NAg in CFA exhibited less severe disease as compared to the rats that received NAg in CFA. Compared with NAg, GMCSF-NAg ($P \leq 0.001$ for all comparisons) and MCSF-NAg ($P \leq 0.038$ for all comparisons) significantly diminished mean cumulative scores, maximal scores and the number of days rats exhibited severe EAE. The data from this experiment provided the first indication that GMCSF-NAg and MCSF-NAg had tolerogenic potential. Statistical analyses were performed with one-way ANOVA with Bonferroni post-hoc tests. This experiment was performed one time.

Challenge	Incidence of EAE	Mean Cumulative Score	Median Cumulative Score	Mean Maximal Intensity	Median Maximal Intensity	Mean Day of Onset	Incidence of Severe EAE	Mean # Days with Severe EAE
NAg in CFA	5 of 5	10.6 ± 2.1	10.2	3.0 ± 0.0	2.8 ± 0.4	11.4 ± 0.9	5 of 5	3.2 ± 0.8
MCSF-NAg in CFA	4 of 4	5.0 ± 2.0	5	2.0 ± 0.8	2.2 ± 0.3	9.0 ± 6.0	3 of 4	1.5 ± 1.0
GMCSF-NAg in CFA	2 of 4	1.2 ± 1.6	0.6	0.6 ± 1.0	2.0 ± 0.0	6.5 ± 7.5	1 of 4	0.3 ± 0.5

Figure 3.16: GMCSF-NAg was a potent tolerogen that prevented the development of severe EAE. Rats were pre-treated with 4 nmoles of GMCSF-NAg, MCSF-NAg, and NAg on days -21, -14 and -7 days before challenge with 50 μg of DHFR-NAg in CFA on day 0. Rats were scored twice a day at approximate 12 hour intervals and weights were recorded daily. Shown are the time-courses of clinical scores (A) and weight loss (B) for experiment 1 (Table 3.2). The NAg pre-treatment control group exhibited a typical disease progression characterized by severe EAE (ataxia, partial or full hind limb paralysis) on days 11.5 – 15 and significant weight loss (defined as a 10 - 20% weight loss) between days 14 and 23. The daily group EAE scores and the daily percent maximal weight loss showed that GMCSF-NAg (EAE scores: $P \leq 0.037$ for days 12 – 14; Weight loss: $P \leq 0.035$ for days 11 - 28) and MCSF-NAg (EAE scores: $P \leq 0.017$ for days 10.5, 12 – 13; Weight loss: $P \leq 0.042$ for days 15 - 22) pre-treatment regimens significantly reduced EAE severity when compared to the NAg pre-treatment group. GMCSF-NAg was significantly more protective than MCSF-NAg with respect to EAE scores ($P \leq 0.029$ on day 14) and EAE associated weight loss ($P \leq 0.029$ for days 16 - 23). Statistical analyses were performed with one-way ANOVA with Bonferroni post-hoc tests.

GM CSF-NAg
M CSF-NAg
NAg

A

Severity of EAE

2.5
2.0
1.5
1.0
0.5
0.0

8   10   12   14   16   18

B

Percent Initial Weight

120
110
100
90
80

10 12 14 16 18 20 22 24 26 28

Days since encephalitogenic challenge
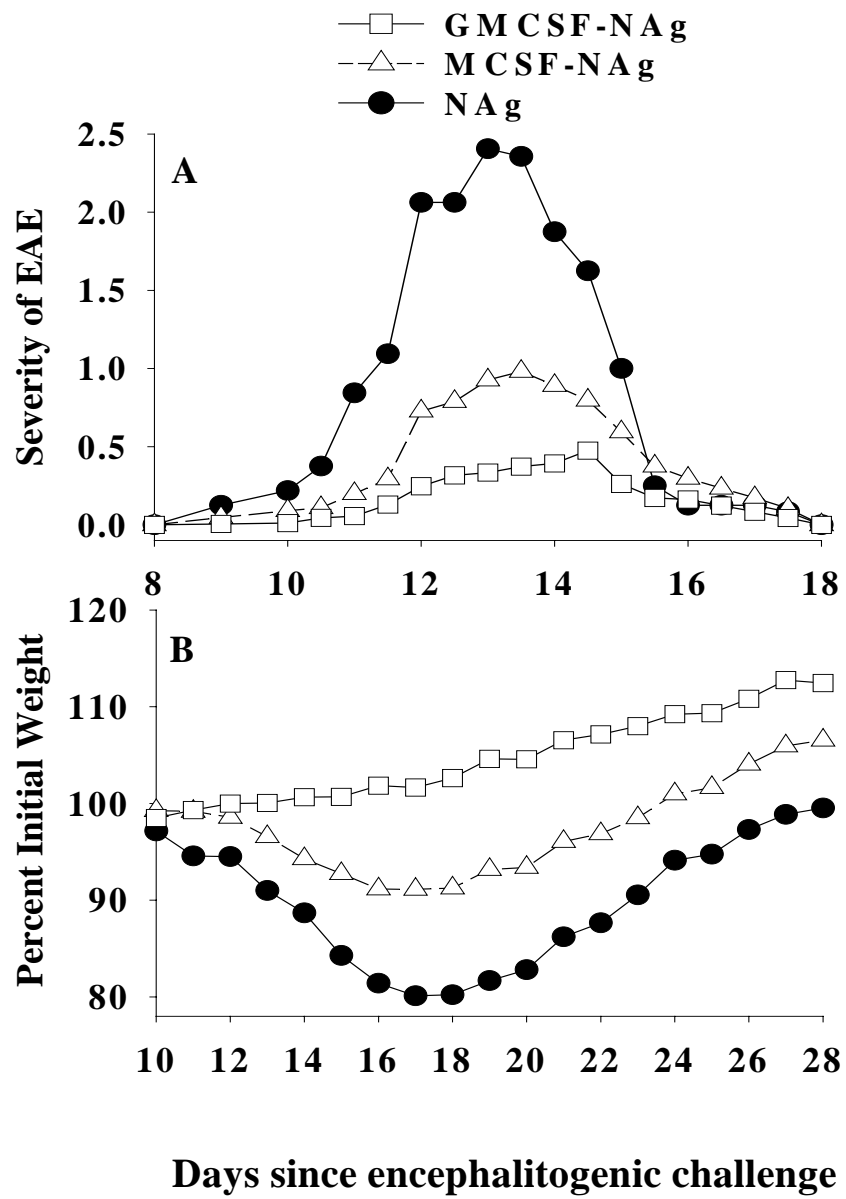
Table 3.2: GMCSF-NAg was a potent tolerogen that required covalent linkage between the cytokine and NAg domains when administered before encephalitogenic challenge. Rats were pre-treated with 4 nmoles of GMCSF-NAg, MCSF-NAg, NAg, 'GM-CSF + NAg' as separate molecules, and 'M-CSF + NAg' as separate molecules on days -21, -14 and -7 days before challenge on day 0. Rats were scored twice a day at approximate 12 hour intervals and weights were recorded daily. Severe EAE was defined by disease scores of 1.0 - 3.0. [b]Experiments 1-3 were combined for statistical analysis. Statistical significance with respect to cumulative and maximal disease scores, incidence and duration of disease, and percentage weight loss between pre-treatment groups is listed as follows: GMCSF-NAg ($P \leq 0.001$) and MCSF-NAg ($P \leq 0.008$) pre-treatment regimens were significantly more tolerogenic than NAg, the GMCSF-NAg pre-treatment regimens was significantly more tolerogenic than the 'GM-CSF + NAg' ($P \leq 0.001$) and 'M-CSF + NAg' ($P \leq 0.001$) regimens, and the MCSF-NAg pre-treatment regimen was significantly more tolerogenic than the 'MCSF + NAg' ($P \leq 0.033$) and 'GMCSF + NAg' ($P \leq 0.008$) regimens. GMCSF-NAg presented as a more profound inhibitor of EAE than MCSF-NAg ($P \leq 0.013$) with respect to cumulative and maximal disease scores, and percentage weight. No significant differences were noted among treatment groups regarding day of onset.

110

Exp.	Pre-Treatment [a]	Incidence	Mean Cum. Score	Median Cum. Score	Mean Max. Score	Median Max. Score	% Weight Loss	Incidence of Severe EAE	Mean # Days with Severe EAE
1	NAg	8 of 8	16.9 ± 5.8	17.3	2.8 ± 0.7	3.0	18.8 ± 5.5	8 of 8	2.9 ± 1.0
	MCSF-NAg	5 of 5	4.3 ± 0.9	4.0	0.8 ± 0.7	0.5	10.1 ± 2.9	1 of 5	0.2 ± 0.5
	GMCSF-NAg	5 of 5	1.8 ± 0.8	1.5	0.3 ± 0.0	0.3	0.6 ± 1.9	0 of 5	0.0 ± 0.0
2	NAg	7 of 7	15.4 ± 5.2	16.0	2.9 ± 1.0	3.0	17.2 ± 2.8	7 of 7	2.7 ± 0.9
	GM-CSF + NAg	4 of 4	14.9 ± 4.4	16.4	2.9 ± 0.3	3.0	15.9 ± 1.6	4 of 4	2.8 ± 0.3
	M-CSF + NAg	4 of 4	10.6 ± 4.0	11.6	2.5 ± 1.0	3.0	14.9 ± 1.7	4 of 4	2.3 ± 0.5
	MCSF-NAg	4 of 4	6.7 ± 3.7	7.8	2.1 ± 1.3	2.5	13.4 ± 2.1	3 of 4	1.4 ± 1.0
	GMCSF-NAg	4 of 4	1.3 ± 0.5	1.1	0.3 ± 0.1	0.3	5.3 ± 3.2	0 of 4	0.0 ± 0.0
3	NAg	6 of 6	12.5 ± 8.2	12.9	2.1 ± 1.0	2.5	18.0 ± 2.0	6 of 6	2.2 ± 1.2
	GM-CSF + NAg	6 of 6	14.9 ± 5.8	12.9	3.0 ± 0.0	3.0	17.7 ± 2.0	6 of 6	2.8 ± 0.9
	M-CSF + NAg	6 of 6	12.4 ± 7.3	13.9	2.3 ± 1.2	3.0	19.7 ± 1.6	5 of 6	2.3 ± 1.3
	MCSF-NAg	5 of 5	6.0 ± 7.0	2.7	1.2 ± 1.2	0.5	14.5 ± 1.3	2 of 5	1.0 ± 1.4
	GMCSF-NAg	2 of 6	0.5 ± 0.8	0.0	0.1 ± 0.1	0.0	7.8 ± 4.4	0 of 6	0.0 ± 0.0
1-3 [b]	NAg	21 of 21	15.1 ± 6.3	17.3	2.6 ± 0.7	3.0	17.9 ± 3.8	21 of 21	2.6 ± 1.0
	GM-CSF + NAg	10 of 10	14.9 ± 5.0	14.3	3.0 ± 0.2	3.0	17.0 ± 2.0	10 of 10	2.8 ± 0.7
	M-CSF + NAg	10 of 10	11.7 ± 6.0	12.8	2.4 ± 1.1	3.0	17.8 ± 2.9	9 of 10	2.3 ± 1.0
	MCSF-NAg	14 of 14	5.6 ± 4.4	4.1	1.3 ± 1.1	0.5	12.6 ± 2.8	6 of 14	0.8 ± 1.1
	GMCSF-NAg	11 of 15	1.2 ± 0.9	1.3	0.2 ± 0.1	0.3	5.0 ± 4.3	0 of 15	0.0 ± 0.0

Figure 3.17: The tolerogenic potential of GMCSF-NAg required covalent linkage between the GM-CSF and NAg domains. Rats were pre-treated with 4 nmoles of GMCSF-NAg, MCSF-NAg, a mixture of GM-CSF and NAg (GM-CSF + NAg), or a mixture of M-CSF and NAg (M-CSF + NAg) on days -21, -14 and -7 days before challenge day 0. Rats were scored twice a day at approximate 12 hour intervals and weights were recorded daily. Shown are the time-courses of clinical scores (A) and weight loss (B) for experiments 2 and 3 (reference Table 3.2). Analysis of the daily group EAE scores and the daily percent maximal weight loss revealed that GMCSF-NAg was a significantly better tolerogen than the 'GMCSF + NAg' (EAE scores: $P \leq 0.002$ for days 9 - 12; Weight loss: $P \leq 0.029$ for days 9 - 19), 'MCSF + NAg' (EAE scores: $P \leq 0.003$ for days 9,5, 11 – 13.5; Weight loss: $P \leq 0.012$ for days 12 - 21), and MCSF-NAg (EAE scores: $P \leq 0.02$ for days 13.5 and 14.5; Weight loss: $P \leq 0.012$ for days 14 - 20) pre-treatment regimens. MCSF-NAg was a significantly better tolerogen than 'GMCSF + NAg' (EAE scores: $P \leq 0.007$ for days 9 – 10.5; Weight loss: $P \leq 0.017$ for days 9 – 10, 12) and 'MCSF + NAg' (EAE scores: $P \leq 0.016$ on day 9.5). Together, these data showed that the tolerogenic nature of GMCSF-NAg and MCSF-NAg required covalent linkage between the cytokine and NAg domains, and was not due to the intrinsic activity of the cytokine alone.

GMCSF-NAg

GM-CSF + NAg
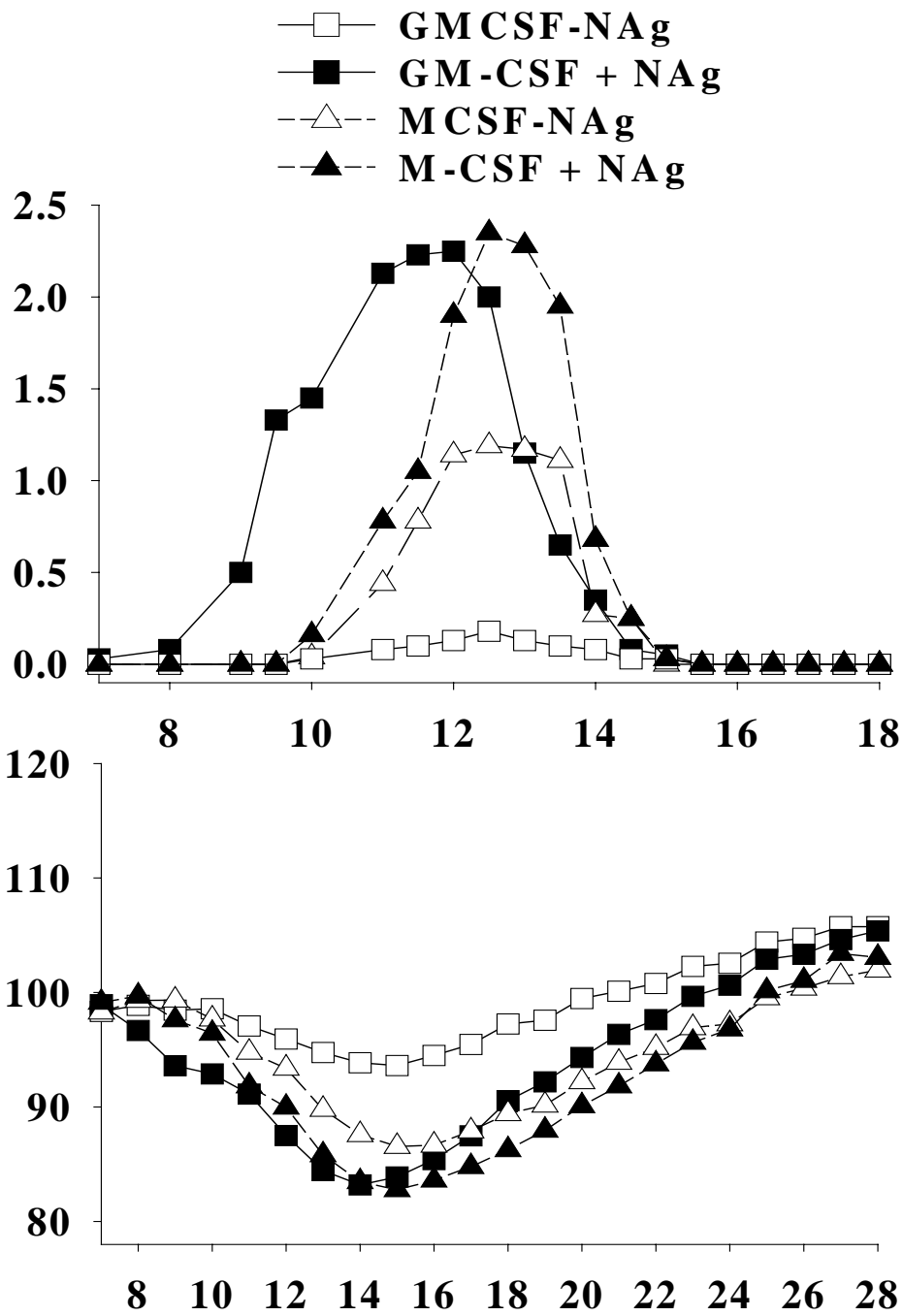
MCSF-NAg

M-CSF + NAg

3.8 GMCSF-NAg AND MCSF-NAg TREATMENT REGIMENS WERE TOLEROGENIC AFTER THE ONSET OF EAE

We additionally investigated whether the tolerogenic potential of GMCSF-NAg and MCSF-NAg could be utilized to treat Lewis rats with active EAE. GMCSF-NAg was emphasized in the treatment experiments due to its greater tolerogenic potential than MCSF-NAg, as seen in the pre-treatment experiments. In the treatment experiments, rats were challenged subcutaneously with 50 μg DHFR-NAg in CFA at the base of the tail on day 0 (Table 3.3, experiments 1 – 3) with an additional administration of 400 ng pertussis toxin intraperitoneally on days 0 and 1 (Table 3.3, experiment 3). Pertussis toxin was administered to induce hyperacute EAE, a more severe form of EAE characterized by severe paralytic disease and high mortality. The hyperacute model was examined because it presented a more rigorous test for the tolerogenic activity of GMCSF-NAg. Rats were monitored for the early manifestations of EAE (distal limp and full limp tail). On the day of initial treatment, rats were matched into treatment groups based on early clinical signs of EAE. In other words, the rats matched in one treatment group exhibited an average disease score comparable to the rats in another treatment group. Rats were treated with equal molar doses of MCSF-NAg, GMCSF-NAg, 'GM-CSF + NAg' as separate molecules or NAg alone. Specifically, the rats in experiment 1 and 2 (Table 3.3) were treated with 1 nmole of designated protein (s) on days 9, 10, 12, and 14 (experiment 1), and on days 10, 11 and 13 (experiment 2). The rats in experiment 3 (Table 3.3) were treated with 4 nmoles on day 8 and 1 nmole on day 11. The variations in dose concentration and treatment duration between experiments 1, 2, and 3 were made to assess the minimum number of doses required to induce tolerance.

114

Rats were monitored for clinical manifestations of EAE, which included EAE severity and weight loss. The GMCSF-NAg treatment was significantly more protective than 'GM-CSF + NAg' ($P \leq 0.020$), or NAg ($P \leq 0.004$) with respect to cumulative and maximal disease scores, incidence and duration of disease, and percentage weight loss (Table 3.3, combined experiments 1 - 3). Additionally, MCSF-NAg was significantly more protective than NAg ($P < 0.05$) with respect to cumulative and maximal disease scores, incidence and duration of disease, and percentage weight loss (Table 3.3, experiment 1). There was no significant difference between the MCSF-NAg and GMCSF-NAg treatment groups. Overall, these data indicated that GMCSF-NAg must be covalently linked in order to effectively block the development of severe EAE. The treatment duration of 4 days versus 3 days between experiments 1 and 3 (Table 3.3) respectively did not influence the treatment outcome. The GMCSF-NAg treatment regimen for experiment 3 (Table 3.3) appeared to be slightly less effective than the regimens for experiments 1 and 2. This difference is mostly like due to the fact that experiment 3 tested the ability of GMCSF-NAg to induce tolerance in the hyperacute EAE model (DHFR-NAg in CFA plus pertussis toxin), a more severe EAE model, in comparison with the traditional EAE model (DHFR-NAg in CFA) studied in experiments 1 and 2. The fact that GMCSF-NAg was tolerogenic in both the traditional and hyperacute EAE models supports the idea that GMCSF-NAg is a potent tolerogen.

The daily group EAE scores (experiments 1 – 3 combined) and the daily percent maximal weight changes (experiments 1 – 3 combined) for rats treated with GMCSF-NAg, 'GM-CSF + NAg', or NAg also indicated that EAE severity was significantly diminished by the GMCSF-NAg treatment regimen (Figure 3.18). The NAg treatment control group exhibited severe EAE (ataxia, partial or full hind limb paralysis) on days 10.5 – 12.5 and significant weight loss (10 -

25% weight loss) between days 11 and 18 (Figure 3.18). The 'GM-CSF + NAg' treatment group exhibited severe EAE on days 12.5 – 13.5 and significant weight loss (10 - 25% weight loss) between days 11 and 18. The GMCSF-NAg group exhibited significant weight loss between days 12 and 17, but did not exhibit severe EAE. In comparison of the daily average scores, all treatment groups exhibited some reduction of EAE severity. Typically, the average peak of EAE severity for a no treatment control group would be between a score of 2 – 3 (data not shown). Yet EAE severity for the NAg treatment group peaked at a score of ~1.4 on day 11.5, the 'GM-CSF + NAg' treatment group peaked at ~1.2 on day 13, and the GMCSF-NAg peaked at a score of 0.5. Overall, GMCSF-NAg was a more significant tolerogen than 'GM-CSF + NAg' (EAE scores: $P \leq 0.022$ for days 11 – 13.5; Weight loss: $P \leq 0.022$ for days 12, 13, 15 – 18) or NAg (EAE scores: $P \leq 0.015$ for days 10 – 12.5; Weight loss: $P \leq 0.007$ for days 12, 13, 15 – 18), indicating that the effectiveness of GMCSF-NAg treatment was due to covalent linkage between GM-CSF and NAg. This experiment showed that GMCSF-NAg could promote antigen-specific tolerance under inflammatory conditions, which contradicts the dogma that tolerance can only be induced in the steady state.

Table 3.3: GMCSF-NAg was a potent tolerogen that required covalent linkage between the cytokine and NAg domains when administered during the onset of EAE. [a]Rats were challenged with 50 μg of DHFR-NAg in CFA on day 0 (experiments 1-3) and also with pertussis toxin (400 ng i.p.) on days 0 and 1 (experiment 3). During disease onset, rats were matched for clinical signs of EAE such that the rats in one treatment group exhibited an average disease score comparable to the rats in another treatment group. The range of average clinical scores per group for experiments 1 - 3 respectively was 0.36 - 0.39, 0.28 - 0.29, and 0.29 on the day of the initial treatment. Rats were treated with 1 nmole of the designated proteins on days 9, 10, 12, and 14 (experiment 1), days 10, 11 and 13 (experiment 2), or 4 nmoles on day 8 and 1 nmole on day 11 (experiment 3). GM-CSF and NAg in the 'GMCSF + NAg' regimen were administered as a mixture of equal molar doses. [b]Experiment 1: MCSF-NAg was significantly more protective than NAg with respect to mean and median cumulative scores ($P \leq 0.003$), mean and median maximal scores ($P < 0.05$), percent weight loss ($P < 0.001$), the incidence of severe EAE ($P = 0.0256$), and mean number of days with severe EAE ($P < 0.001$) (experiment 1). [c]Combined experiments 1 – 3: The GMCSF-NAg treatment was significantly more protective than 'GM-CSF + NAg' ($P \leq 0.020$), or NAg ($P \leq 0.004$) with respect to cumulative and maximal disease scores, incidence and duration of disease, and percentage weight loss.

Exp.	Treatment [a]	Incidence	Mean Cum. Score	Median Cum. Score	Mean Max. Score	Median Max. Score	% Weight Loss	Incidence of Severe EAE	Mean # Days with Severe EAE
1 [b]	NAg	7 of 7	9.4 ± 3.3	8.3	2.4 ± 0.8	3.0	20.3 ± 3.0	7 of 7	2.1 ± 0.5
	MCSF-NAg	8 of 8	3.6 ± 2.4	2.6	1.1 ± 1.2	0.4	13.7 ± 4.5	3 of 8	0.4 ± 0.7
	GM-CSF + NAg	8 of 8	4.4 ± 2.2	3.5	1.0 ± 1.0	0.5	20.9 ± 2.4	3 of 8	0.5 ± 0.8
	GMCSF-NAg	9 of 9	2.8 ± 0.8	2.5	0.6 ± 0.6	0.5	12.7 ± 3.8	2 of 9	0.1 ± 0.2
2	NAg	9 of 9	6.4 ± 5.1	4.5	1.6 ± 1.1	1.0	18.2 ± 2.6	7 of 9	1.7 ± 1.5
	GM-CSF + NAg	7 of 7	9.0 ± 5.7	11.0	2.1 ± 1.2	3.0	21.3 ± 3.6	5 of 7	1.6 ± 1.5
	GMCSF-NAg	8 of 8	2.2 ± 0.5	2.3	0.4 ± 0.1	0.4	13.6 ± 2.2	0 of 8	0.0 ± 0.0
3	NAg	6 of 6	9.2 ± 6.9	6.4	1.9 ± 1.2	2.0	26.2 ± 2.9	5 of 6	1.8 ± 1.3
	GM-CSF + NAg	7 of 7	10.6 ± 5.3	10.8	2.4 ± 1.0	3.0	25.1 ± 1.7	7 of 7	1.9 ± 0.8
	GMCSF-NAg	7 of 7	5.1 ± 3.6	3.5	1.4 ± 1.2	1.0	19.8 ± 4.7	5 of 7	0.6 ± 0.7
1-3 [c]	NAg	22 of 22	8.1 ± 5.1	6.6	2.0 ± 1.1	2.0	21.1 ± 4.3	19 of 22	1.8 ± 1.2
	GM-CSF + NAg	22 of 22	7.8 ± 5.2	6.1	1.8 ± 1.2	2.0	22.3 ± 3.2	15 of 22	1.3 ± 1.2
	GMCSF-NAg	24 of 24	3.3 ± 2.3	2.6	0.8 ± 0.8	0.5	15.1 ± 4.7	7 of 24	0.2 ± 0.5

Figure 3.18: GMCSF-NAg required covalent linkage between the cytokine and NAg domains to effectively block the progression of EAE when treatment was initiated after disease onset. Rats were challenged with 50 μg of DHFR-NAg in CFA on day 0 (experiments 1 - 3) and with pertussis toxin (400 ng i.p.) on days 0 and 1 (experiment 3). On the day of initial treatment, rats were matched into treatment groups based on clinical signs of EAE. Rats were treated with 1 nmole of the designated proteins on days 9, 10, 12, and 14 (experiment 1), days 10, 11 and 13 (experiment 2), or 4 nmoles on day 8 and 1 nmole on day 11 (experiment 3). Shown are the compiled time-course data for clinical EAE scores (A) and weight loss (B) for experiments 1, 2, and 3 of Table 3.3. GMCSF-NAg was a more significant tolerogen than 'GM-CSF + NAg' (EAE scores: $P \leq 0.022$ for days $11 - 13.5$; Weight loss: $P \leq 0.022$ for days 12, 13, $15 - 18$) or NAg (EAE scores: $P \leq 0.015$ for days $10 - 12.5$; Weight loss: $P \leq 0.007$ for days 12, 13, $15 - 18$), indicating that the effectiveness of GMCSF-NAg treatment was due to covalent linkage between GM-CSF and NAg.
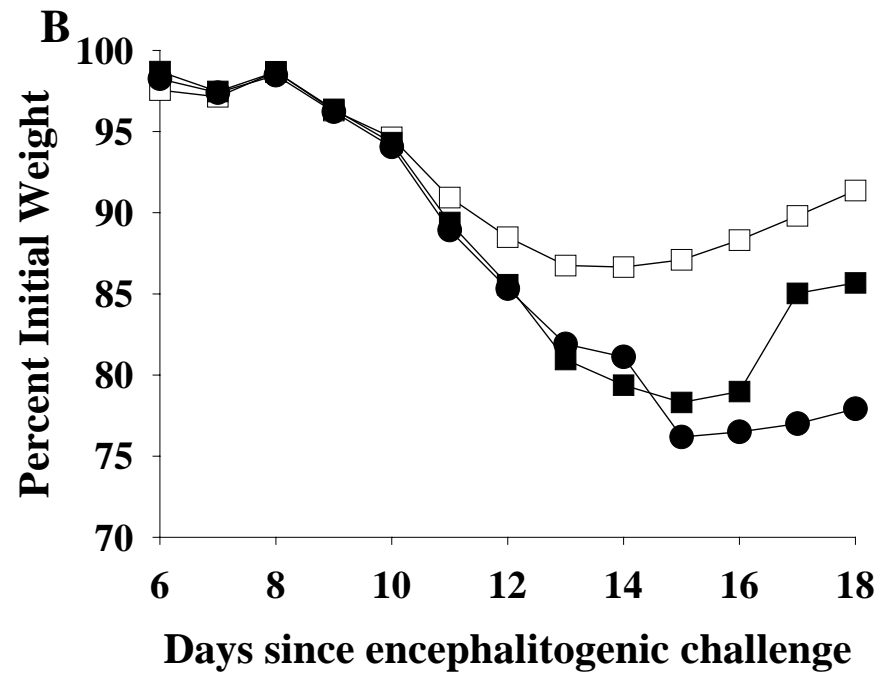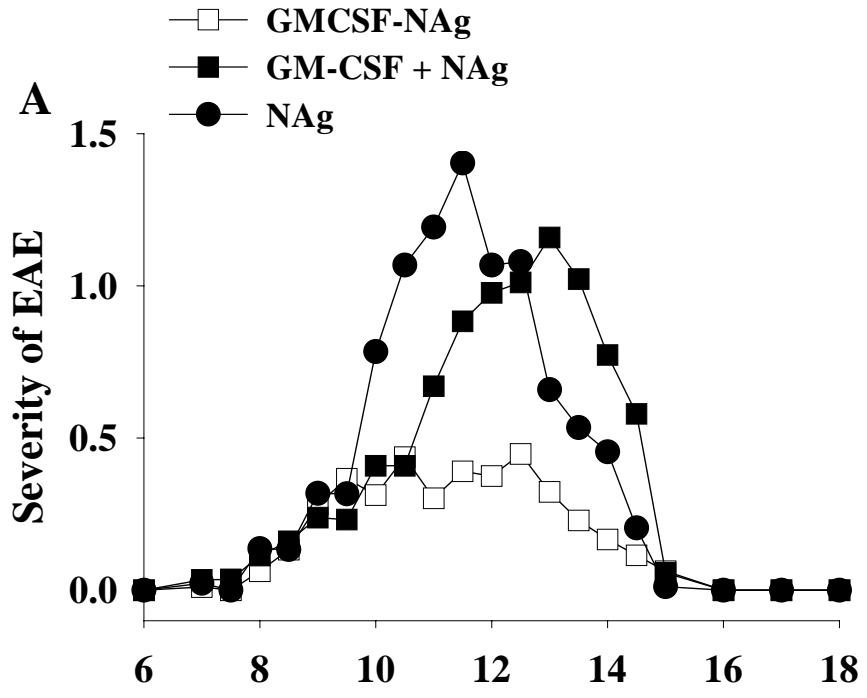
3.9 GMCSF-NAg DID NOT ENHANCE NAg SPECIFIC ANTIBODY PRODUCTION

EAE results from cell mediated damage against neuroantigens in the CNS, however the presence of neuroantigen-specific antibodies can exacerbate EAE. Therefore, antibody production against neuroantigens is an important consideration in the pathogenesis of EAE. We examined whether pre-treatment with NAg, GMCSF-NAg, or MCSF-NAg prior to encephalitogenic challenge (50 μg DHFR-NAg in CFA on day 0) significantly altered antibody production against NAg (Figure 3.19A). Serum samples were obtained from terminal bleeds of GMCSF-NAg and MCSF-NAg pretreated rats from experiment 1 (Table 3.2 and Figure 16). Terminal bleeds were performed four weeks post-challenge, when the rats had fully recovered from EAE. ELISA was used to analyze serum IgG and IgM reactivity against NAg. NAg ($P \leq$ 0.005) and MCSF-NAg ($P \leq$ 0.002) pre-treatments resulted in significant decrease in antibody between the titration points of 1 / 1,000 and 1 / 10,000 when compared to the no pre-treatment control serum. GMCSF-NAg ($P \leq$ 0.002) pre-treatment also resulted in a significant decrease in antibody between the titration points of 1 / 10 and 1 / 1,000 when compared to the no pre-treatment control serum. For all samples, the serum reactivity against NAg titrated to 1 / 10,000. These data showed that pre-treatment with NAg, MCSF-NAg, and GMCSF-NAg did not enhance NAg specific antibody production.

Next we examined whether the GMCSF-NAg, GM-CSF, 'GM-CSF + NAg', or NAg treatment regimens altered NAg specific antibody titers (Figure 3.19B). Rats were challenged with 50 μg DHFR-NAg in CFA on day 0 and subsequently monitored for the early manifestations of EAE (distal limp and full limp tail). On the day of initial treatment, rats were matched into treatment groups based on early clinical signs of EAE. Rats were treated with equal molar doses of GMCSF-NAg, 'GM-CSF + NAg' as separate molecules, GM-CSF, or NAg

on days 9, 10, 12, and 14 (Table 3.3, experiment 1). Terminal bleeds were performed four weeks post-challenge, when the rats had fully recovered from EAE. ELISA was used to analyze serum IgG and IgM reactivity against NAg. GM-CSF ($P \leq 0.006$), 'GM-CSF + NAg' ($P \leq 0.001$), and GMCSF-NAg ($P < 0.001$) treatments resulted in significant decrease in antibody between the titration points of 1 / 100 and 1 / 1,000 when compared to the no treatment control serum. The NAg ($P \leq 0.002$) treatment alone resulted in a significant decreased antibody at 1 / 100 when compared to the no treatment control serum. For all samples, the serum reactivity against NAg titrated to 1 / 10,000. These data showed that treatment with NAg, GMCSF-NAg, 'GM-CSF + NAg' as separate molecules, GM-CSF, or NAg did not enhance NAg specific antibody production.

Figure 3.19: Pre-treatment and treatment with GMCSF-NAg does not enhance NAg specific antibody production in Lewis rats. Terminal bleeds were performed four weeks post-challenge, when the rats had fully recovered from EAE. ELISA was performed to test serum reactivity against NAg. Goat anti-rat IgM+ IgG conjugated to NPP was used as the secondary antibody to detect rat serum reactive to the NAg peptide. (A) Rats were pre-treated with 4 nmoles of GMCSF-NAg, MCSF-NAg, or NAg on days -21, -14 and -7 days before challenge on day 0. Serum samples were obtained from terminal bleeds of pretreated rats from experiment 1 (Table 3.2). The NAg ($P \leq 0.005$) and MCSF-NAg ($P \leq 0.002$) pre-treatment resulted in a significant decrease in antibody titers between 1 / 1,000 and 1 / 10,000 when compared to the no pre-treatment control serum. Titers from the GMCSF-NAg ($P \leq 0.002$) pre-treatment group were significantly diminished between 1 / 10 and 1 / 1,000 when compared to the no pre-treatment control serum. These data were representative of two experiments. (B) Rats were challenged on day 0. On the day of initial treatment, rats were matched into treatment groups based on clinical signs of EAE. Rats were treated with 1 nmole of the GMCSF-NAg, 'GM-CSF + NAg', GM-CSF, or NAg on days 9, 10, 12, and 14 post-challenge (Table 3.3, experiment 1). GM-CSF ($P \leq 0.006$), 'GM-CSF + NAg' ($P \leq 0.001$), and GMCSF-NAg ($P < 0.001$) treatments resulted in a significant decrease in antibody titers between 1 / 100 and 1 / 1,000, while antibody titers from the NAg ($P \leq 0.002$) treatment only resulted in a significant decreased antibody at 1 / 100 when compared to the no treatment control serum. This experiment was performed once.
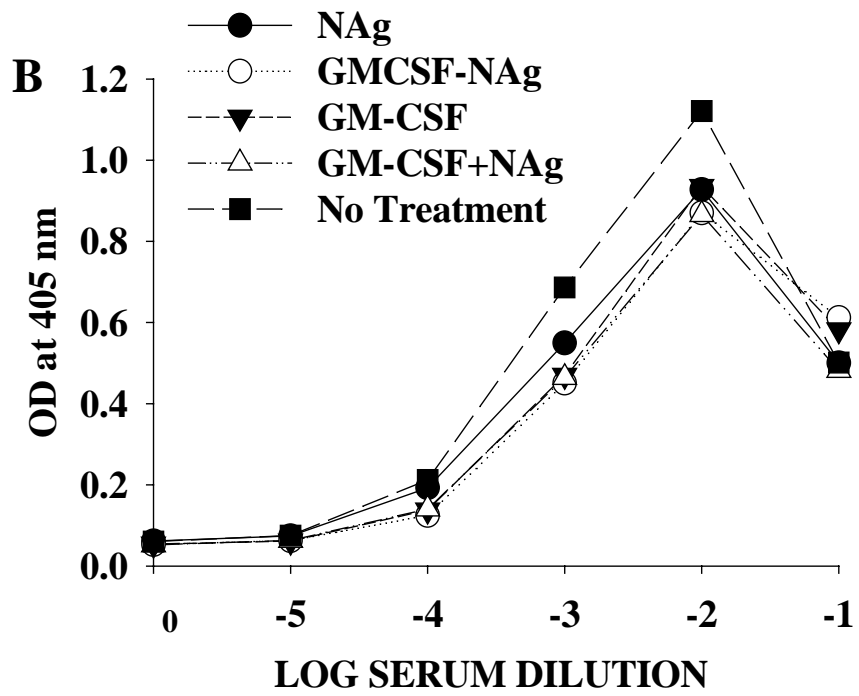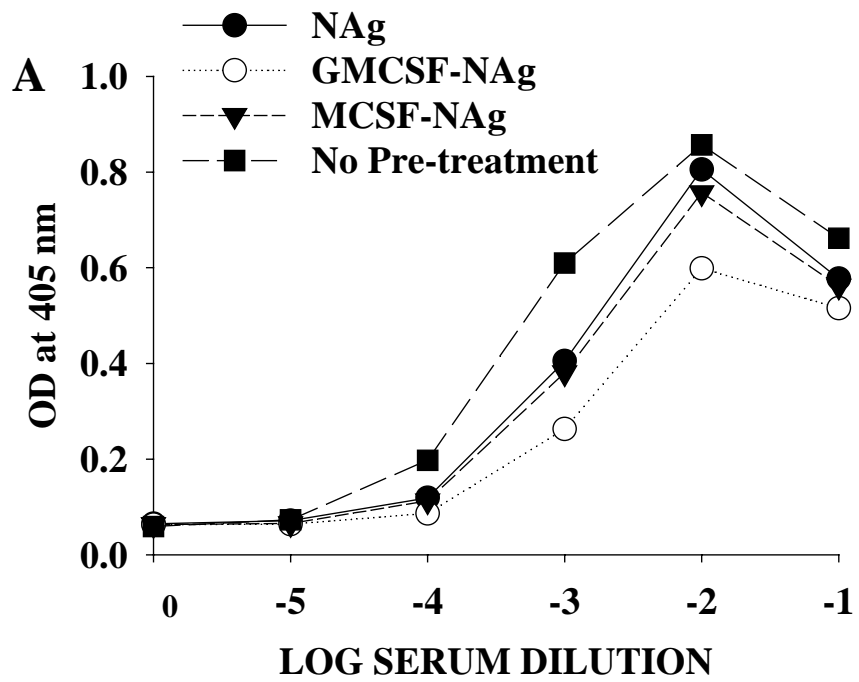
3.10 GENERATION OF IL2-NAg-GFP CONSTRUCTS

We have designed GFP tagged cytokines as tools for potential applications that might involve tracking specific cell populations by immunohistochemistry or flow cytometry. We have engineered and expressed five GFP tagged cytokines, including GMCSF-NAg-GFP, MCSF-NAg-GFP, GFP-NAg-IL16, IL4-NAg-GFP, and IL2-NAg-GFP. Only the experiments describing the IL2-NAg-GFP data will be presented because it was the most successfully studied fusion protein. The significance of IL2-NAg-GFP fusion proteins lies with the ability of IL-2 to target GFP to T cells bearing a functional IL-2 receptor. The capacity of IL2-NAg-GFP to label T cells could be utilized in studies that examine the localization of encephalitogenic T cells or regulatory T cells.

The IL2-NAg-GFP fusion protein was constructed by covalently linking the genes encoding GFP and IL2-NAg (previously generated on the pFastBac-1 plasmid) by a two-step, overlap and extension PCR. The overlap and extension PCR was performed with NAg-GFP fusion primers. The sequences of the upstream fusion primers (60 base pairs in length) contained a 5' end complimentary to the NAg domain and a 3' end complimentary to the N-terminus of the GFP domain. The downstream primer (69 base pairs in length) was composed of a 5' – 3' sequence that complimented the pFastBac-1 plasmid sequence, a stop codon, the C-terminal histidine tag of IL2-NAg, 2 additional histidine residues, and a 3' end that complimented C-terminus of the GFP domain. Ultimately, the upstream and downstream primers converged at the GFP domain. In the first PCR step, GFP was amplified from the pKB2 plasmid (encoding GFP) using the NAg-GFP (2850) upstream fusion primer plus the downstream GFP fusion primer (2852). The predicted amplification product of the first step PCR was 795 base pairs, which ran out around the 800 base pair standard on the agarose gel (Figure 3.20). The high

molecular weight band (~1,600 base pairs) seen in the gel could have been the result of dimerized GFP PCR products.

In the second PCR step, the amplified GFP product served as the extension primer. The GFP PCR product encoded NAg, GFP, an 8 histidine tag, a stop codon, and a portion of the pFastBac-1 plasmid sequence. The GFP PCR product was extended into the parental pFastBac-1 plasmid encoding IL2-NAg. The resulting product was ~5.9 kilobases in length and fell around the 4361 base pair Hind III fragment (Figure 3.21). Parental plasmids remaining in the extension reaction were digested with DpnI prior to transformation. The digestion was performed to increase transformation efficiency of the IL2-NAg-GFP extension product into electrocompetent Top10 *E. coli* by digesting away the parental plasmid. Restriction enzyme digestion of the extension product did not result in visible digest products of parental plasmid, presumably due to the low level of contaminating parental plasmid. Therefore, positive and negative controls, i.e. parental plasmid in the presence or absence of restriction enzyme, were run to test for enzyme reactivity. Colonies of Top10 *E. coli* transformed with pFastBac-1 plasmids were selected in ampicillin, and PCR screened for the presence of GFP (Figure 3.22). Colonies were screened with the upstream NAg-GFP fusion primer (2850) and the downstream GFP fusion primer (2852). Colonies that were positive for IL2-NAg-GFP yielded an amplicon around 800 base pairs. Plasmids were isolated from the GFP positive colonies, and were subsequently sequenced. No point mutations were identified in the IL2-NAg-GFP fusion construct. Asterisks denoted the colony that contained the IL2-NAg-GFP construct without mutation.

Figure 3.20: Amplification of GFP using NAg-GFP fusion primers. IL2-NAg-GFP fusion

proteins were generated by a 2 step PCR process. In the first PCR step, GFP was amplified

using an upstream primer that consisted of two domains. The 5' domain was complimentary to

the NAg domain and a 3' domain complimentary to the N-terminus of GFP. The 5' to 3'

sequence of the downstream primer complemented the pFastBac-1 plasmid sequence, a stop

codon, the C-terminal his-tag of IL2-NAg, and the C-terminus of the GFP domain. The

predicted band size for the GFP amplicon was 795 base pairs, which ran near the 800 base pair

standard on the 1.0 % agarose gel. Lane 1 contained the 100-base pair ladder. Lanes 2 - 4

contained the GFP PCR products run on the gel in triplicate.
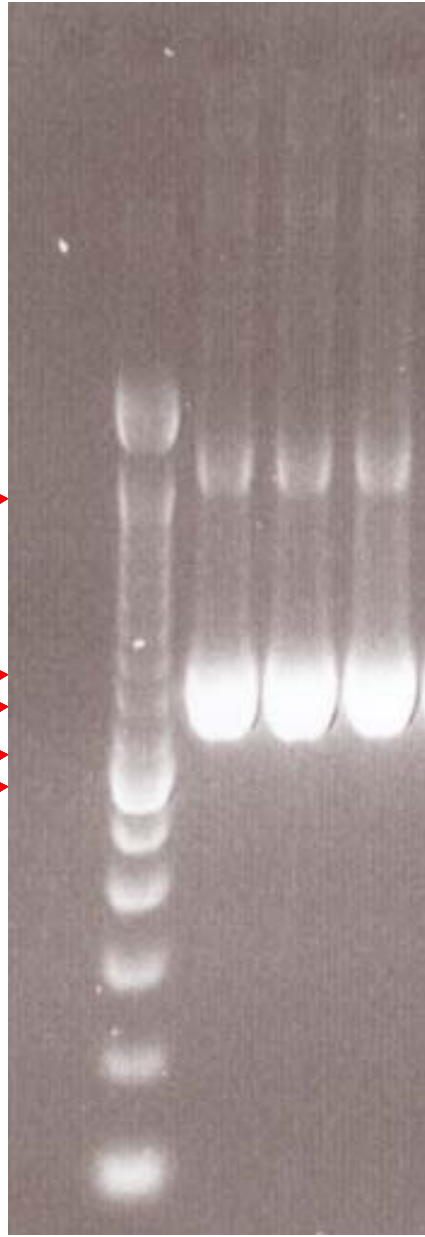
Figure 3.21: Extension of GFP into the pFastBac-1 plasmid encoding IL2-NAg. IL2-NAg-GFP fusion proteins were generated by a 2-step PCR process. In the second PCR step, the amplified GFP PCR product, from Figure 3.20, served as the extension primer. The GFP amplicon encoded for NAg, GFP, an 8 his-tag, a stop codon, and a portion of the pFastBac-1 plasmid sequence. Lane 2, GFP was extended into the pFastBac-1 plasmid encoding IL2-NAg, as shown by generation of the high molecular weight product of approximately 5.9 kb. Methylated parental plasmids (without the GFP insert) were digested from the extension reaction with the Dpn I restriction enzyme. Lane 4 showed the DpnI digest product from the IL2-NAg-GFP extension reaction. Lanes 5 and 6 served as controls for the restriction enzyme digest. Lane 6 showed the GM-CSF pFastBac-1 parental plasmid digested with DpnI (positive control) and GM-CSF parental plasmid in the absence of Dpn I (negative control). Lanes 1 and 3 contained the Hind III molecular weight standards on the 1.0 % agarose gel. The high molecular weight band of IL2-NAg-GFP appeared as high molecular weight band above the 4361 base pair standard.
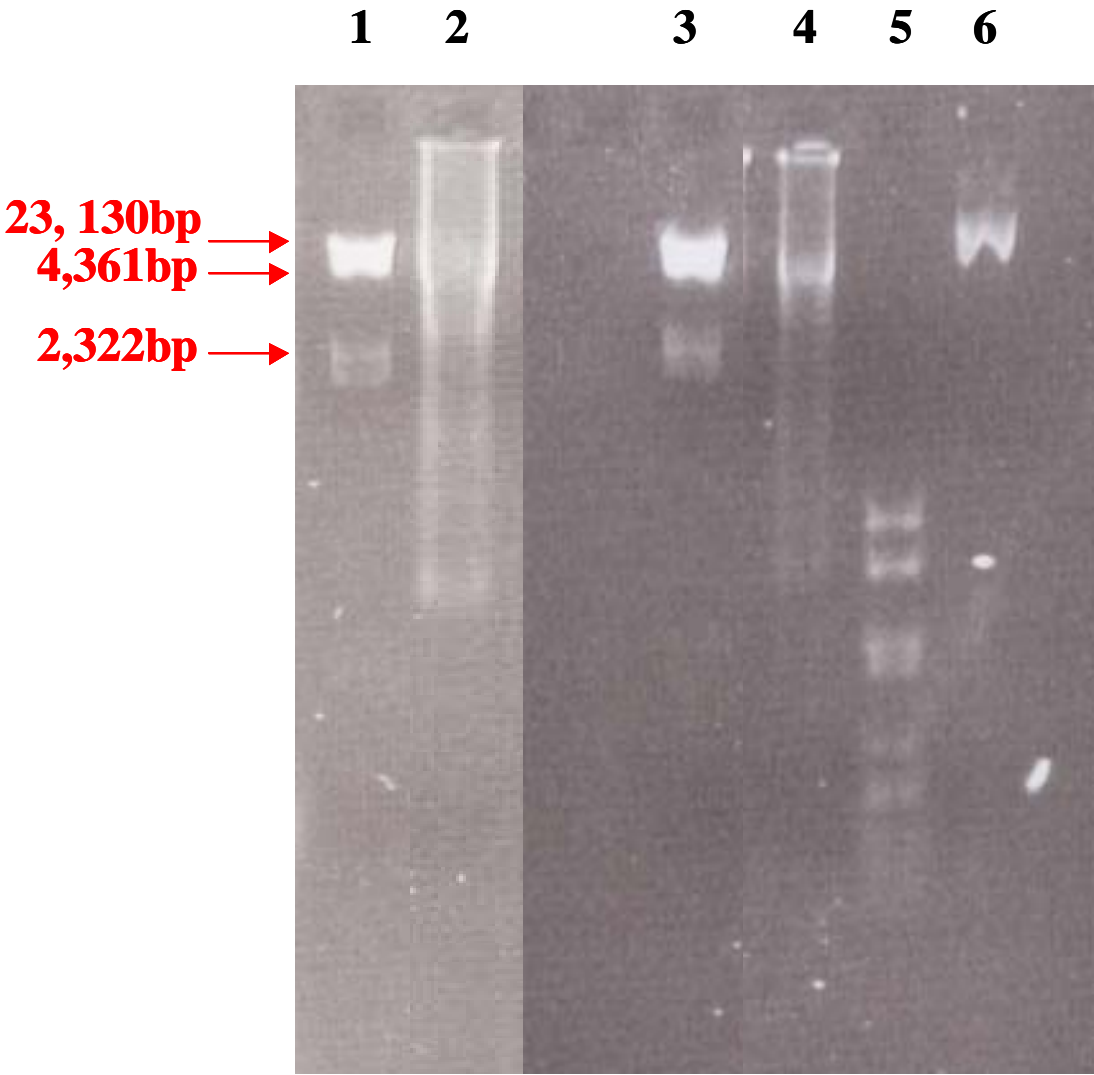
Figure 3.22: PCR screen of *E. coli* transformed with IL2-NAg-GFP. Top 10 *E. coli* colonies were transformed with pFastbac-1 plasmids encoding IL2-NAg-GFP. Colonies were selected for ampicillin resistance encoded by the pFastBac-1 plasmid. Colonies were screened with the upstream NAg-GFP fusion primer (2850) and the downstream GFP fusion primer (2852). Lane 1 contained the 100 base pair molecular weight standard. (Lanes 2 - 7) Colonies that exhibited bands around 800 base pairs were considered positive for transformation with the pFastBac-1 plasmid encoding IL2-NAg-GFP. Lane 3 did not exhibit a GFP amplicon and was therefore considered to be negative for the transformation. The bands that appeared below the 100 base pair standard were considered to be primer dimers. PCR products were run on a 1.0% agarose gel. Asterisks denoted the positive colony that contained no point mutations.
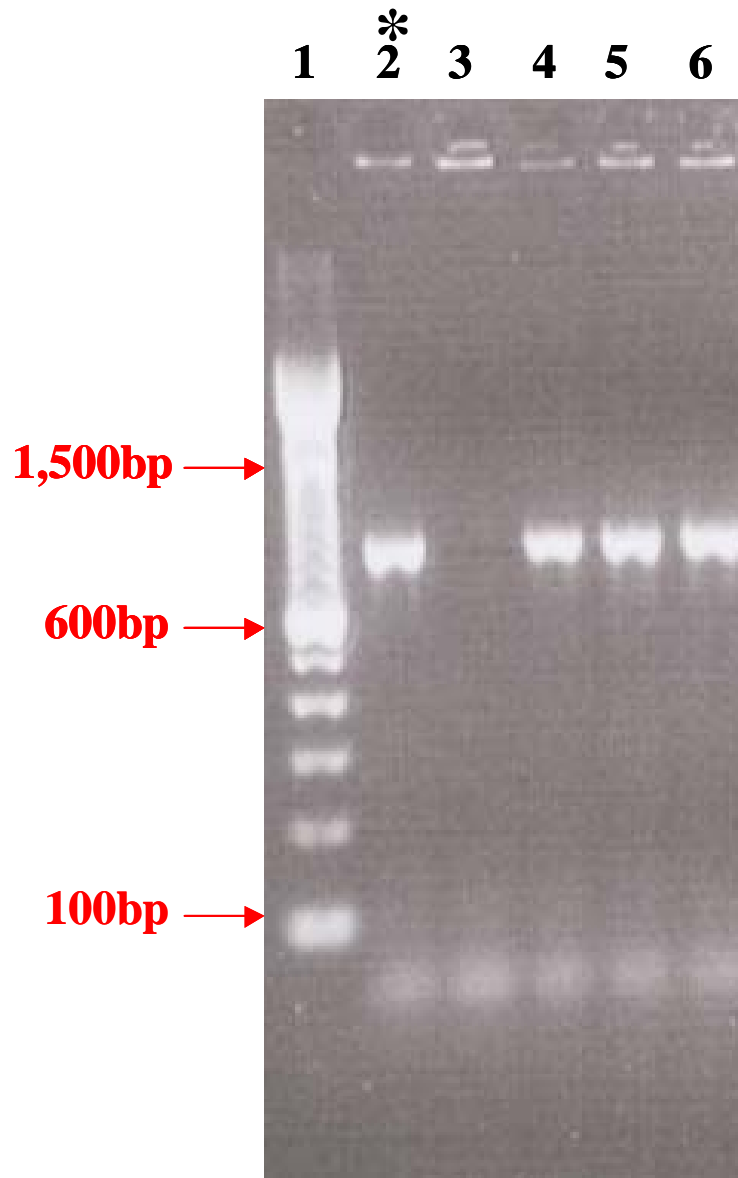
3.11 GENERATION OF AN IL2-NAg-GFP EXPRESSION SYSTEM

The DNA encoding IL2-NAg-GFP was transposed from pFastBac-1 into a baculoviral vector within *E. coli* DH10Bac. The pFastBac-1 plasmids encoding IL2-NAg-GFP were electroporated into *E. coli* DH10Bac. Site-specific transposition was mediated by the Tn7 transposase encoded in a helper plasmid within DH10Bac *E. coli*. The transposase Tn7 translocated the IL2-NAg-GFP constructs (flanked by mini-Tn7 sequences) from pFastBac-1 into the bacmid DNA vector (containing a mini-*att*Tn7 site). Colonies that had undergone transposition were detected through blue and white screening in the presence of Bluo-Gal and the LacI repressor IPTG. White colonies were presumably positive for baculoviral vectors that encoded IL2-NAg-GFP because transposition at the bacmid *att*Tn7 site disrupted the lacZα gene, such that β-galactosidase was not present. Transformed DH10Bac colonies were selected in the presence of kanamycin, gentamicin and tetracycline, and were subsequently PCR screened for GFP.

Baculoviral vectors encoding IL2-NAg-GFP were transfected into Sf9 insect cells. Seven days post-transfection, biological activity (i.e., fluorescence) of the GFP domain was tested by flow cytometry of infected Sf9 insect cells. GFP fluorescence was excited at 488 nm and emission was detected with the FITC filter set at 530 nm using the Becton Dickinson FACScan flow cytometer. Sf9 cells transfected with the IL2-NAg-GFP1.7 or IL2-NAg-GFP3.3 baculovirus exhibited GFP fluorescence when compared to untransfected Sf9 cells (Figure 3.24). Untransfected Sf9 cells displayed a mean fluorescence intensity of 9.5, while IL2-NAg-GFP1.7 and IL2-NAg-GFP3.3 transfected Sf9 cells exhibited a mean fluorescence of 22.9 and 36.7 respectively. The GFP domain was not overwhelming fluorescent. This is likely due to the fact

that 488 nm excites GFP at the secondary excitation peak (395 nm is the primary excitation peak), perhaps resulting in a weak emission.

Baculoviruses were released into the media after establishing a lytic infection within the Sf9 culture. Individual viruses that encoded IL2-NAg-GFP were isolated by plaque purification. In other words, individual viruses were isolated by co-culturing Sf9 insect cells with limiting dilutions of baculovirus supernatant. Viruses were selected based on their ability to promote a strong lytic infection and generate protein. IL2-NAg-GFP proteins were designed to be secreted in the supernatant of baculoviral infected Sf9 insect cells, which made the fusion proteins readily available for biological testing. Bioassays were performed on supernatants from the plaque purification assay in order to assess the biological activity of the NAg domain (Figure 3.24). RsL.11 T cells were co-cultured with irradiated, splenic APC (Lewis rat) plus supernatant from the plaque assay. Antigenic proliferation of RsL.11 T cells was detected by [^{3}H]thymidine incorporation. Cultures were pulsed with [^{3}H]thymidine on day 2 of a 3-day culture.

The plaque purified IL2-NAg-GFP.1.7.D4 baculovirus was expanded in Sf9 cells for 6-8 days to generate viral stocks for future protein expressions. Proteins were expressed in large-scale Sf9 cultures that were infected for four days with the baculovirus. On day four of culture, supernatants were harvested and clarified of Sf9 cells. Supernatants were ultimately concentrated and purified by affinity chromatography column consisting of immobilized single-chain antibodies against the C-terminal histidine tag of IL2-NAg-GFP. Purified IL2-NAg-GFP was analyzed on 12% SDS-PAGE to check for protein purity and size (Figure 3.25). Protein purity was not essential for the use of IL2-NAg-GFP with *in vitro* applications, therefore only one purification step was performed. Mature IL2-NAg-GFP (45.3 kDa) had no N-linked glycosylation sites and therefore the major band represented in the gel was likely an

unglycosylated form of IL2-NAg-GFP. IL2-NAg-GFP appears as a band located between the 37

kDa and 48 kDa molecular weight standards. There are contaminating bands in this preparation

due to purification by only one affinity column.

Figure 3.23: Biological activity of the GFP domain of IL2-NAg-GFP. Baculoviral vectors encoding IL2-NAg-GFP were transfected into Sf9 insect cells. Seven days post-transfection, biological activity of the GFP domain was assessed by flow cytometry using infected Sf9 cells. GFP fluorescence was excited at 488 nm and detected with the FITC filter set at 530 nm using the Becton Dickinson FACScan. Data were analyzed with the CELLQuest software program. Untransfected Sf9 cells (represented by the filled in peak) displayed a mean fluorescence intensity of 9.5, while IL2-NAg-GFP1.7 and IL2-NAg-GFP3.3 transfected Sf9 cells exhibited a mean fluorescence of 22.9 and 36.7 respectively.
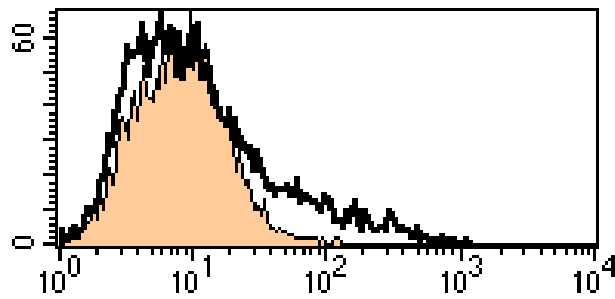
Sf9 + IL2-NAg-GFP1.7
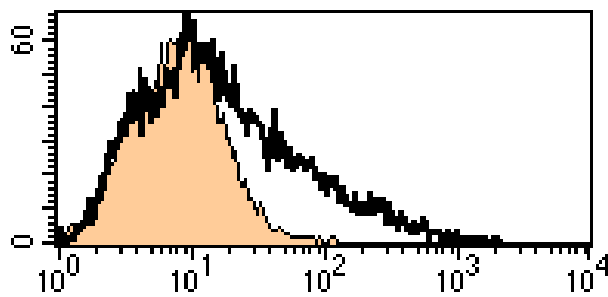
Sf9 + IL2-NAg-GFP3.3

Fluorescence

Figure 24: Plaque purification of baculoviruses that encoded IL2-NAg-GFP. Individual baculoviruses that encoded IL2-NAg-GFP were plaque purified. Sf9 insect cells (10^4 / well) were infected with a limiting dilution of designated baculovirus (10^{-5} - 10^{-8}). On day 9 of infection, supernatants from individual wells were tested for bioactivity. Fusion proteins were secreted into the supernatant of baculoviral infected Sf9 insect cells and therefore readily available for biological testing by a NAg specific bioassay. Irradiated splenic APC ($5x10^5$ / well) and NAg-specific RsL.11 T cells were cultured with supernatant from wells of the plaque purification assay. Cultures were pulsed with [^{3}H]thymidine on day 2 of a 3-day culture in order to assess RsL.11 proliferation. The shaded well designated the baculovirus chosen for expansion.

IL2-NAg-GFP.1.7					
Dilution 10^{-5}			Dilution 10^{-6}		
7147	12879	12557	3674	11337	227
14660	14843	12952	9400	11942	263
17315	16262	15873	110	6305	2658
13482	14857	11926	11753	8492	123
15531	18478	12817	143	10129	152
9667	12978	16138	375	3949	6527
10206	20485	17272	128	103	7573
3550	15639	18712	9988	255	3374

Figure 3.25: The purity of IL2-NAg-GFP was determined by SDS-PAGE. IL2-NAg-GFP fusion proteins were expressed in large-scale Sf9 insect cell cultures. Supernatants were concentrated and subsequently purified by means of the 8 his-tag engineered at the C-terminus. IL2-NAg-GFP was purified by an affinity column consisting of immobilized single-chain antibodies against the C-terminal histidine tag. Purified IL2-NAg-GFP was analyzed on 12% SDS-PAGE. Lanes 1, 2, and 3 were respectively loaded with the protein ladder, purified IL2-NAg-GFP, and the affinity column flow thru. Purified IL2-NAg-GFP (45.3 kDa) had no N-linked glycosylation sites. IL2-NAg-GFP appears as a band located between the 37 kDa and 49 kDa molecular weight standards. There are upper contaminating bands present at weights of 49 kDa and greater. Lower contaminating bands are also present.
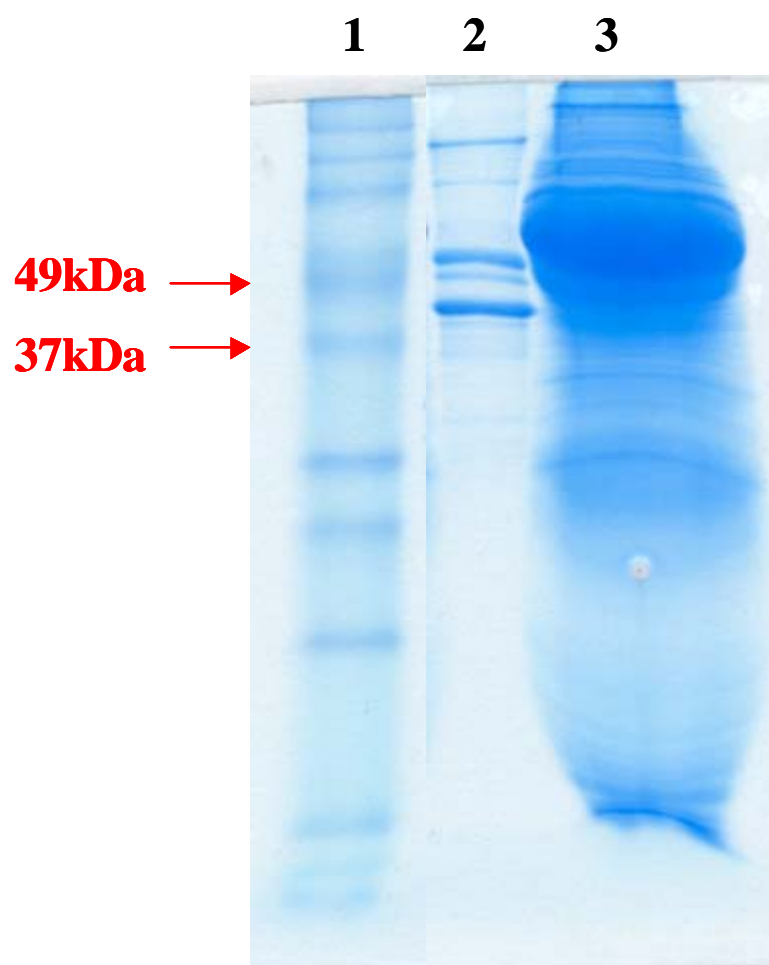
3.12 BIOLOGICAL ACTIVITY OF THE IL-2 DOMAIN

An IL-2 bioassay was performed on purified IL2-NAg-GFP in order to assess the biological activity of the cytokine domain (Figure 3.26). CTLL indicator cells (10^4 / well) were cultured with IL2-NAg-GFP or IL2-NAg titrated on a log scale from 100 nM – 10 fM. Cultures were pulsed with MTS / PMS after 48 hours and the color production was read at 492 nm. Biological activity of the IL-2 domains from IL2-NAg-GFP and IL2-NAg facilitated the survival and growth of CTLL cells. Biological activity of IL2-NAg-GFP titrated to a concentration of 1 nM, while IL2-NAg titrated to a concentration of 100 pM. The half maximal IL-2 activity of IL2-NAg-GFP was diminished 10 fold when compared to the half maximal activity of IL2-NAg. The 10 fold reduction was potentially due to hindrance of the IL-2 domain by the covalently linked GFP or due to the diminished purity of IL2-NAg-GFP in comparison to IL2-NAg (data not shown).

The cytokine activity of IL2-NAg-GFP was alternatively tested for the ability to target GFP to cells expressing the high affinity IL-2 receptor (α, β, γ subunits). The IL-2 dependent R1T T cell clone and the BW5147 thymoma cell line, an IL-2 independent T cell hybridoma, served as the experimental variables (Figure 3.27). BW5147 cells and IL-2 starved R1T cells (10^5 / well) were cultured with 100 nM IL2-NAg-GFP for 1 hour at 37°C. R1T and BW5147 were stained with propidium iodide to discern the dead cell population by flow cytometry. The mean fluorescence intensity of unstained BW5147 (represented by the filled in peak) was 47 and IL2-NAg-GFP stained BW5147 was 70. The mean fluorescence intensity of unstained R1T (represented by the filled in peak) was 80 and IL2-NAg-GFP stained R1T was 327. These data indicated that IL2-NAg-GFP could be effectively utilized as a fluorescent ligand to identify those cells that express the high affinity IL-2 receptor.

The idea that IL2-NAg-GFP could target GFP specifically to cells expressing the high affinity IL-2 receptor was supported by an inhibition assay (Figure 3.28). This assay was designed such that the IL-2 receptors on splenic APC were saturated or "inhibited" prior to the addition of IL2-NAg-GFP. IL-2 receptor saturation would hypothetically prevent IL2-NAg-GFP from binding to the high affinity IL-2 receptor, resulting in diminished GFP fluorescence. Lewis rat splenocytes (devoid of red blood cells) were activated with ConA and LPS for 24 hours. ConA and LPS served as mitogens for T cells and B cells, respectively. After activation, splenocytes were washed and cultured overnight in the absence of IL-2, in order to empty the IL-2 receptors. Splenocytes (10^5 / well) were pre-treated with 100 nM of GM-CSF, M-CSF, IL-4, IL-2 or no cytokine for 3 hours at 37^oC before incubation with 100 nM IL2-NAg-GFP for 1 hour. Cells were stained with propidium iodide to discern the dead cell population by flow cytometry. The mean fluorescence intensities of IL2-NAg-GFP labeled splenocytes with no cytokine pre-treatment, with GM-CSF, M-CSF, or IL-4 pre-treatment were 470, 475, 471, and 486 respectively. Splenocytes pretreated with IL-2 prior to staining with IL2-NAg-GFP exhibited a mean fluorescence intensity of 216. The decreased fluorescence indicated that IL-2 competitively blocked IL2-NAg-GFP from binding the high affinity IL-2 receptor. GM-CSF, M-CSF, and IL-4 pre-treatment did not competitively inhibit IL2-NAg-GFP binding and therefore exhibited no decrease in GFP intensity. Therefore, IL2-NAg-GFP was a specific marker of for cells that expressed the high affinity IL-2 receptor because the cytokine domain of IL2-NAg-GFP targeted GFP to APC by a mechanism that was competitively and specifically blocked by IL-2.

Figure 3.26: IL-2 bioassay to assess the cytokine activity of IL2-NAg-GFP. CTLL indicator cells (10^4 / well) were cultured with IL2-NAg-GFP or IL2-NAg titrated on a log scale from 100 nM – 10 fM (x-axis). Cultures were pulsed with MTS / PMS after 48 hours and color production resulting from MTS reduction was read at 492 nm. Biological activity of the IL-2 domains from IL2-NAg-GFP and IL2-NAg facilitated the survival and growth of CTLL. The half maximal IL-2 activity of IL2-NAg-GFP was diminished 10 fold in comparison to the half maximal activity of IL2-NAg. This experiment was performed once.
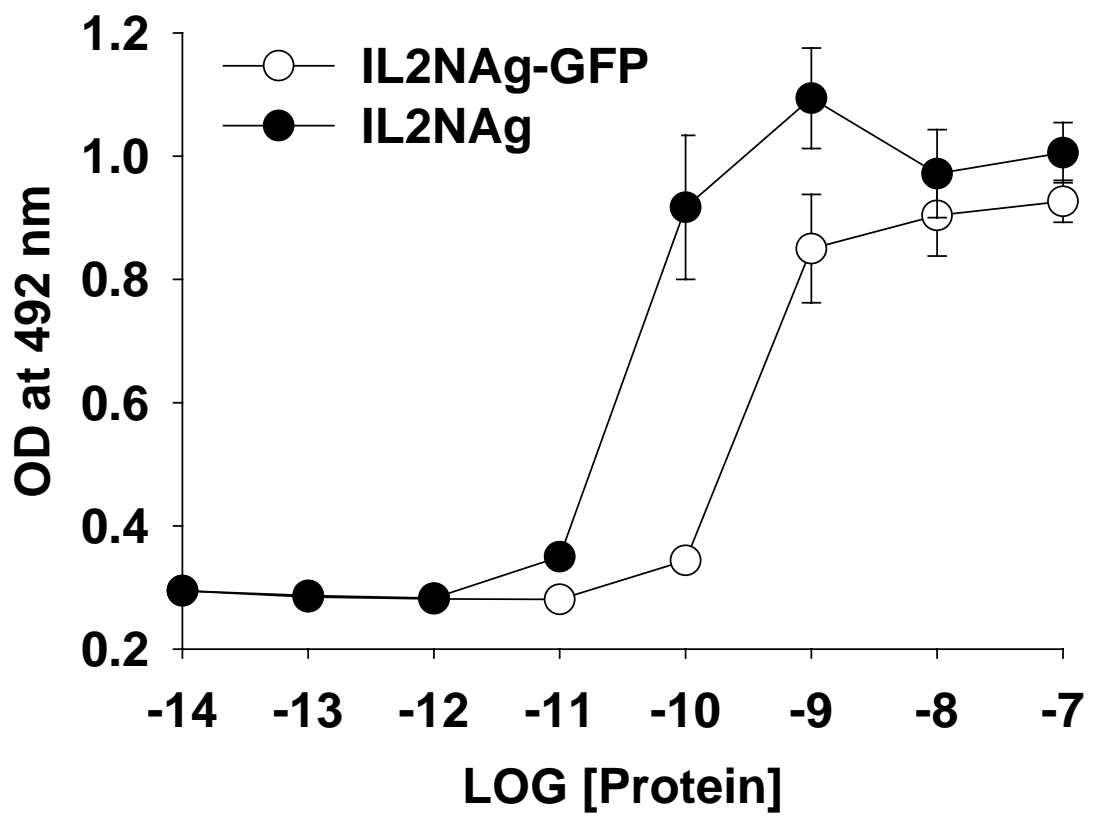
Figure 3.27: IL2-NAg-GFP specifically stained R1T cells that expressed surface IL-2 receptors. IL-2 starved R1T cells, an IL-2 dependent T cell clone, and BW5147 thymoma cells, an IL-2 independent T cell hybridoma, (10^5 / well) were cultured with 100 nM IL2-NAg-GFP for 1 hour. Cells were not washed after the hour incubation period. R1T and BW5147 cells were stained with 2.0 μg / ml of propidium iodide to discern the dead cell population. The Becton Dickinson LSRII flow cytometer was used to detect propidium iodide and GFP fluorescence. GFP fluorescence was excited at 405 nm and detected with the AmCyan filter at 530 / 30 nm. Propidium iodide fluorescence was excited at 488 nm and detected with the PE-Cy5 filter at 660 / 20 nm. Data were analyzed with the FLOWJO software program. The mean fluorescence intensity of unstained BW5147 (represented by the filled in peak) was 47 and IL2-NAg-GFP stained BW5147 was 70. The mean fluorescence intensity of unstained R1T (represented by the filled in peak) was 80 and IL2-NAg-GFP stained R1T was 327. All experimental conditions were performed in duplicate.

BW5147
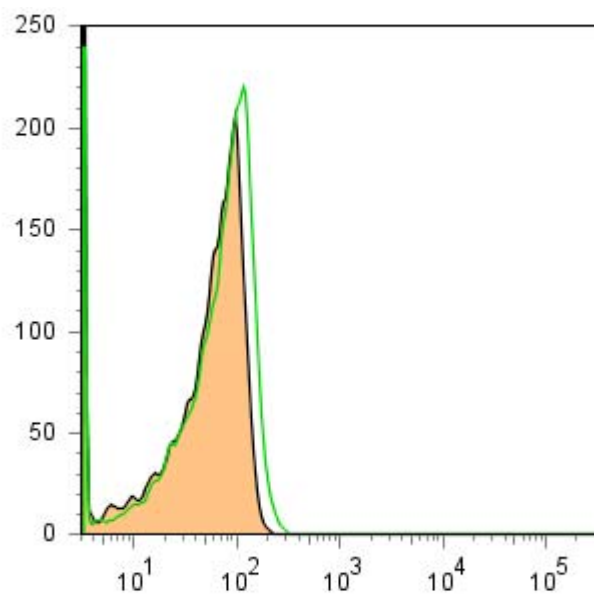
R1T
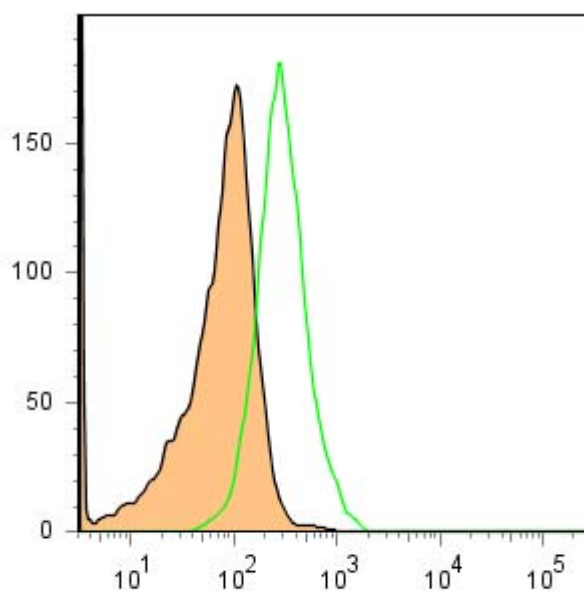
GFP Fluorescence

Figure 3.28: The cytokine domain of IL2-NAg-GFP targeted GFP to APC by a mechanism that was competitively and specifically blocked by IL-2. Lewis rat splenocytes (devoid of red blood cells), were activated with 2.5 μg / ml ConA and 10.0 μg / ml LPS for 24 hours. ConA and LPS served as mitogens for T cells and B cells, respectively. After activation, splenocytes were washed and cultured overnight in cRPMI (without IL-2). Splenocytes (10^5 / well) were pretreated with 100 nM of GM-CSF, M-CSF, IL-4, IL-2 or no cytokine for 3 hours before the addition of IL2-NAg-GFP (100 nM). Cells were not washed after the hour incubation period. Splenocytes were stained with 2.0 μg / ml of propidium iodide to discern the dead cell population. Splenocytes were analyzed with the Becton Dickinson LSRII flow cytometer along with the FLOWJO analysis software. The mean fluorescence intensities of IL2-NAg-GFP labeled splenocytes with no cytokine pre-treatment, with GM-CSF, M-CSF, or IL-4 pre-treatment were 470, 475, 471, and 486 respectively. Splenocytes pretreated with IL-2 prior to staining with IL2-NAg-GFP exhibited a mean fluorescence intensity of 216. This indicated that IL-2 competitively blocked IL2-NAg-GFP. Therefore, IL2-NAg-GFP was a specific marker of for cells that expressed the IL-2 receptor. All experimental conditions were performed in duplicate.

IL2-NAg-GFP plus GM-CSF
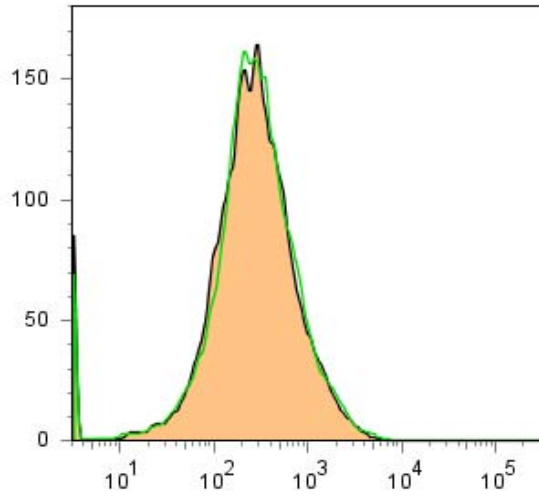
IL2-NAg-GFP plus M-CSF
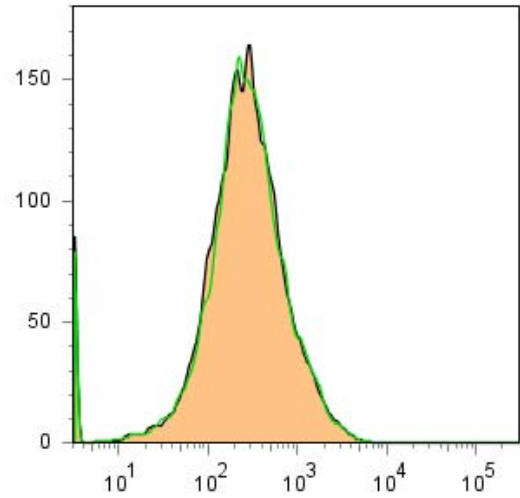
IL2-NAg-GFP plus IL-4
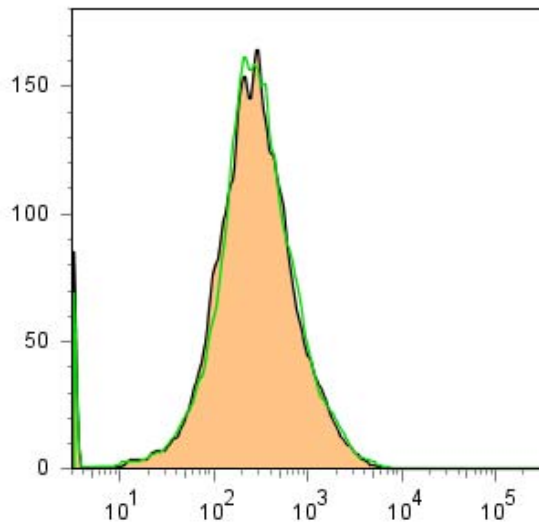
IL2-NAg-GFP plus IL-2
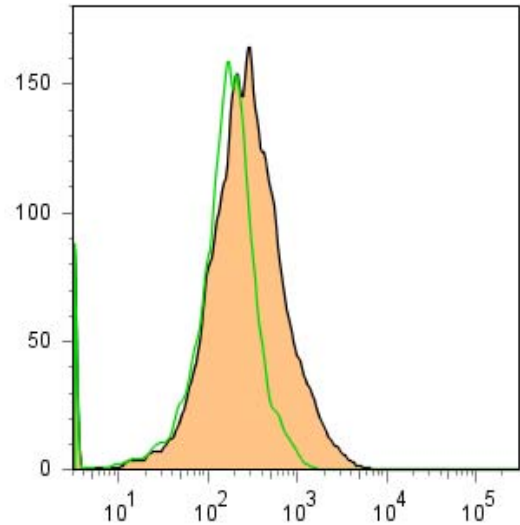
CHAPTER 4

DISCUSSION

4.1 SIGNIFICANCE

Cytokine-antigen fusion proteins have been previously studied as therapeutic vaccines to promote immunity against cancer and infectious agents (60-62). More recently, cytokine-antigen fusion proteins have proven to be efficacious as tolerogenic vaccines in the EAE autoimmune disease model (28, 64, 65). Data presented here showed that GMCSF-NAg, and to a lesser extent MCSF-NAg, prevented the development of severe paralytic EAE in the Lewis rat model when administered before or after disease onset. The novelty of the cytokine-antigen fusion proteins was that they could promote antigen-specific tolerance during both steady state and inflammatory environments. The ability to induce tolerance in an inflammatory environment was significant because it contradicted the dogma that tolerance is induced under steady state, i.e., non-inflammatory conditions. Furthermore, the ability of a GM-CSF fusion protein to regulate tolerance induction was novel because GM-CSF is considered to be a critical mediator of EAE. The mechanistic data revealed that GMCSF-NAg, and to a lesser extent MCSF-NAg, could enhance antigenic proliferation of T cell clones, *in vitro*, by targeting the tethered NAg domain to APC via the respective cytokine receptor. We proposed that APC targeting likely accounted for the tolerogenic response elicited by GMCSF-NAg *in vivo*. A unique feature of GMCSF-NAg was that it could target NAg to specific APC subsets, including dendritic cells, macrophages, activated B cells and NK cells, unlike other laboratories that target one APC type, specifically dendritic cells. Overall, these fusion proteins provide a potential platform for understanding how to regulate the balance between tolerance and immunity.

4.2 TARGETING ANTIGEN TO ANTIGEN PRESENTING CELL SUBSETS BY MEANS OF FUSION PROTEINS

The ability to target antigen to APC, particularly DC, by means of fusion proteins is not a new concept. Antigen can be targeted to APC through protein or DNA based strategies that take advantage of cell surface receptors that are endocytosed upon binding ligand (92, 93). In brief, numerous cell surface molecules have been targeted including C-type lectin receptors, integrins, Fcγ receptors, T cell and APC co-stimulatory molecules, toll-like receptors, MHC molecules, molecules associated with antigen processing pathways, as well as cytokine and growth factor receptors (Table 4.1). The idea being that these fusion proteins would target antigen to APC and enhance processing and presentation of antigen by MHC class I or class II molecules (or both) in order to augment immune responses. In addition to antigen targeting, fusion proteins could potentially initiate different APC activation programs i.e., promoting APC maturation in order to enhance T cell activation or promoting the expression of chemoattractants to increase the number of immune responders (92, 93).

Extensive research has been performed with antigen fusion proteins that target C-type lectins, specifically DEC-205. Nussenzweig's laboratory showed that targeting antigen to DC by antibodies against DEC-205 enhanced antigen presentation by a specific CD8$^+$ DC subset and in turn augmented T cell proliferation (75, 94). Augmented presentation was associated with the ability of DEC-205 to localize to late endosomes and lysosomes that contain MHC class II molecules, thereby facilitating antigen loading on MHC class II (95). Noteworthy is that *in vivo* administration of anti-DEC205-Ag promoted a significant antigenic burst of T cells within 48 hours but the antigen-specific T cells were not sustained over time (7 to 20 days) (75). The tolerogenic mechanism was associated with the induction of T cell anergy or deletion. This

mechanism may be applicable to what we have seen in our studies with GMCSF-NAg. GMCSF-NAg, and to a lesser extent MCSF-NAg, significantly augmented proliferation of T cell clones *in vitro* yet preliminary *in vivo* data did not reflect a sustained NAg-specific T cell repertoire (data not shown). In this preliminary experiment rats were challenged with GP69-88, MCSF-NAg or GMCSF-NAg in CFA (see Table 3.1). The rats challenged with GMCSF-NAg or MCSF-NAg exhibited significantly reduced disease than the GP69-88 control group. Rats were monitored for one month, after which lymph nodes were harvested and tested for NAg activity, i.e. T cell priming. The assay suggested that lymph node cells from the GMCSF-NAg group exhibited diminished activity when compared to the proliferative response of the GP69-88 and MCSF-NAg groups. Potentially, NAg-specific T cells were being deleted or anergized as a result of GM-CSF targeting NAg to DC and macrophages. The overall importance of antigen fusion proteins is that they provide a tool to target antigen to APC *in vivo* with the endpoint of influencing T cell immune responses to be immunogenic or tolerogenic.

Table 4.1: Published studies of antigen fusion proteins.

Category	Target	Ag Fusion	Type	Effect	Mechanism
C-type lectin	DEC-205	αDEC205 / OVA (75, 76, 95)	Protein vaccine	Enhanced CD4$^+$ and CD8$^+$ T cell priming, facilitated Ag cross presentation	Targeting steady state CD11c$^+$ DC and localization to endosomal / lysosomal compartment
	DCIR2	33D1 Ab / avidin (96)	Protein vaccine	Enhanced Ab response against avidin and promoted immunological memory	DC targeting and endocytosis
Integrin	CD11c	αCD11c / goat IgG (97)	Protein vaccine	Enhanced Ab response against goat IgG	APC targeting and endocytosis
Fc receptors	Fcγ receptor	OVA / αOVAIgG (98)	Protein vaccine	Enhanced DC maturation, enhanced Ag cross presentation by DC and MHC class II presentation of Ag by B cells	APC targeting (DC and B cell examined *in vitro*), phagocytosis and DC activation
		HBVe / IgG (99)	DNA vaccine	Enhanced Ag cross presentation *in vivo*, enhanced Ab response against HBV	CD11c$^+$ DC targeting and phagocytosis
		hαFcγRI (CD64) / PSA (100)	Protein vaccine	Enhanced Ag presentation by HLA-A	Targeting APC and phagocytosis
T cell co-stimulatory molecules	CD3	αCD3 / avidin (96)	Protein vaccine	Enhanced Ab response against avidin	T cell targeting and endocytosis
	CD4	αCD4 / avidin (96)	Protein vaccine	Enhanced Ab response against avidin	T cell and APC targeting, endocytosis
	CD45	αCD45 / avidin (96)	Protein vaccine	Enhanced Ab response against avidin	Leukocyte targeting and endocytosis

Abbreviations: α (anti-), Ab (antibody), Ag (antigen), OVA (ovalbumin), 33D1 (monoclonal Ab against DC1R2), DCIR2 (DC inhibitory receptor 2), Fc (Ab fragment crystallizable), HBVe (hepatitis B virus protein e), hα FcγRI (human anti-Fcγ receptor I), PSA (prostrate specific antigen)

Category	Target	Ag Fusion	Type	Effect	Mechanism
B cell receptor	sIgG2a	αIgG2a / avidin (96)	Protein vaccine	Enhanced Ab response against avidin	B cell targeting and endocytosis
	sIg	Pc / αIg (101)	Protein	Enhanced Ag uptake and presentation, that involves BCR targeting to MIIC compartment(102)	B cell targeting (*in vitro*)
MHC molecules or antigen processing pathways	MHC class II	αI-A/E / avidin, αI-A^k / avidin, αI-A^b / avidin (96)	Protein vaccine	Enhanced Ab response against avidin and promoted immunological memory	APC targeting and endocytosis
		Pc / αI-A (101)	Protein	Enhanced Ag uptake and presentation	B cell targeting (*in vitro*)
	Lysosome-endosomal compartment	Signal peptide of LAMP1 / HPV E7 protein / LAMP-1	Retroviral transduced DC vaccine (103)	Increased CD4$^+$ and CD8$^+$ T cell responses *in vitro* and *in vivo* and the DC vaccine diminished tumor load in mice	Enhanced loading on MHC class II by intracellularly targeting E7 to lysosome/MIIC compartment
			Recombinant vaccinia virus (104)	Increased CD4$^+$ and CD8$^+$ T cell responses *in vitro* and *in vivo*, enhanced E7 antibody	
	MHC class I processing pathway	Calreticulin / HPV E7 protein (105)	DNA vaccine	Enhanced CD8$^+$ T cell activation *in vivo*, enhanced E7 antibody response, protected against tumor challenge	Targeted to MHC class I processing pathway
		E7 / Hsp70 (106)	DNA vaccine	Enhanced CD8$^+$ T cell activation *in vivo*, protected against tumor challenge	Targeted to MHC class I processing pathway
		Pc / αI-K (101)	Protein	Enhanced Ag uptake and presentation	B cell targeting (*in vitro*)

<u>Abbreviations</u>: BCR (B cell receptor), Pc (pigeon cytochrome c), MIIC (MHC class II compartment), I-A/E (MHC class II molecules), LAMP-1 (lysosomal associated membrane protein −1), HPV E7 (human papillomavirus protein E7), I-K (MHC class I molecule)

Category	Target	Ag Fusion	Type	Effect	Mechanism
Toll-like receptors	TLR9	Unmethylated CpG / gp120 (107)	DNA-protein vaccine	Enhanced serum IFNγ levels, enhanced Ab response and enhanced CD8$^+$ T cell response to gp120	Targeting to and maturation of APC
		OVA / unmethylated CpG (108-111)		Enhanced Ag uptake by CD11c$^+$ DC, enhanced Ag presentation on MHC class I and enhanced DC maturation, protected against lethal challenge with LM-OVA. CD8$^+$ T cell response was dependent on TLR9 but TLR9 was not required for APC targeting.	APC targeting, particularly DC (*in vivo*) and B cells, maturation of APC, targeting to endosomal / lysosomal compartment
Cytokines or growth factors	Flt3 receptor	Flt3 ligand / HPV E7 protein (112)	DNA vaccine	Enhanced E7 specific CD8$^+$ T cell tumor immunity, FL (pre-treatment and treatment) protected against lethal tumor challenge	APC targeting (DC examined *in vitro*) and endocytosis
	GM-CSF receptor	GM-CSF / sIg of 38C13 B cell tumor Ag (62)	Protein vaccine	Enhanced antibody production against the tumor antigen, protected from a lethal tumor challenge	APC targeting
	IL-2 receptor	IL2 / HSV glycoprotein D (60)	Protein vaccine	Enhanced antibody titers and the CD8$^+$ T cell response	T cell targeting or T cell activation
APC co-stimulatory molecules	B7	CTLA4 / hIgG (113)	DNA vaccine	Enhanced Ab response against hIgG	APC targeting and endocytosis
		CTLA4 / hIgG / HA (114)		Enhanced Ab response against HA & enhanced viral clearance	
	CD40	(40AdE7) bispecific Ab conjugate αCD40-αAd fiber knob protein / adenovirus expressing HPV E7 protein (115)	Adenovirus based DNA vaccine	Enhanced MOI, induced DC maturation, 40AdE7 infected DC (pre-treatment and treatment) protected mice against lethal tumor challenge	APC targeting (DC examined *in vitro*) and endocytosis

Abbreviations: CpG (cytosine, guanine oligodeoxynucleotides), gp120 (Human Immunodeficiency Virus glycoprotein 120), LM-OVA (*Listeria monocytogenes* expressing OVA), FL (Flt 3 ligand), hIgG (human IgG), HA (influenza hemagglutinin), Ad (adenovirus), MOI (multiplicity of infection)

4.3 CYTOKINE – ANTIGEN FUSION PROTEINS: HANGING IN THE BALANCE BETWEEN TOLERANCE AND IMMUNITY

Cytokine-antigen fusion proteins were initially designed to enhance the immunogenicity of weak antigens without the need for adjuvants and carrier proteins. For instance, fusion proteins comprised of IL-2 fused to viral glycoproteins, bacterial or cancer antigens enhanced production of antigen-specific antibody titers and protected animals from a lethal challenge with the respective infectious agent or tumor cell line when compared to controls (60, 62, 116). In contrast we showed IL2-NAg fusion proteins to be significantly tolerogenic in the EAE model (64, 65). IL2-NAg prevented a cell-mediated autoimmune response against NAg when administered as a pre-treatment or treatment regimen (64, 65). This balance between tolerance and immunity was also seen with GMCSF-antigen fusion proteins. GM-CSF fusion proteins acted as an adjuvant to enhance antigen-specific immunity against viral, bacterial and cancer antigens, while inducing antigen-specific tolerance in EAE (61, 62, 116, 117). The dichotomy of cytokine-antigen fusion proteins in regulating immunity versus tolerance raises the concern of how to effectively employ this platform technology to prevent rather than enhance an autoimmune response.

In the previous examples, the common variable between the immunogenic and tolerogenic models was the cytokine domain. This leads one to believe that the cytokine domain, while influencing the immune response, is not the only consideration for regulating the balance between immunity and tolerance. In other words, the antigenic domain maybe an important consideration in the design of cytokine-antigen fusion proteins (117). For instance, self-antigen has been shown to drive regulatory T cell responses (37, 118). Oral administration of low dose self antigen prior to encephalitogenic challenge suppressed paralytic EAE by a regulatory T cell

phenotype (37). Additionally, intrathymic injection of MBP into Lewis rats before, but not after, encephalitogenic challenge significantly protected rats from the development of severe EAE when compared to controls (118, 119). The mechanism potentially involved the induction of thymus-derived, regulatory T cells because removal of the thymus 72 hours after intrathymic injection abrogated the protective effect (118).

The use of APL or altered self-antigens, on the other hand, have been controversial due to the exacerbation of MS in clinical trials (44). Single amino acid changes to self peptide can result in a heteroclitic response, depending on the alteration (120, 121). A heteroclitic response could occur if the APL elicits a greater immune response than the immunizing self antigen (117). For instance, the T cell clone Q1.1B6 generated a heteroclitic response to the altered PLP ligand (L144) when compared to the cognate PLP peptide (Q144). The TCR of Q1.1B6 exhibited a similar affinity for the immunizing Q144 peptide and L144, yet L144 behaved as a superagonist by enhancing T cell proliferation and increasing IFNγ, IL-2 and IL-4 expression when compared to the cognate peptide. This heteroclitic response was seen in different T cell clones and was therefore not specific to Q1.1B6. Interestingly, T cell activation during the heteroclitic response had little to no requirement for co-stimulatory molecules. These data may have implications for the etiology of autoimmune disease such that foreign antigen / self protein mimic could cross react and hyperstimulate autoreactive T cells with little co-stimulation, resulting in a pathogenic Th1 immune response (120, 121).

Pulmonary alveolar proteinosis (PAP) is an example where self-antigen can be used therapeutically during an autoimmune response. PAP is classified as a rare autoimmune disease marked by the accumulation of lipid material in lung alveoli (122). The pathology of PAP is associated with a GM-CSF deficiency mediated by autoantibodies against the cytokine (122,

123). Treatment with subcutaneous GM-CSF improved lung function in some patients without significant side effects (122, 123). Currently the therapeutic effect of GM-CSF is associated with increased lipid catabolism by alveolar macrophages. A role for GM-CSF in regulating T cell and B cell responses in PAP has not been examined in detail, however data have shown that GM-CSF treatment could reduce anti-GMCSF antibody titers in a subset of patients (123). In our study GM-CSF fused to the NAg self peptide (GMCSF-NAg) was able to significantly protect animals from EAE. These data imply that administration of self-antigen such as GM-CSF in the case of PAP and GMCSF-NAg in the case of EAE has the potential to regulate an ongoing autoimmune response.

The ability of GM-CSF, as a component of GMCSF-NAg, to promote tolerance in EAE contradicts the dogma that GM-CSF is a critical mediator of the disease. For instance, GM-CSF knockout mice were found to be resistant to the induction of EAE and disease susceptibility was restored after subcutaneous administration of GM-CSF (124). Furthermore, T cells were shown to be the major source of GM-CSF required for the induction of EAE (125, 126). The requirement for GM-CSF was mostly associated with T cell reactivation in the CNS, i.e., the effector phase of the disease. During the effector phase, encephalitogenic T cells enter the CNS and become reactivated upon recognition of neuroantigen:MHC complexes on APC. MBP specific T cells from GM-CSF knockout mice were unable to induce severe disease upon adoptive transfer into irradiated, wild type mice (125). T cell derived GM-CSF was apparently required for the activation of APC within the CNS in order to promote inflammation (125). These data were supported by the fact that encephalitogenic T cells transduced with GM-CSF promoted chronic EAE (126). Collectively, these data and our GMCSF-NAg data suggested that GM-CSF may have a unique role in regulating the balance between immunity and tolerance.

The finding that GMCSF-NAg could promote tolerance during an on-going autoimmune response was significant because it contradicted the belief that tolerance could only be induced under steady state or non-inflammatory conditions. Tolerance induced by steady state dendritic cells via anti-DEC205-Ag fusion proteins resulted in antigen-specific T cell anergy that was reversed by increased co-stimulation delivered by an anti-CD40 antibody, *in vitro* (75). This research supported the idea that inflammatory conditions, marked by enhanced co-stimulation, could inhibit the development of tolerance, at least in the case of anergy-induced tolerance. On the contrary, there is growing support for the induction of tolerance under inflammatory conditions. For instance, mature, activated dendritic cells expressing high levels of co-stimulatory molecules could promote T cell tolerance via mechanisms that involved deletion or expansion of regulatory T cell populations (74). Autologous, LPS matured DC promoted the development of T cells capable of suppressing an allogeneic mixed lymphocyte reaction via a contact independent mechanism associated with increased FOXP3 expression by T cells (127). Alternatively, LPS matured DC could be differentiated into a regulatory DC phenotype in the presence of splenic endothelial cells (128). The differentiated regulatory DC inhibited T cell proliferation via a mechanism associated with increased nitric oxide production (128). Overall, these examples support the possibility that self-antigen could theoretically be used to induce antigen-specific tolerance in patients with on-going autoimmune disease.

4.4 ANTIGEN PRESENTING CELL SUBSETS AND NK CELLS: EVIDENCE FOR REGULATING TOLERANCE

The GM-CSF domain of GMCSF-NAg potentially enhanced the tolerogenic nature of the tethered NAg self-peptide by targeting NAg to specific APC subsets. In this study we saw that

159

GMCSF-NAg largely targeted NAg to dendritic cells and macrophages. Other laboratories have indicated a tolerogenic role for these APC subsets in EAE, as previously discussed. In addition to dendritic cells and macrophages, our studies also indicated that perhaps activated B cells and NK cells could have a role in tolerance induction. GMCSF-NAg weakly targeted NAg to activated B cells and NK cells, while T cell APC were not targeted by GMCSF-NAg at all. The fact that GMCSF-NAg could target NAg to a variety of APC *in vitro* suggested that the tolerogenic nature of GMCSF-NAg *in vivo* may be associated with a collaborative effort among APC subsets. In this way, our APC targeting strategy differs from other laboratories that focus on targeting antigen to one APC subset, specifically dendritic cells. Targeting antigen to dendritic cells has been effectively used to induce tolerance in animal models, however it precludes the role of other cell types (macrophages, B cells and NK cells) in the induction of tolerance. In fact, NK cells and B cells have been examined for tolerogenic roles in EAE.

Clinically there is indirect evidence supporting a regulatory role for NK cells in MS patients. For instance, patients exhibited reduced brain inflammation during clinical trials with daclizumab, a mAb to the high affinity IL-2 receptor α subunit, via a mechanism that correlated with a significant increase in peripheral blood CD56^{bright} NK cells and a modest decrease in CD4$^+$ and CD8$^+$ T cells (129). *In vitro* assays indicated that CD56^{bright} NK cells were potentially responsible for the therapeutic effects of daclizumab. The T cell cytotoxicity mediated by NK cells appeared to be contact dependent; cytotoxicity was enhanced by the activation of NK and T cells in the presence of IL-2 (129). Some EAE models have also supported a role for NK cells and tolerance (130, 131). Deletion of NK cells, and inadvertently NK-T cells, in C57B6 mice by the administration of an antibody against NK1.1 (C-type lectin integral membrane protein) one day before challenge significantly enhanced EAE severity and mortality compared to isotype

controls (130). Furthermore, β2m knockout mice, purportedly deficient in CD8$^+$ T cells and NK-T cells, only exhibited severe EAE and increased mortality in the presence of anti-NK1.1. This suggested that NK cells, rather than NK-T cells or CD8$^+$ T cells, were involved in preventing severe EAE in mice (130). In another example, activated NK cells were associated with the suppression of EAE in SJL mice following Hsp70-pc (heat shock protein 70 - protein complexes derived from CNS of EAE mice) treatment as compared to Hsp70 alone and Hsp70-pc from normal mice (132). NK cells from Hsp70-pc treated mice reduced PLP specific T cell proliferation *in vitro* and suppressed EAE *in vivo* when NK cells were adoptively transferred after disease onset (132).

B cells have also been associated with the regulation of tolerance in EAE. For instance, B cell deficient mice (μ knockout) did not spontaneously recover after an acute phase of EAE when compared to wild type B10.PL controls (133). The data suggested that B cells somehow played a role in spontaneous recovery / tolerance in this mouse model. In another experiment, B cells retrovirally transfected with MOG were tolerogenic when administered as a pre-treatment or treatment suggesting a role in tolerance in two different animal models C57B6 and PL10 (134). The B cells in this study were likely activated because the cells were transduced in the presence of LPS. The aforementioned studies lend support for the role of multiple cell types (B cells, NK cells, macrophages and DC) in the induction of tolerance within the EAE model, particularly after the administration of GMCSF-NAg.

4.5 CONCLUSION

GMCSF-NAg fusion proteins were potent inducers of antigen-specific tolerance in the Lewis rat model of EAE. The tolerogenic mechanism is not fully understood at this point,

however *in vivo* data indicated that the fusion of NAg to GM-CSF was crucial for tolerance induction. Based on *in vitro* data, we propose that the delivery of NAg to APC subsets, *in vivo*, likely accounted for the tolerogenic mechanism of GMCSF-NAg. The *in vitro* assays indicated that NAg was targeted to specific APC subsets, namely macrophages and dendritic cells, via the GM-CSF cytokine domain. The fact that GM-CSF largely targeted NAg to dendritic cells and macrophages suggests that the tolerogenic mechanism could involve myeloid suppressor cells. Myeloid (dendritic cells or macrophages) suppressor cells could then drive tolerance through the induction of antigen-specific regulatory T cells or through high dose, deletional tolerance resulting from enhanced NAg uptake and presentation by APC. Furthermore, it is unclear whether the tolerogenic mechanism associated with the GMCSF-NAg pre-treatment regimen would be the same as the mechanism associated with the treatment regimen. Perhaps there is a novel tolerogenic mechanism at work because GMCSF-NAg was capable of targeting various APC subsets, i.e., DC, MO, activated B cells, and NK cells. The ability of cytokine-antigen fusion proteins to promote antigen-specific tolerance in both steady state and inflammatory environments suggested that these fusion proteins could be important tools for understanding how to regulate the balance between tolerance and immunity.

The purpose of this research was to design a tolerogenic vaccine that would promote a neuroantigen-specific regulatory response, which is proposed to be deficient in MS patients. Whether GMCSF-NAg could be used to treat human patients is debatable, due to safety concerns with GM-CSF and the uncertainty of which neuroantigen to therapeutically target. Despite the fact that GM-CSF is used in cancer patients to promote hematopoietic recovery following radiation therapy, the involvement of GM-CSF in the inflammatory processes of autoimmune disease models, including EAE, cannot be ignored. Perhaps APC can be loaded *ex vivo* and then

162

administered back to the patient in order to avoid safety concerns regarding the systemic administration of GM-CSF. This has been done in clinical trials with another GMCSF-fusion protein GMCSF-PAP (prostatic acid phosphatase) (135). Furthermore, a consideration for our research is identifying the appropriate neuroantigen(s) to target because the antigen specificity may change over time (epitope spreading) and may differ among patients. At the least, our technology presents a tool for basic science research to study the mechanisms that promote antigen-specific tolerance. Despite the potential future hurdles, we cannot ignore the success we have seen with GMCSF-NAg in our EAE models.

CHAPTER 5

REFERENCES

1.   Murray, T. J. 2009. The history of multiple sclerosis: the changing frame of the disease over the centuries. *J Neurol Sci* 277 Suppl 1:S3-8.

2.   Raine, C. S., McFarland, H.F., Hohlfeld, R, ed. 2008. *Multiple Sclerosis: A Comprehensive Text* Saunders Elsevier Philadelphia, PA.

3.   Lublin, F. D., and S. C. Reingold. 1996. Defining the clinical course of multiple sclerosis: results of an international survey. National Multiple Sclerosis Society (USA) Advisory Committee on Clinical Trials of New Agents in Multiple Sclerosis. *Neurology* 46:907-911.

4.   Esiri, M. M. 2009. MS: is it one disease? *Int MS J* 16:39-41.

5.   Anderson, D. W., J. H. Ellenberg, C. M. Leventhal, S. C. Reingold, M. Rodriguez, and D. H. Silberberg. 1992. Revised estimate of the prevalence of multiple sclerosis in the United States. *Ann Neurol* 31:333-336.

6.   Baxter, A. G. 2007. The origin and application of experimental autoimmune encephalomyelitis. *Nat Rev Immunol* 7:904-912.

7.   Gold, R., C. Linington, and H. Lassmann. 2006. Understanding pathogenesis and therapy of multiple sclerosis via animal models: 70 years of merits and culprits in experimental autoimmune encephalomyelitis research. *Brain* 129:1953-1971.

8.   Furtado, G. C., D. Olivares-Villagomez, M. A. Curotto de Lafaille, A. K. Wensky, J. A. Latkowski, and J. J. Lafaille. 2001. Regulatory T cells in spontaneous autoimmune encephalomyelitis. *Immunol Rev* 182:122-134.

9.   Steinman, L., and S. S. Zamvil. 2006. How to successfully apply animal studies in experimental allergic encephalomyelitis to research on multiple sclerosis. *Ann Neurol* 60:12-21.

10.   Rivers, T. M., D. H. Sprunt, and G. P. Berry. 1933. Observations on Attempts to Produce Acute Disseminated Encephalomyelitis in Monkeys. *J Exp Med* 58:39-53.

11.   Rivers, T. M., and F. F. Schwentker. 1935. Encephalomyelitis Accompanied by Myelin Destruction Experimentally Produced in Monkeys. *J Exp Med* 61:689-702.

12.   Olitsky, P. K., and R. H. Yager. 1949. Experimental disseminated encephalomyelitis in white mice. *J Exp Med* 90:213-224.

13.   Kabat, E. A., A. Wolf, and A. E. Bezer. 1946. Rapid Production of Acute Disseminated Encephalomyelitis in Rhesus Monkeys by Injection of Brain Tissue With Adjuvants. *Science* 104:362-363.

14.   Zamvil, S. S., and L. Steinman. 1990. The T lymphocyte in experimental allergic encephalomyelitis. *Annu Rev Immunol* 8:579-621.

15.   Paterson, P. Y. 1960. Transfer of allergic encephalomyelitis in rats by means of lymph node cells. *J Exp Med* 111:119-136.

16.   Gonatas, N. K., and J. C. Howard. 1974. Inhibition of experimental allergic encephalomyelitis in rats severely depleted of T cells. *Science* 186:839-841.

17.   Arnason, B. G., B. D. Jankovic, B. H. Waksman, and C. Wennersten. 1962. Role of the thymus in immune reactions in rats. II. Suppressive effect of thymectomy at birth on reactions of delayed (cellular) hypersensitivity and the circulating small lymphocyte. *J Exp Med* 116:177-186.

18.   Ortiz-Ortiz, L., R. M. Nakamura, and W. O. Weigle. 1976. T cell requirement for experimental allergic encephalomyelitis induction in the rat. *J Immunol* 117:576-579.

19.   Waldor, M. K., S. Sriram, R. Hardy, L. A. Herzenberg, L. A. Herzenberg, L. Lanier, M. Lim, and L. Steinman. 1985. Reversal of experimental allergic encephalomyelitis with monoclonal antibody to a T-cell subset marker. *Science* 227:415-417.

20.   Brostoff, S. W., and D. W. Mason. 1984. Experimental allergic encephalomyelitis: successful treatment in vivo with a monoclonal antibody that recognizes T helper cells. *J Immunol* 133:1938-1942.

21.   Kabat, E. A., A. Wolf, and A. E. Bezer. 1947. The Rapid Production of Acute Disseminated Encephalomyelitis in Rhesus Monkeys by Injection of Heterologous and Homologous Brain Tissue with Adjuvants. *J Exp Med* 85:117-130.

22.   Kibler, R. F., R. B. Fritz, F. Chou, C. H. Jen Chou, N. Y. Peacocke, N. M. Brown, and D. E. McFarlin. 1977. Immune response of Lewis rats to peptide C1 (residues 68-88) of guinea pig and rat myelin basic proteins. *J Exp Med* 146:1323-1331.

23.   Ortiz-Ortiz, L., and W. O. Weigle. 1976. Cellular events in the induction of experimental allergic encephalomyelitis in rats. *J Exp Med* 144:604-616.

24.   Sabatino, J. J., Jr., K. M. Rosenthal, and B. D. Evavold. 2009. Manipulating Antigenic Ligand Strength to Selectively Target Myelin-Reactive CD4+ T Cells in EAE. *J Neuroimmune Pharmacol*.

25.   Billiau, A., and P. Matthys. 2001. Modes of action of Freund's adjuvants in experimental models of autoimmune diseases. *J Leukoc Biol* 70:849-860.

26. Verma, A., D. K. Deb, A. Sassano, S. Uddin, J. Varga, A. Wickrema, and L. C. Platanias. 2002. Activation of the p38 mitogen-activated protein kinase mediates the suppressive effects of type I interferons and transforming growth factor-beta on normal hematopoiesis. *J Biol Chem* 277:7726-7735.

27. Wandinger, K. P., C. S. Sturzebecher, B. Bielekova, G. Detore, A. Rosenwald, L. M. Staudt, H. F. McFarland, and R. Martin. 2001. Complex immunomodulatory effects of interferon-beta in multiple sclerosis include the upregulation of T helper 1-associated marker genes. *Ann Neurol* 50:349-357.

28. Mannie, M. D., D. J. Abbott, and J. L. Blanchfield. 2009. Experimental autoimmune encephalomyelitis in Lewis rats: IFN-beta acts as a tolerogenic adjuvant for induction of neuroantigen-dependent tolerance. *J Immunol* 182:5331-5341.

29. Gran, B., L. R. Tranquill, M. Chen, B. Bielekova, W. Zhou, S. Dhib-Jalbut, and R. Martin. 2000. Mechanisms of immunomodulation by glatiramer acetate. *Neurology* 55:1704-1714.

30. Treatments: FDA approved disease modifying agents. National Multiple Sclerosis Society

31. Lutterotti, A., M. Sospedra, and R. Martin. 2008. Antigen-specific therapies in MS - Current concepts and novel approaches. *J Neurol Sci* 274:18-22.

32. Critchfield, J. M., M. K. Racke, J. C. Zuniga-Pflucker, B. Cannella, C. S. Raine, J. Goverman, and M. J. Lenardo. 1994. T cell deletion in high antigen dose therapy of autoimmune encephalomyelitis. *Science* 263:1139-1143.

33. Weishaupt, A., S. Jander, W. Bruck, T. Kuhlmann, M. Stienekemeier, T. Hartung, K. V. Toyka, G. Stoll, and R. Gold. 2000. Molecular mechanisms of high-dose antigen therapy in experimental autoimmune encephalomyelitis: rapid induction of Th1-type cytokines and inducible nitric oxide synthase. *J Immunol* 165:7157-7163.

34. Minguela, A., S. Pastor, W. Mi, J. A. Richardson, and E. S. Ward. 2007. Feedback regulation of murine autoimmunity via dominant anti-inflammatory effects of interferon gamma. *J Immunol* 178:134-144.

35. Faria, A. M., and H. L. Weiner. 2006. Oral tolerance: therapeutic implications for autoimmune diseases. *Clin Dev Immunol* 13:143-157.

36. Buckner, J. H., and S. F. Ziegler. 2004. Regulating the immune system: the induction of regulatory T cells in the periphery. *Arthritis Res Ther* 6:215-222.

37. Miyamoto, K., C. I. Kingsley, X. Zhang, C. Jabs, L. Izikson, R. A. Sobel, H. L. Weiner, V. K. Kuchroo, and A. H. Sharpe. 2005. The ICOS molecule plays a crucial role in the development of mucosal tolerance. *J Immunol* 175:7341-7347.

38.   Conde, A. A., B. Stransky, A. M. Faria, and N. M. Vaz. 1998. Interruption of recently induced immune responses by oral administration of antigen. *Braz J Med Biol Res* 31:377-380.

39.   Yu, P., R. K. Gregg, J. J. Bell, J. S. Ellis, R. Divekar, H. H. Lee, R. Jain, H. Waldner, J. C. Hardaway, M. Collins, V. K. Kuchroo, and H. Zaghouani. 2005. Specific T regulatory cells display broad suppressive functions against experimental allergic encephalomyelitis upon activation with cognate antigen. *J Immunol* 174:6772-6780.

40.   Legge, K. L., B. Min, J. J. Bell, J. C. Caprio, L. Li, R. K. Gregg, and H. Zaghouani. 2000. Coupling of peripheral tolerance to endogenous interleukin 10 promotes effective modulation of myelin-activated T cells and ameliorates experimental allergic encephalomyelitis. *J Exp Med* 191:2039-2052.

41.   Nicholson, L. B., J. M. Greer, R. A. Sobel, M. B. Lees, and V. K. Kuchroo. 1995. An altered peptide ligand mediates immune deviation and prevents autoimmune encephalomyelitis. *Immunity* 3:397-405.

42.   Ben-Nun, A., N. Kerlero de Rosbo, N. Kaushansky, M. Eisenstein, L. Cohen, J. F. Kaye, and I. Mendel. 2006. Anatomy of T cell autoimmunity to myelin oligodendrocyte glycoprotein (MOG): prime role of MOG44F in selection and control of MOG-reactive T cells in H-2b mice. *Eur J Immunol* 36:478-493.

43.   Karin, N., D. J. Mitchell, S. Brocke, N. Ling, and L. Steinman. 1994. Reversal of experimental autoimmune encephalomyelitis by a soluble peptide variant of a myelin basic protein epitope: T cell receptor antagonism and reduction of interferon gamma and tumor necrosis factor alpha production. *J Exp Med* 180:2227-2237.

44.   Bielekova, B., B. Goodwin, N. Richert, I. Cortese, T. Kondo, G. Afshar, B. Gran, J. Eaton, J. Antel, J. A. Frank, H. F. McFarland, and R. Martin. 2000. Encephalitogenic potential of the myelin basic protein peptide (amino acids 83-99) in multiple sclerosis: results of a phase II clinical trial with an altered peptide ligand. *Nat Med* 6:1167-1175.

45.   Ford, M. L., and B. D. Evavold. 2003. Regulation of polyclonal T cell responses by an MHC anchor-substituted variant of myelin oligodendrocyte glycoprotein 35-55. *J Immunol* 171:1247-1254.

46.   Margot, C. D., M. L. Ford, and B. D. Evavold. 2005. Amelioration of established experimental autoimmune encephalomyelitis by an MHC anchor-substituted variant of proteolipid protein 139-151. *J Immunol* 174:3352-3358.

47.   Ho, P. P., P. Fontoura, M. Platten, R. A. Sobel, J. J. DeVoss, L. Y. Lee, B. A. Kidd, B. H. Tomooka, J. Capers, A. Agrawal, R. Gupta, J. Zernik, M. K. Yee, B. J. Lee, H. Garren, W. H. Robinson, and L. Steinman. 2005. A suppressive oligodeoxynucleotide enhances the efficacy of myelin cocktail/IL-4-tolerizing DNA vaccination and treats autoimmune disease. *J Immunol* 175:6226-6234.

48. Garren, H., P. J. Ruiz, T. A. Watkins, P. Fontoura, L. T. Nguyen, E. R. Estline, D. L. Hirschberg, and L. Steinman. 2001. Combination of gene delivery and DNA vaccination to protect from and reverse Th1 autoimmune disease via deviation to the Th2 pathway. *Immunity* 15:15-22.

49. Ruiz, P. J., H. Garren, I. U. Ruiz, D. L. Hirschberg, L. V. Nguyen, M. V. Karpuj, M. T. Cooper, D. J. Mitchell, C. G. Fathman, and L. Steinman. 1999. Suppressive immunization with DNA encoding a self-peptide prevents autoimmune disease: modulation of T cell costimulation. *J Immunol* 162:3336-3341.

50. Ferber, I. A., S. Brocke, C. Taylor-Edwards, W. Ridgway, C. Dinisco, L. Steinman, D. Dalton, and C. G. Fathman. 1996. Mice with a disrupted IFN-gamma gene are susceptible to the induction of experimental autoimmune encephalomyelitis (EAE). *J Immunol* 156:5-7.

51. Bourquin, C., A. Iglesias, T. Berger, H. Wekerle, and C. Linington. 2000. Myelin oligodendrocyte glycoprotein-DNA vaccination induces antibody-mediated autoaggression in experimental autoimmune encephalomyelitis. *Eur J Immunol* 30:3663-3671.

52. Garren, H., W. H. Robinson, E. Krasulova, E. Havrdova, C. Nadj, K. Selmaj, J. Losy, I. Nadj, E. W. Radue, B. A. Kidd, J. Gianettoni, K. Tersini, P. J. Utz, F. Valone, and L. Steinman. 2008. Phase 2 trial of a DNA vaccine encoding myelin basic protein for multiple sclerosis. *Ann Neurol* 63:611-620.

53. Xu, L. Y., Y. M. Huang, J. S. Yang, P. H. Van Der Meide, H. Link, and B. G. Xiao. 2000. Suppression of ongoing experimental allergic encephalomyelitis (EAE) in Lewis rats: synergistic effects of myelin basic protein (MBP) peptide 68-86 and IL-4. *Clin Exp Immunol* 120:526-531.

54. Mathisen, P. M., M. Yu, J. M. Johnson, J. A. Drazba, and V. K. Tuohy. 1997. Treatment of experimental autoimmune encephalomyelitis with genetically modified memory T cells. *J Exp Med* 186:159-164.

55. Cua, D. J., H. Groux, D. R. Hinton, S. A. Stohlman, and R. L. Coffman. 1999. Transgenic interleukin 10 prevents induction of experimental autoimmune encephalomyelitis. *J Exp Med* 189:1005-1010.

56. Cash, E., A. Minty, P. Ferrara, D. Caput, D. Fradelizi, and O. Rott. 1994. Macrophage-inactivating IL-13 suppresses experimental autoimmune encephalomyelitis in rats. *J Immunol* 153:4258-4267.

57. Brod, S. A., M. Khan, R. H. Kerman, and M. Pappolla. 1995. Oral administration of human or murine interferon alpha suppresses relapses and modifies adoptive transfer in experimental autoimmune encephalomyelitis. *J Neuroimmunol* 58:61-69.

58.   Yu, M., A. Nishiyama, B. D. Trapp, and V. K. Tuohy. 1996. Interferon-beta inhibits progression of relapsing-remitting experimental autoimmune encephalomyelitis. *J Neuroimmunol* 64:91-100.

59.   Floris, S., S. R. Ruuls, A. Wierinckx, S. M. van der Pol, E. Dopp, P. H. van der Meide, C. D. Dijkstra, and H. E. De Vries. 2002. Interferon-beta directly influences monocyte infiltration into the central nervous system. *J Neuroimmunol* 127:69-79.

60.   Hinuma, S., M. Hazama, A. Mayumi, and Y. Fujisawa. 1991. A novel strategy for converting recombinant viral protein into high immunogenic antigen. *FEBS Lett* 288:138-142.

61.   Tao, M. H., and R. Levy. 1993. Idiotype/granulocyte-macrophage colony-stimulating factor fusion protein as a vaccine for B-cell lymphoma. *Nature* 362:755-758.

62.   Chen, T. T., M. H. Tao, and R. Levy. 1994. Idiotype-cytokine fusion proteins as cancer vaccines. Relative efficacy of IL-2, IL-4, and granulocyte-macrophage colony-stimulating factor. *J Immunol* 153:4775-4787.

63.   Mannie, M. D., J. L. Devine, B. A. Clayson, L. T. Lewis, and D. J. Abbott. 2007. Cytokine-neuroantigen fusion proteins: new tools for modulation of myelin basic protein (MBP)-specific T cell responses in experimental autoimmune encephalomyelitis. *J Immunol Methods* 319:118-132.

64.   Mannie, M. D., B. A. Clayson, E. J. Buskirk, J. L. DeVine, J. J. Hernandez, and D. J. Abbott. 2007. IL-2/neuroantigen fusion proteins as antigen-specific tolerogens in experimental autoimmune encephalomyelitis (EAE): correlation of T cell-mediated antigen presentation and tolerance induction. *J Immunol* 178:2835-2843.

65.   Mannie, M. D., and D. J. Abbott. 2007. A fusion protein consisting of IL-16 and the encephalitogenic peptide of myelin basic protein constitutes an antigen-specific tolerogenic vaccine that inhibits experimental autoimmune encephalomyelitis. *J Immunol* 179:1458-1465.

66.   Sadlack, B., J. Lohler, H. Schorle, G. Klebb, H. Haber, E. Sickel, R. J. Noelle, and I. Horak. 1995. Generalized autoimmune disease in interleukin-2-deficient mice is triggered by an uncontrolled activation and proliferation of CD4+ T cells. *Eur J Immunol* 25:3053-3059.

67.   Martin, D., and S. L. Near. 1995. Protective effect of the interleukin-1 receptor antagonist (IL-1ra) on experimental allergic encephalomyelitis in rats. *J Neuroimmunol* 61:241-245.

68.   Mathy, N. L., N. Bannert, S. G. Norley, and R. Kurth. 2000. Cutting edge: CD4 is not required for the functional activity of IL-16. *J Immunol* 164:4429-4432.

69.   Cruikshank, W. W., K. Lim, A. C. Theodore, J. Cook, G. Fine, P. F. Weller, and D. M. Center. 1996. IL-16 inhibition of CD3-dependent lymphocyte activation and proliferation. *J Immunol* 157:5240-5248.

70. Patel, D. M., P. Y. Arnold, G. A. White, J. P. Nardella, and M. D. Mannie. 1999. Class II MHC/peptide complexes are released from APC and are acquired by T cell responders during specific antigen recognition. *J Immunol* 163:5201-5210.

71. Patel, D. M., R. W. Dudek, and M. D. Mannie. 2001. Intercellular exchange of class II MHC complexes: ultrastructural localization and functional presentation of adsorbed I-A/peptide complexes. *Cell Immunol* 214:21-34.

72. Hamilton, J. A. 2008. Colony-stimulating factors in inflammation and autoimmunity. *Nat Rev Immunol* 8:533-544.

73. Martinez-Moczygemba, M., and D. P. Huston. 2003. Biology of common beta receptor-signaling cytokines: IL-3, IL-5, and GM-CSF. *J Allergy Clin Immunol* 112:653-665; quiz 666.

74. Cools, N., P. Ponsaerts, V. F. Van Tendeloo, and Z. N. Berneman. 2007. Balancing between immunity and tolerance: an interplay between dendritic cells, regulatory T cells, and effector T cells. *J Leukoc Biol* 82:1365-1374.

75. Hawiger, D., K. Inaba, Y. Dorsett, M. Guo, K. Mahnke, M. Rivera, J. V. Ravetch, R. M. Steinman, and M. C. Nussenzweig. 2001. Dendritic cells induce peripheral T cell unresponsiveness under steady state conditions in vivo. *J Exp Med* 194:769-779.

76. Bonifaz, L., D. Bonnyay, K. Mahnke, M. Rivera, M. C. Nussenzweig, and R. M. Steinman. 2002. Efficient targeting of protein antigen to the dendritic cell receptor DEC-205 in the steady state leads to antigen presentation on major histocompatibility complex class I products and peripheral CD8+ T cell tolerance. *J Exp Med* 196:1627-1638.

77. Hawiger, D., R. F. Masilamani, E. Bettelli, V. K. Kuchroo, and M. C. Nussenzweig. 2004. Immunological unresponsiveness characterized by increased expression of CD5 on peripheral T cells induced by dendritic cells in vivo. *Immunity* 20:695-705.

78. Xiao, B. G., Y. M. Huang, J. S. Yang, L. Y. Xu, and H. Link. 2001. Bone marrow-derived dendritic cells from experimental allergic encephalomyelitis induce immune tolerance to EAE in Lewis rats. *Clin Exp Immunol* 125:300-309.

79. Huang, Y. M., J. S. Yang, L. Y. Xu, H. Link, and B. G. Xiao. 2000. Autoantigen-pulsed dendritic cells induce tolerance to experimental allergic encephalomyelitis (EAE) in Lewis rats. *Clin Exp Immunol* 122:437-444.

80. Ganesh, B. B., D. M. Cheatem, J. R. Sheng, C. Vasu, and B. S. Prabhakar. 2009. GM-CSF-induced CD11c+CD8a--dendritic cells facilitate Foxp3+ and IL-10+ regulatory T cell expansion resulting in suppression of autoimmune thyroiditis. *Int Immunol* 21:269-282.

81. Cheatem, D., B. B. Ganesh, E. Gangi, C. Vasu, and B. S. Prabhakar. 2009. Modulation of dendritic cells using granulocyte-macrophage colony-stimulating factor (GM-CSF)

delays type 1 diabetes by enhancing CD4+CD25+ regulatory T cell function. *Clin Immunol* 131:260-270.

82.   Li, G., Young-June Kim and Hal E. Broxmeyer 2005. Macrophage Colony-Stimuliong Factor Drives Cord Blood Monocyte Differentiation into IL-10highIL-12absent Dendritic Cells with Tolerogenic Potential. *Journal of Immunology* 174:4706-2717.

83.   Nishina, T., Y. Naomoto, A. Gouchi, M. Gunduz, Y. Shirakawa, T. Nobuhisa, T. Motoki, S. Kusaka, M. Haisa, J. Matsuoka, E. Nakayama, and N. Tanaka. 2004. Macrophage colony-stimulating factor inhibits tumor necrosis factor production and prolongs skin graft survival. *Transplantation* 77:456-459.

84.   Guan, Y., S. Yu, Z. Zhao, B. Ciric, G. X. Zhang, and A. Rostami. 2007. Antigen presenting cells treated in vitro by macrophage colony-stimulating factor and autoantigen protect mice from autoimmunity. *J Neuroimmunol* 192:68-78.

85.   Zhu, B., Y. Bando, S. Xiao, K. Yang, A. C. Anderson, V. K. Kuchroo, and S. J. Khoury. 2007. CD11b+Ly-6C(hi) suppressive monocytes in experimental autoimmune encephalomyelitis. *J Immunol* 179:5228-5237.

86.   Pixley, F. J., and E. R. Stanley. 2004. CSF-1 regulation of the wandering macrophage: complexity in action. *Trends Cell Biol* 14:628-638.

87.   Chitu, V., and E. R. Stanley. 2006. Colony-stimulating factor-1 in immunity and inflammation. *Curr Opin Immunol* 18:39-48.

88.   Perry, S. E., S. M. Mostafa, R. Wenstone, A. Shenkin, and P. J. McLaughlin. 2004. HLA-DR regulation and the influence of GM-CSF on transcription, surface expression and shedding. *Int J Med Sci* 1:126-136.

89.   Mannie, M. D., J. M. Rosser, and G. A. White. 1995. Autologous rat myelin basic protein is a partial agonist that is converted into a full antagonist upon blockade of CD4. Evidence for the integration of efficacious and nonefficacious signals during T cell antigen recognition. *J Immunol* 154:2642-2654.

90.   Arnold, P. Y., D. K. Davidian, and M. D. Mannie. 1997. Antigen presentation by T cells: T cell receptor ligation promotes antigen acquisition from professional antigen-presenting cells. *Eur J Immunol* 27:3198-3205.

91.   Mannie, M. D., D. J. Fraser, and T. J. McConnell. 2003. IL-4 responsive CD4+ T cells specific for myelin basic protein: IL-2 confers a prolonged postactivation refractory phase. *Immunol Cell Biol* 81:8-19.

92.   Foged, C., A. Sundblad, and L. Hovgaard. 2002. Targeting vaccines to dendritic cells. *Pharm Res* 19:229-238.

93.   Ahlers, J. D., and I. M. Belyakov. 2009. Strategies for recruiting and targeting dendritic cells for optimizing HIV vaccines. *Trends Mol Med* 15:263-274.

94.   Dudziak, D., A. O. Kamphorst, G. F. Heidkamp, V. R. Buchholz, C. Trumpfheller, S. Yamazaki, C. Cheong, K. Liu, H. W. Lee, C. G. Park, R. M. Steinman, and M. C. Nussenzweig. 2007. Differential antigen processing by dendritic cell subsets in vivo. *Science* 315:107-111.

95.   Mahnke, K., M. Guo, S. Lee, H. Sepulveda, S. L. Swain, M. Nussenzweig, and R. M. Steinman. 2000. The dendritic cell receptor for endocytosis, DEC-205, can recycle and enhance antigen presentation via major histocompatibility complex class II-positive lysosomal compartments. *J Cell Biol* 151:673-684.

96.   Skea, D. L., and B. H. Barber. 1993. Studies of the adjuvant-independent antibody response to immunotargeting. Target structure dependence, isotype distribution, and induction of long term memory. *J Immunol* 151:3557-3568.

97.   Wang, H., M. N. Griffiths, D. R. Burton, and P. Ghazal. 2000. Rapid antibody responses by low-dose, single-step, dendritic cell-targeted immunization. *Proc Natl Acad Sci U S A* 97:847-852.

98.   Regnault, A., D. Lankar, V. Lacabanne, A. Rodriguez, C. Thery, M. Rescigno, T. Saito, S. Verbeek, C. Bonnerot, P. Ricciardi-Castagnoli, and S. Amigorena. 1999. Fcgamma receptor-mediated induction of dendritic cell maturation and major histocompatibility complex class I-restricted antigen presentation after immune complex internalization. *J Exp Med* 189:371-380.

99.   You, Z., X. Huang, J. Hester, H. C. Toh, and S. Y. Chen. 2001. Targeting dendritic cells to enhance DNA vaccine potency. *Cancer Res* 61:3704-3711.

100.   Wallace, P. K., J. L. Romet-Lemonne, M. Chokri, L. H. Kasper, M. W. Fanger, and C. E. Fadul. 2000. Production of macrophage-activated killer cells for targeting of glioblastoma cells with bispecific antibody to FcgammaRI and the epidermal growth factor receptor. *Cancer Immunol Immunother* 49:493-503.

101.   Casten, L. A., and S. K. Pierce. 1988. Receptor-mediated B cell antigen processing. Increased antigenicity of a globular protein covalently coupled to antibodies specific for B cell surface structures. *J Immunol* 140:404-410.

102.   Cheng, P. C., C. R. Steele, L. Gu, W. Song, and S. K. Pierce. 1999. MHC class II antigen processing in B cells: accelerated intracellular targeting of antigens. *J Immunol* 162:7171-7180.

103.   Kang, T. H., J. H. Lee, H. C. Bae, K. H. Noh, J. H. Kim, C. K. Song, B. C. Shin, C. F. Hung, T. C. Wu, J. S. Park, and T. W. Kim. 2006. Enhancement of dendritic cell-based vaccine potency by targeting antigen to endosomal/lysosomal compartments. *Immunol Lett* 106:126-134.

104.   Wu, T. C., F. G. Guarnieri, K. F. Staveley-O'Carroll, R. P. Viscidi, H. I. Levitsky, L. Hedrick, K. R. Cho, J. T. August, and D. M. Pardoll. 1995. Engineering an intracellular

pathway for major histocompatibility complex class II presentation of antigens. *Proc Natl Acad Sci U S A* 92:11671-11675.

105.   Cheng, W. F., C. F. Hung, C. Y. Chai, K. F. Hsu, L. He, M. Ling, and T. C. Wu. 2001. Tumor-specific immunity and antiangiogenesis generated by a DNA vaccine encoding calreticulin linked to a tumor antigen. *J Clin Invest* 108:669-678.

106.   Chen, C. H., T. L. Wang, C. F. Hung, Y. Yang, R. A. Young, D. M. Pardoll, and T. C. Wu. 2000. Enhancement of DNA vaccine potency by linkage of antigen gene to an HSP70 gene. *Cancer Res* 60:1035-1042.

107.   Tighe, H., K. Takabayashi, D. Schwartz, R. Marsden, L. Beck, J. Corbeil, D. D. Richman, J. J. Eiden, Jr., H. L. Spiegelberg, and E. Raz. 2000. Conjugation of protein to immunostimulatory DNA results in a rapid, long-lasting and potent induction of cell-mediated and humoral immunity. *Eur J Immunol* 30:1939-1947.

108.   Maurer, T., A. Heit, H. Hochrein, F. Ampenberger, M. O'Keeffe, S. Bauer, G. B. Lipford, R. M. Vabulas, and H. Wagner. 2002. CpG-DNA aided cross-presentation of soluble antigens by dendritic cells. *Eur J Immunol* 32:2356-2364.

109.   Heit, A., T. Maurer, H. Hochrein, S. Bauer, K. M. Huster, D. H. Busch, and H. Wagner. 2003. Cutting edge: Toll-like receptor 9 expression is not required for CpG DNA-aided cross-presentation of DNA-conjugated antigens but essential for cross-priming of CD8 T cells. *J Immunol* 170:2802-2805.

110.   Heit, A., K. M. Huster, F. Schmitz, M. Schiemann, D. H. Busch, and H. Wagner. 2004. CpG-DNA aided cross-priming by cross-presenting B cells. *J Immunol* 172:1501-1507.

111.   Heit, A., F. Schmitz, M. O'Keeffe, C. Staib, D. H. Busch, H. Wagner, and K. M. Huster. 2005. Protective CD8 T cell immunity triggered by CpG-protein conjugates competes with the efficacy of live vaccines. *J Immunol* 174:4373-4380.

112.   Hung, C. F., K. F. Hsu, W. F. Cheng, C. Y. Chai, L. He, M. Ling, and T. C. Wu. 2001. Enhancement of DNA vaccine potency by linkage of antigen gene to a gene encoding the extracellular domain of Fms-like tyrosine kinase 3-ligand. *Cancer Res* 61:1080-1088.

113.   Boyle, J. S., J. L. Brady, and A. M. Lew. 1998. Enhanced responses to a DNA vaccine encoding a fusion antigen that is directed to sites of immune induction. *Nature* 392:408-411.

114.   Deliyannis, G., J. S. Boyle, J. L. Brady, L. E. Brown, and A. M. Lew. 2000. A fusion DNA vaccine that targets antigen-presenting cells increases protection from viral challenge. *Proc Natl Acad Sci U S A* 97:6676-6680.

115.   Tillman, B. W., T. L. Hayes, T. D. DeGruijl, J. T. Douglas, and D. T. Curiel. 2000. Adenoviral vectors targeted to CD40 enhance the efficacy of dendritic cell-based vaccination against human papillomavirus 16-induced tumor cells in a murine model. *Cancer Res* 60:5456-5463.

116.   Wortham, C., L. Grinberg, D. C. Kaslow, D. E. Briles, L. S. McDaniel, A. Lees, M. Flora, C. M. Snapper, and J. J. Mond. 1998. Enhanced protective antibody responses to PspA after intranasal or subcutaneous injections of PspA genetically fused to granulocyte-macrophage colony-stimulating factor or interleukin-2. *Infect Immun* 66:1513-1520.

117.   Blanchfield, J. L., and M. D. Mannie. 2010. A GMCSF-neuroantigen fusion protein is a potent tolerogen in experimental autoimmune encephalomyelitis (EAE) that is associated with efficient targeting of neuroantigen to APC. *J Leukoc Biol* 87:509-521.

118.   Khoury, S. J., M. H. Sayegh, W. W. Hancock, L. Gallon, C. B. Carpenter, and H. L. Weiner. 1993. Acquired tolerance to experimental autoimmune encephalomyelitis by intrathymic injection of myelin basic protein or its major encephalitogenic peptide. *J Exp Med* 178:559-566.

119.   Khoury, S. J., L. Gallon, W. Chen, K. Betres, M. E. Russell, W. W. Hancock, C. B. Carpenter, M. H. Sayegh, and H. L. Weiner. 1995. Mechanisms of acquired thymic tolerance in experimental autoimmune encephalomyelitis: thymic dendritic-enriched cells induce specific peripheral T cell unresponsiveness in vivo. *J Exp Med* 182:357-366.

120.   Nicholson, L. B., H. Waldner, A. M. Carrizosa, A. Sette, M. Collins, and V. K. Kuchroo. 1998. Heteroclitic proliferative responses and changes in cytokine profile induced by altered peptides: implications for autoimmunity. *Proc Natl Acad Sci U S A* 95:264-269.

121.   Nicholson, L. B., A. C. Anderson, and V. K. Kuchroo. 2000. Tuning T cell activation threshold and effector function with cross-reactive peptide ligands. *Int Immunol* 12:205-213.

122.   Kavuru, M. S., E. J. Sullivan, R. Piccin, M. J. Thomassen, and J. K. Stoller. 2000. Exogenous granulocyte-macrophage colony-stimulating factor administration for pulmonary alveolar proteinosis. *Am J Respir Crit Care Med* 161:1143-1148.

123.   Venkateshiah, S. B., T. D. Yan, T. L. Bonfield, M. J. Thomassen, M. Meziane, C. Czich, and M. S. Kavuru. 2006. An open-label trial of granulocyte macrophage colony stimulating factor therapy for moderate symptomatic pulmonary alveolar proteinosis. *Chest* 130:227-237.

124.   McQualter, J. L., R. Darwiche, C. Ewing, M. Onuki, T. W. Kay, J. A. Hamilton, H. H. Reid, and C. C. Bernard. 2001. Granulocyte macrophage colony-stimulating factor: a new putative therapeutic target in multiple sclerosis. *J Exp Med* 194:873-882.

125.   Ponomarev, E. D., L. P. Shriver, K. Maresz, J. Pedras-Vasconcelos, D. Verthelyi, and B. N. Dittel. 2007. GM-CSF production by autoreactive T cells is required for the activation of microglial cells and the onset of experimental autoimmune encephalomyelitis. *J Immunol* 178:39-48.

126.   Marusic, S., J. S. Miyashiro, J. Douhan, 3rd, R. F. Konz, D. Xuan, J. W. Pelker, V. Ling, J. P. Leonard, and K. A. Jacobs. 2002. Local delivery of granulocyte macrophage colony-

stimulating factor by retrovirally transduced antigen-specific T cells leads to severe, chronic experimental autoimmune encephalomyelitis in mice. *Neurosci Lett* 332:185-189.

127. Verhasselt, V., O. Vosters, C. Beuneu, C. Nicaise, P. Stordeur, and M. Goldman. 2004. Induction of FOXP3-expressing regulatory CD4pos T cells by human mature autologous dendritic cells. *Eur J Immunol* 34:762-772.

128. Zhang, M., H. Tang, Z. Guo, H. An, X. Zhu, W. Song, J. Guo, X. Huang, T. Chen, J. Wang, and X. Cao. 2004. Splenic stroma drives mature dendritic cells to differentiate into regulatory dendritic cells. *Nat Immunol* 5:1124-1133.

129. Bielekova, B., M. Catalfamo, S. Reichert-Scrivner, A. Packer, M. Cerna, T. A. Waldmann, H. McFarland, P. A. Henkart, and R. Martin. 2006. Regulatory CD56(bright) natural killer cells mediate immunomodulatory effects of IL-2Ralpha-targeted therapy (daclizumab) in multiple sclerosis. *Proc Natl Acad Sci U S A* 103:5941-5946.

130. Zhang, B., T. Yamamura, T. Kondo, M. Fujiwara, and T. Tabira. 1997. Regulation of experimental autoimmune encephalomyelitis by natural killer (NK) cells. *J Exp Med* 186:1677-1687.

131. Smeltz, R. B., N. A. Wolf, and R. H. Swanborg. 1999. Inhibition of autoimmune T cell responses in the DA rat by bone marrow-derived NK cells in vitro: implications for autoimmunity. *J Immunol* 163:1390-1397.

132. Galazka, G., A. Jurewicz, W. Orlowski, M. Stasiolek, C. F. Brosnan, C. S. Raine, and K. Selmaj. 2007. EAE tolerance induction with Hsp70-peptide complexes depends on H60 and NKG2D activity. *J Immunol* 179:4503-4512.

133. Wolf, S. D., B. N. Dittel, F. Hardardottir, and C. A. Janeway, Jr. 1996. Experimental autoimmune encephalomyelitis induction in genetically B cell-deficient mice. *J Exp Med* 184:2271-2278.

134. Xu, B., and D. W. Scott. 2004. A novel retroviral gene therapy approach to inhibit specific antibody production and suppress experimental autoimmune encephalomyelitis induced by MOG and MBP. *Clin Immunol* 111:47-52.

135. Small, E. J., P. Fratesi, D. M. Reese, G. Strang, R. Laus, M. V. Peshwa, and F. H. Valone. 2000. Immunotherapy of hormone-refractory prostate cancer with antigen-loaded dendritic cells. *J Clin Oncol* 18:3894-3903.

February 10, 2009

Mark Mannie, Ph.D.
Department of Micro/Immuno
Brody 5E-106
ECU Brody School of Medicine

Dear Dr. Mannie:

Your Animal Use Protocol entitled, "Antigen-Specific Vaccines," (AUP #K144a) was reviewed by this institution's Animal Care and Use Committee on 2/10/09. The following action was taken by the Committee:

   "Approved as submitted"

A copy is enclosed for your laboratory files. Please be reminded that all animal procedures must be conducted as described in the approved Animal Use Protocol. Modifications of these procedures cannot be performed without prior approval of the ACUC. The Animal Welfare Act and Public Health Service Guidelines require the ACUC to suspend activities not in accordance with approved procedures and report such activities to the responsible University Official (Vice Chancellor for Health Sciences or Vice Chancellor for Academic Affairs) and appropriate federal Agencies.

Sincerely yours,

Robert G. Carroll, Ph.D.
Chairman, Animal Care and Use Committee

RGC/jd

enclosure

Marcus Jeannette
Warren Life Science Bldg. Room 188
East Carolina University
Greenville, NC 27834

June 9, 2010

Mark Mannie, Ph.D.
ECU Brody School of Medicine
Department of Microbiology/Immunology
Brody 5E-106

Dr. Mannie,

For your records, this letter has been written to acknowledge that Jennifer Lori Blanchfield successfully completed radiation safety training in August of 2004. Completion of this training permitted her to use radioactive material in your laboratory. Tritiated [methyl-3H] thymidine has been the radioactive material currently approved for *in vitro* use in your laboratory.

Sincerely,

Marcus Jeannette
Basic Sciences Radiation Officer